INFORMATION TO USERS

This manuscript has been reproduced from the microfilm master. UMI films the text directly from the original or copy submitted. Thus, some thesis and dissertation copies are in typewriter face, while others may be from any type of computer printer.

The quality of this reproduction is dependent upon the quality of the copy submitted. Broken or indistinct print, colored or poor quality illustrations and photographs, print bleedthrough, substandard margins, and improper alignment can adversely affect reproduction.

In the unlikely event that the author did not send UMI a complete manuscript and there are missing pages, these will be noted. Also, if unauthorized copyright material had to be removed, a note will indicate the deletion.

Oversize materials (e.g., maps, drawings, charts) are reproduced by sectioning the original, beginning at the upper left-hand corner and continuing from left to right in equal sections with small overlaps.

ProQuest Information and Learning
300 North Zeeb Road, Ann Arbor, MI 48106-1346 USA
800-521-0600

dizzy, a Novel Gene Required for Axon Guidance in the Visual System of *Drosophila*

by

Anthony G. Bottalico

A Dissertation Submitted to the Graduate Faculty in Biology in Partial Fulfillment of the Requirements for the Degree of Doctor of Philosophy, The City University of New York

2003

This manuscript has been read and accepted for the Graduate Faculty in Biology in satisfaction of the dissertation requirement for the degree of Doctor of Philosophy.

4.14.2003
Date

Chair of Examining Committee
Dr. He Qi, Brooklyn College

4.24.03
Date

Executive Officer
Dr. Richard L. Chappell

Dr. Jennifer Basil, Brooklyn College

Dr. Charlene Forest, Brooklyn College

Dr. Theodore Muth, Brooklyn College

Dr. George Ojakian, SUNY Downstate Medical Center

Supervisory Committee

THE CITY UNIVERSITY OF NEW YORK

Abstract

dizzy, a Novel Gene Required for Axon Guidance in the Visual System of *Drosophila*

by

Anthony G. Bottalico

Advisor: Dr. Qi He

Retinal axons in the *Drosophila* visual system traverse long distance and make several critical projection decisions en route. Elucidating genes required for retinal axon pathfinding is thus essential for understanding mechanisms governing the development of the CNS. Identified in our screening for genes required for the visual system development, *dizzy* encodes a protein regulating the pathfinding of the retinal axons. In *dizzy* mutants, retinal axons make abnormal projections to their targets in the lamina while the photoreceptors appear normal. The full cDNA sequence for *dizzy* has been obtained and it encodes a novel guanine nucleotide exchange factor of 1573 amino acids with a Ras/Rap1A-associating domain. The combined molecular, cellular and genetic analyses demonstrate that Dizzy is a critical mediator of axon pathfinding with a

possible regulatory role in the growth cone cytoskeleton reorganization.

To my family

Acknowledgements

I would like to express my deep appreciation to my mentor Dr. Qi He for providing me with the guidance to complete my doctorate.

I am grateful for other members of my doctoral committee, Drs. Jennifer Basil, Dan Eshel, Charlene Forest, Theodore Muth, and George Ojakian.

My thanks also go to Dr. Martin P. Schreibman for his mentorship and guidance in completing my M.S., Dr. James Nishiura for providing me with my first undergraduate research project and continual advice, Dr. Katherine Flynn for her early assistance in the doctoral process and her continued friendship, and Dr. Ray H. Gavin, for advice and the opportunity of teaching at Brooklyn College.

I am indebted to my friend and laboratory partner, Melissa Garcia, for collaborative efforts in the laboratory and for sharing research ideas, techniques, and experiences.

Many thanks to those CUNY undergraduates that I was fortunate enough to coach.

Last but not least, my special gratitude goes to all my friends for the many great experiences that we have shared throughout the years.

Table of Contents

Chapter 5 Molecular Analysis of the *dizzy* Locus

Chapter 6 General Discussion

List of Figures

Chapter 1

Introduction

1.1 History of Neuroscience

Understanding the cellular and molecular mechanisms that regulate the formation of precise and selective connections between neurons during development of the central nervous system (CNS) is a challenging problem in neurobiology (Albright et al., 2000; Dickson, 2002; Mueller, 1999; Tessier-Lavigne and Goodman, 1996). Such highly specific communications between neurons are required for the establishment of functional neuronal circuits in mature brains. The human brain for instance has over one trillion neurons and each one contains over one thousand neural synapses. One critical issue in neuroscience thus concerns understanding how neuronal circuits are assembled in the complex three-dimensional architecture of the brain.

1.1a Holistic and Reductionist Approaches

Historically, there have been two approaches to understanding this complex problem. The first is the holistic approach, referred to as a top-down approach, that studies

the role of a large system of neurons in intact experimental systems. The second is the reductionist approach, referred to as the bottom-up approach, that investigates the basic functional components in the nervous system. In this approach one can focus on individual neuronal circuits, neurons, or molecules (Albright et al., 2000). Both of these approaches have limitations, but they were successfully applied at the end of the 19th century to understanding the nervous system.

Holistic Approach - Paul Pierre Broca

Paul Pierre Broca was a pioneer in shaping the holistic approach when he discovered the speech center of the brain while examining the brains of aphasic (unable to talk) patients (Jay, 2002; Lukacs, 1980; Opp, 1994). He found that these individuals had a specific lesion located in the third circumvolution of the frontal lobe in the brain, which enabled him to conclude that different regions of the cerebral cortex of the human brain are functionally different.

Reductionist Approach - Santiago Ramon y Cajal

The reductionist approach was by far the most widely used strategy in elucidating the functions of the brain. Santiago Ramon y Cajal was among the first neuroscientists to probe the brain utilizing the methodology (Andres-Barquin, 2001; DeFelipe, 2002). Among many of his discoveries was the finding that neurons serve as the functional signaling units of the nervous system and that neurons connect to one another in a precise manner (Jones, 1999). Cajal also demonstrated that the nervous system tissue is comprised of discrete neurons with the help of two technological improvements: First, he chose to use young brains when the density of neurons is still low and the expansion of the dendritic tree modest. Second, Cajal applied Camillo Golgi's silver staining method to label occasional neurons in their entirety (Albright et al., 2000).

Cajal was able to identify several types of neurons and demonstrated that these cells can communicate with one another only at specialized points of apposition contacts that

Sherrington later called synapses (Berlucchi, 1999). These findings led him to formulate the principles of dynamic polarization and connection specificity.

1.1b Principle of Dynamic Polarization

According to the principle of dynamic polarization, electrical signals are first propagated in the neural cell body and then sent down the axon to the axonal terminus of the cell (Changeux, 2001). By identifying the directionality of information flow in the nervous system, dynamic polarization provided a logic set of rules for mapping the individual pathways in the brain that constitute a coherent neuronal circuit. While mapping developing neuronal circuits in the hippocampus of new-born animals, Cajal recognized a stereotypical pattern of connections between neurons, supporting his principle of connection specificity.

1.1c Principal of Connection Specificity

The principle of connection specificity is the idea that a given neuron will form specific connections with only some neurons and not with others. Cajal provided dramatic illustrations of embryonic neurons in the process of extending

their axons guided by a specialized structure at the leading edge he named the growth cone (Baas and Luo, 2001; Tanaka and Sabry, 1995). Cajal hypothesized that these neurons were potentially guided to their target by factors present in the surrounding milieu in a process called chemotaxis (Sotelo, 1999).

Chemotaxis was accepted as the primary mechanism for wiring the CNS until it was challenged by the antiselectivity movement, which favored a predominantly mechanical interpretation. It was Roger Sperry who conducted definitive experiments to establish Cajal's hypothesis for a chemically based axon guidance mechanism.

Chemoaffinity Hypothesis – Roger Sperry

Roger Sperry formulated the chemoaffinity hypothesis, where the most plausible explanation for the selectivity apparent in the formation of developing neural connections is a precise system of matching chemical labels conferring positional information (Marin et al., 2001; Sperry, 1963). Sperry studied neuronal connectivity in the vertebrate visual system between retinal photoreceptor neurons and their

postsynaptic targets in the tectum of the brain. He selected the visual system for good reason – the visual system is topographically organized so that the relative positions of photoreceptors along the anterior-posterior (AP) and dorsal-ventral (DV) axis in the eye match the corresponding targets in the tectum.

In his first set of experiments, Sperry severed photoreceptor axons at the optic stalk and observed that the regenerated photoreceptor axons were capable of forming phenotypically wild-type retinotopic connections with their target neurons in the tectum. In the second set of experiments, he inverted the eye 180 degrees following the severing of photoreceptor axons at the optic stalk. The retinal axons of these animals managed to form stereotypical connections with their targets; however, these frogs had an inverted representation of the visual world (Meyer, 1998; Sperry, 1963). Sperry concluded that instead of a specific guidance cue for each photoreceptor cell, a gradient of guidance cues along the AP and DV axis could account for

the formation of topographic maps (Goodhill and Richards, 1999).

1.2 Modern Neuroscience

The advances in brain imaging techniques and the application of molecular biology in developmental neuroscience have extended our understanding of the nervous system significantly, including the mechanisms underlining the wiring of the neural circuitry (Albright et al., 2000; Dickson, 2002; Habib et al., 1996; Huber et al., 2000; Tessier-Lavigne and Goodman, 1996). A widely held theory holds that the complex pattern of neuronal connections of the CNS is generated through two overlapping stages. Initially, axons are guided to their targets solely by guidance cues without any input from the neural activities. It is thus referred to as an activity-independent process, which creates the crude neuronal connections. Later on, after the establishment of the coarse interactions, the neural activities will drive the fine-tuning process in the activity-dependent phase to complete the synapse formation and the functional neural network (Barth et al., 1997; Goodman and Shatz,

1993; Hall, 1998; Heisenberg et al., 1995; Spinelli et al., 1972; Tessier-Lavigne and Goodman, 1996).

1.2a Steering the Growth Cone

Growth Cone Morphology

The projection of a neuronal axon is guided by the growth cone, a specialized extension at the tip of a neuronal axon with finger-like projections, filopodia, and web-like veils called lamellipodia (Figure 1A) (Mueller, 1999). Filopodia are about 0.2-0.5 μm thin spike-like projections up to 40 μm in length that grow and retract at a rate of up to 12 μm/min, while lamella spread and retract between filopodia (Tanaka and Sabry, 1995). It is clear that the shape and motility of the growth cone is determined by the dynamics of the cytoskeleton. Specifically, the motor is the polymerization and depolymerization of the actin filaments within the growth cone, resulting in large-scale changes of the overall morphology and the physical movement of the growth cone (Dent and Kalil, 2001; Gordon-Weeks, 1988).

Growth Cone Actin Cytoskeleton

The shape of the growth cone is largely determined by the organization of the actin cytoskeleton which forms an interwoven network of filaments at the leading edge of the filopodia and lamellipodia. At the core of each filopodium is a dense and cross linked bundle of actin filaments extending into the lamella, while in the lamella, long actin filaments form a network appearing like woven fabric. The actin filaments in both filopodia and lamella are predominately oriented with their faster growing ends at the periphery and their slower growing ends towards the center of the cell. Drugs disrupting F-actin cause lamellipodial and filopodial collapse and block the ability of axons to navigate (Dent and Kalil, 2001).

At the leading edge of the growth cone, a highly dynamic peripheral region extends and retracts actin-filled filopodia. These filopodia are thought to play an active role in synaptic targeting, in part by serving as antennae that scout in advance of the axonal growth to sample a large volume of their environment (Mueller, 1999). The regulation of

polymerization and depolymerization of the actin cytoskeleton and microtubules determines the directional path of a growing axon (Zhou and Cohan, 2001).

Growth Cone Microtubules

In growing neurons, microtubules are intimately associated with the dynamic actin-based protrusions in the growth cone and play a critical role in turning decisions. Microtubules in the axon form highly stabilized cross-linked bundles, but as they emerge from the axon into the growth cone, they spread into single filaments that continuously extend into and retract from the peripheral areas of the lamella and the bases of filopodia (Buck and Zheng, 2002). This constant exploration is attributable to a property of microtubules called dynamic instability, by which individual microtubules randomly transit between phases of polymerization in growth cones at 11 μm/min and depolymerization at 10 μm/min. In growth cones the more dynamic positive ends of the microtubules are pointed toward the periphery of the growth cone. The precise role of microtubules in growth cone motility is not yet clear.

Disrupting microtubule assembly and inhibiting microtubule motors in moving cells reduce lamellipodial protrusions and persistent migration (Dent and Kalil, 2001). This suggests that the penetration of microtubules into the lamella promotes their formation either by local membrane insertion or by modulation of actin organization (Tanaka and Sabry, 1995).

Growth Cone Guidance Cues

Growth cones are guided to their targets by long-range diffusible cues and short-range contact dependent cues (Tessier-Lavigne and Goodman, 1996). There are four types of guidance cues including long-range chemoattraction and chemorepulsion, and short-range contact attraction and contact repulsion (Figure 1B). Long-range cues are diffusible proteins distributed in a spatially graded manner in the surrounding milieu of the growth cone, whereas short-range cues are bound locally to components of the extracellular matrix or to the surface of adjacent cells. Growth cones respond to the coordinate actions of all four types of guidance

cues, steering towards or away from specific sites (Mueller, 1999).

1.3 Molecular Biology of Axon Guidance

The identification and characterization of guidance cues, their receptors, and intracellular signaling molecules involved have progressed significantly in recent years, thanks to, in large part, the utilization of molecular biology in neuroscience (Albright et al., 2000; Dickson, 2002). In the *Drosophila* model in particular, two experimental approaches have been especially fruitful.

1) Forward genetics: where a large collection of fly mutants is created and screened for various developmental defects, followed by the identification of the genes responsible. This has been the core of the modern version of traditional fly genetics.

2) Reverse genetics: where *Drosophila* homologs of genes first identified in other species are elucidated and their functions analyzed by generating mutant animals lacking the expression of these genes. This strategy is especially

promising in the post-genome era when the entire genome sequence of the animal is available.

The combination of these approaches has yielded a frame work of understanding about the molecular basis of axon pathfinding. Specifically, the guidance molecules of the netrins, slit, semaphorins and ephrins have formed the best characterized guidance mechanisms. Collectively, they create a scaffold of the signaling steps leading to the responses of a growing axon (Dickson, 2002).

1.3a Guidance Cues and Their Receptors

Netrins

Proteins of the Netrin family are bifunctional capable of exerting both chemoattractive and chemorepulsive forces on axon projections (Chan et al., 1996; Hong et al., 1999; Song et al., 1997). The discovery of Netrins came as a remarkable convergence in the search for a chemoattractant for vertebrate commissural axons, and the analysis of genes required for circumferential axon guidance in the nematode *Caenorhabditis elegans* (*C. elegans*) (Dickson, 2002).

Following the initial lead that the ventral most portion of the vertebrate spinal cord, the floor plate, is capable of secreting an apparently chemoattractive guidance cue, Kennedy et al. chose a biochemical approach aimed at identifying this elusive factor(s). They uncovered two forms of the protein, Netrin-1 and Netrin-2 (Kennedy et al., 1994). Surprisingly, Netrins show a remarkable degree of identity to Unc-6, a protein characterized earlier in *C. elegans* (Chan et al., 1996; Hedgecock et al., 1990). Furthermore, Unc-6 was identified as a guidance molecule responsible for the navigation of the ventral bound axons (Chan et al., 1996; Hedgecock et al., 1990). Together, it becomes clear that the Netrins are the vertebrate Unc-6 critical for organizing the axon pathfinding in the CNS.

Shortly afterward, two *Drosophila* homologs, Netrin-A and Netrin-B were identified (Harris et al., 1996). Apart from sharing a high level of structural conservation, the fly Netrins are also found as pivotal players in wiring the CNS (Harris et al., 1996). Thus, the Netrins constitute an evolutionarily

conserved guidance mechanism spanning over 600 million years in the course of evolution.

Molecularly, the Netrin proteins share a common domain structure and extensive amino acid sequence similarity over the entire length of the protein (Mitchell et al., 1996). These proteins lack a transmembrane domain, consistent with their role as secreted diffusible molecules. Structurally, the Netrin protein contains four domains that include a signal peptide at the amino terminus, followed by domains VI, V, and C toward the carboxy end. In addition, Netrin proteins have three highly conserved epidermal growth factor-like (EGF-like) repeats in the V domain with at least 60% homology (Culotti and Kolodkin, 1996).

Genetic analysis in *C. elegans* to identify potential candidate genes that are in the same pathway of netrin Unc-6 guidance cues led to the identification of the Unc-6 receptor, Unc-40 (Hedgecock et al., 1990). Unc-40 has a vertebrate homolog called Deleted in Colorectal Carcinoma (DCC) (Chan et al., 1996; Culotti and Merz, 1998), and in fruit flies named Frazzled (Kolodziej et al., 1996). The elimination of Unc-40

function results in misrouting of axons normally attracted to a Netrin source in *C. elegans*, *Drosophila*, and vertebrates (Chan et al., 1996; de la Torre et al., 1997; Mitchell et al., 1996).

Collectively, the Unc-6/Unc-40 pathway mediates proper ventral migration of pioneering axons in the CNS of the *C. elegans*, *Drosophila* and the vertebrates, respectively (Tessier-Lavigne and Goodman, 1996; Kolodziej, 1996), indicating the DCC/Unc-40 receptors for Netrins are the prime regulator of the attractive effects of the Netrin proteins.

The picture becomes complicated when unexpectedly, the Netrins were found to repel certain axons (Chan et al., 1996; Culotti and Kolodkin, 1996). It turns out that the outcome of Netrin guidance cues depends on the Netrin receptors. When a Netrin binds to its receptor Unc-5 along with Unc-40, the responding axons expressing these receptors will interpret the Netrin signal as a repulsive cue and steer away (Hong et al., 1999).

Together, the current model suggests that Unc-40 functions as a co-receptor for both repulsive and attractive

Netrin guidance. When Unc-40 is associated with Unc-5, the complex mediates a repulsive response, while if the association is between Unc-40 and one yet unidentified co-receptor X, the complex will receive Netrins as attractive cues (Keleman and Dickson, 2001).

To explore the downstream molecular differences in the attractive and repulsive Netrin guidance cues, *in vitro* studies have been conducted, which have shown that the common secondary messenger systems such as the intracellular levels of cyclic adenosine monophosphate (cAMP), the activity of protein kinase A (PKA), and cellular calcium concentration (Ca^{2+}) are critical for the axonal response (Hong et al., 2000; Hopker et al., 1999; Song et al., 1997). Furthermore, these investigations show that the downstream components, not the surface receptors may determine the final axonal responses to the Netrin cues (Hong et al., 2000; Hopker et al., 1999; Song et al., 1997). If these components such as the cAMP concentration were artificially changed, the same growth cone will respond differently to the same Netrin

gradient (Hong et al., 2000; Hopker et al., 1999; Song et al., 1997).

The recent characterization of *Drosophila* Dunc-115 has offered one possible downstream pathway of the Netrin guidance cue (Garcia and He, 2003).

Slit

Slit is a large diffusible protein that signals through the Roundabout (Robo) receptor (Nguyen Ba-Charvet et al., 1999; Nguyen-Ba-Charvet and Chedotal, 2002; Rao and Wu, 2000). It was first identified through a genetic screening in *Drosophila* for genes linked to the *roundabout* (*robo*) pathway (Kidd et al., 1998; Seeger et al., 1993; Kidd, 1999).

Characterization of Slit indicates that it is expressed at the midline, where it acts as a short-range repellent through the Robo receptor (Brose et al., 1999; Chan et al., 1996; Zinn and Sun, 1999). Two additional Slit receptors, Robo-2 and Robo-3, specify the lateral positions of axons that run parallel to the midline, presumably in response to long-range gradient of Slit activity diffusing away from the midline (Rajagopalan et al., 2000; Rajagopalan et al., 2000). Subsequent studies

have shown that the Robo/Slit pathway regulates midline axon guidance in an evolutionarily conserved manner across species (Battye et al., 1999; Van Vactor and Flanagan, 1999; Zinn and Sun, 1999). In vertebrates the Slit protein is also expressed in the CNS, and commissural axons are repelled by Slit after they have crossed the midline. In *slit* mutants, axons enter the midline but never leave (Battye et al., 1999; Kidd et al., 1999; Meyer, 1998).

All Slit proteins contain a putative signal peptide, four tandem arrays of leucine rich repeats (LRRs), a long stretch of EGF repeats, an Agrin-Laminin-Perlecan-Slit (ALPS) conserved spacer motif, and a cysteine knot. Mature Slit proteins lack any hydrophobic sequences that may function as a transmembrane domain, indicating that they are secreted proteins.

Extensive genetic and phenotypic analyses in *Drosophila* have provided a comprehensive understanding of the regulatory roles of Robo/Slit pathway in midline axon guidance. Robo appears to function as the "gatekeeper" by controlling midline crossing, where axons that never cross

the midline express a high level of the Robo receptor, while those that do cross have a low Robo expression (Flanagan and Van Vactor, 1998; Georgiou and Tear, 2002; Keleman et al., 2002)

In vertebrates, three Slit and two Robo orthologs have been identified at the developing ventral midline (Brose et al., 1999). Their expression pattern is consistent with a role in repulsive axon guidance at the midline.

Semaphorins

Semaphorins constitute another family of proteins important for mediating axonal pathfinding, fasciculation, branching, and synapse formation in a long-range chemorepulsive, or short-range contact-repulsive manner (Gavazzi, 2001; Kolodkin et al., 1997; Raper, 2000; Winberg et al., 1998). At least thirty semaphorin family members have been identified and subdivided into several classes based on the C-terminus structure of the proteins (Bashaw and Goodman, 1999; Chen et al., 2000).

Semaphorins signal through multimeric receptor complexes that are poorly understood, and almost all Semaphorin receptor complexes include a Plexin protein (Dickson, 2002; Tamagnone and Comoglio, 2000). Recently, Plexin receptors have been characterized in vertebrates and invertebrates that are capable of binding Semaphorins (Ohta et al., 1995; Winberg et al., 1998). Plexins form a large family of transmembrane proteins subclassified into four groups (A to D) based on sequence similarities (Tamagnone et al., 1999). To date, there are nine vertebrate and two invertebrate Plexin homologs that have been identified. Compelling evidence suggests that Plexins are receptors for perhaps all classes of Semaphorins, either alone or in combination with Neuropilins (Mueller, 1999).

Drosophila Plexin-A is a functional receptor for Sema-1a (Winberg et al., 1998), while vertebrate Plexin-As are functional receptors for secreted class 3 Semaphorins (Cheng et al., 2001). Furthermore, receptor complexes for vertebrate class 3 Semaphorins also include Neuropilins that do not have a signaling function, but are required for ligand binding.

Plexins may function as a signal transducer of Neuropilin-Sema III complexes, since Neuropilins have a very short cytoplasmic domain with no obvious signaling motifs and are dispensable for repulsive Semaphorin guidance (Yu and Kolodkin, 1999).

Genetic analysis of Semaphorin function in flies and mice suggests that they primarily act as short-range inhibitory cues that deflect axons away from inappropriate regions and guide them through repulsive corridors (Dickson, 2002; Raper, 2000). Preliminary evidence suggests that some Semaphorins may also act as attractive cues for certain axons, although this remains to be verified by genetic analysis (Bagnard et al., 1998; Song et al., 1998).

Ephrins

The search for graded guidance cues that could support Sperry's chemoaffinity hypothesis have led to the discovery of Ephrins, membrane bound ligands for the Eph family of receptor tyrosine kinases (Goodhill and Richards, 1999; Marin et al., 2001; Orike and Pini, 1996). Ephrins are

grouped into two structural classes, the Ephrin-A anchoring the membrane through the GPI linkage and the Ephrin-B with a typical transmembrane domain (Schmucker and Zipursky, 2001).

The receptors for the Ephrin ligands are members of the the Eph receptor tyrosine kinase (RTK) family, which contains at least thirteen members (Drescher et al., 1997; Wilkinson, 2001). The Eph receptors interacting with Ephrin-A and B are called EphA and EphB, respectively. Eph RTKs and their ligands Ephrins are involved in mediating axon guidance in the developing vertebrate and fly CNS (Dearborn et al., 2002; Drescher, 2002; Holder and Klein, 1999).

Eph receptors have an immunoglobulin (Ig) like domain, a cysteine-rich region and two fibronectin type III repeats in the extracellular portion, and a tyrosine kinase domain in the cytoplasmic region. Eph receptors have been isolated and characterized in both vertebrates and invertebrates, and share extensive structural similarities (Dearborn et al., 2002; Holder, 1999; Hornberger, 1999).

Several studies have shown that the Eph receptor/Ephrin signaling leads to collapse of the neuronal growth cone, suggesting that the Eph signaling pathway mediates axon guidance by inhibition (Brennan et al., 1997; Kennedy et al., 1994). Using an *in vitro* growth cone collapse stripe assay, it has been shown that class A Ephrins expressed in the tectum of mouse, chick and zebra fish cause growth cone collapse or repulsion (Mueller, 1999). Furthermore, growth cone collapse occurs when chick spinal motor neurons expressing EphA4 and EphB2 interact with class A and B Ephrins, respectively (Hornberger et al., 1999).

Eph receptors and Ephrins are important for the formation of topographic maps in the visual system of vertebrates (Birgbauer et al., 2000; Holder and Klein, 1999). Retinal ganglion cell (RGC) axons are guided to their appropriate targets in the optic tectum of the brain by a highly organized developmentally regulated process. Furthermore, retinal neurons express Eph kinase receptors in a gradient along the anterior-posterior axis. In the tectum, Ephrins are expressed in a complimentary gradient along the

anterior-posterior axis of the tectum. This gradient of Eph receptor expression in the developing retina and its repulsive ligand in target tectum is required for appropriate wiring of the visual system (Figure 1C) (Flanagan and Vanderhaeghen, 1998; Goodhill and Richards, 1999; Marin et al., 2001; Tessier-Lavigne, 1995).

Retinal axons with successively higher Eph levels map to successively lower points along the ephrin gradient. *In vivo* and *in vitro* analyses suggest that Ephrin-A2 is repulsive for temporal axons while Ephrin-A5 is repulsive for both temporal and nasal axons (Birgbauer et al., 2000; Hornberger et al., 1999). Both Ephrins are expressed in an anterior-posterior gradient in the tectum, with maximal expression in the posterior, suggesting a role for Eph signaling in establishing appropriate connections in the retinotectal system. Strong evidence suggests that temporal axons with a high level of EphA3 receptors are repelled by Ephrin-A2 and are prevented from entering the posterior tectum, whereas nasal axons with low EphA3 receptor levels are permitted to

cross the Ephrin-A2 gradient and to innervate the posterior region.

A *Drosophila* member of the Eph receptor tyrosine kinase family, EPH, has been isolated and characterized (Dearborn et al., 2002). The *Drosophila* EPH has a high degree of similarity to its vertebrate homologs, indicating a possible conservation in its function. Indeed, the EPH expression in *Drosophila* is required for precise neuronal connectivity between photoreceptor axons and their retinotopic targets in the brain. Thus, as in vertebrates, topographic map formation in the visual system of *Drosophila* requires the activity of Eph receptor kinases in guidance of axonal growth cones.

1.4 Intracellular Signaling Pathways and the Cytoskeleton

Understanding the role of growth cone receptors and their extracellular guidance cues accounts for the turning behavior of the growth cone and its axon during pathfinding, but does not account for the intracellular signaling mechanism that underlies the changes in the growth cone orientation and

shape (Korey and Van Vactor, 2000). It is clear that these extracellular signals must be relayed through a network of intracellular signaling proteins that coordinate responses to the environment that ultimately regulate the growth cone cytoskeleton. Members of the small GTPases have been shown to play a critical role in conveying signals to the cytoskeleton (Bateman and Van Vactor, 2001).

1.4a Small GTPase Proteins

Small GTPase proteins are monomeric G-proteins with molecular masses of 20-40 kDa that have an intrinsic GTPase activity (Ross and Wilkie, 2000). They can exist in an inactive GDP-bound and active GTP-bound form, and are interconvertible by GDP/GTP exchange and GTPase reactions (Figure 1D) (Hall, 1994; Liao et al., 1999; Molnar et al., 2001).

To date, more than 100 small GTPases have been identified in eukaryotes from yeast to human, forming at least five families: the Ras, Rho, Rab, Sar1/Arf, and Ran families (Takai et al., 2001). The functions of many GTPases have recently been elucidated: the Ras subfamily primarily regulates gene expression, while the Rho/Rac/Cdc42 of the

Rho family regulate both cytoskeletal reorganization and gene expression, and the Rab and Sar1/Arf family members mediate intracellular vesicle trafficking. The Ran family on the other hand is involved in the nucleocytoplasmic transport during the G1, S, G2 phases of the cell cycle and microtubule organization during the M phase (Takai et al., 2001).

Acting as molecular switches, the GTPases have two interconvertible forms, GDP-bound inactive and GTP-bound active form. An upstream signal stimulates the dissociation of GDP from the GDP-bound form, which is followed by the binding of GTP, eventually leading to the conformational change of the downstream effector-binding region so that this region interacts with the downstream effector(s) (Gao et al., 2001; Liao et al., 1999). The GTP bound form is converted to the GDP bound form by the intrinsic GTPase activity, this GDP bound form then releases the bound downstream effector(s). In this manner, one cycle of activation and inactivation is achieved. Numerous proteins affecting the GTPase activity, nucleotide exchange rates and membrane localization of the G-protein superfamily members have now

been identified (Mueller, 1999; Ross and Wilkie, 2000; Takai et al., 2001).

1.4b Regulators of GTPase Activity

Activity of the GTPases and their roles are modulated by regulators and effectors that are 10-15 times larger and are often modular structures containing several different types of functional domains capable of interacting with an intricate network of cellular enzymes and structures (Gao et al., 2001; Liao et al., 1999; Mueller, 1999; Ross and Wilkie, 2000). The current biochemical model regarding the regulation of GTPase activity has three key players: guanine nucleotide exchange factors (GEFs), GTPase activating proteins (GAPs), and guanine nucleotide dissociation inhibitors (GDI) (Takai et al., 2001).

These regulators modulate the activity of the G-proteins by regulating GDP/GTP exchange. The rate-limiting step of the GDP/GTP exchange reaction is the dissociation of GDP from the GDP-bound form (Bourne et al., 1990; Takai et al., 1992). This reaction is extremely slow and is stimulated by GEFs. The GTPase activity of each small G-protein is variable

but relatively slow and stimulated by GAPs (Figure 1D). Finally, the GDP/GTP exchange reactions of Rho/Rac/Cdc42 and Rab proteins are further regulated by GDIs that inhibit both the basal and GEF-stimulated dissociation of GDP from the GDP bound form, and keep the GTPase in the inactive GDP bound form.

The importance of the regulators of GTPase activity is reflected by their ability to regulate a wide range of essential intracellular biochemical pathways in all eukaryotic cells. The number of GEFs, GAPs and GDIs clearly exceed the number of GTPases. While the reasons remain speculative, it is likely to reflect, in part, the ability of a single stimulus to activate different subsets of GTPases depending on the cell type and the biological context (Takai et al., 2001).

Guanine Nucleotide Exchange Factors (GEFs)

GEFs are proteins that function upstream of the small GTPases and activate them by catalyzing the exchange of GDP to GTP. GEFs first associate with the GDP-bound form of the GTPase, and GDP then dissociates from this complex at an increased rate, leaving the GEF bound to the empty

GTPase in the absence of nucleotide (Liao et al., 1999). GTP then binds immediately, prompting GEF dissociation and leaving the GTPase in the active form (Figure 1E).

GTPase-Activating Proteins (GAPs)

GAP members negatively regulate GTPases by stimulating the hydrolysis of GTP to GDP (Itoh et al., 2002). GAPs function downstream of the GTPases and assist GTPases to overcome their very low intrinsic GTPase activity (Figure 1D).

Guanine Nucleotide Dissociation Inhibitors (GDIs)

GDIs affect the rate of GDP dissociation from GTPases Rho/Rac/Cdc42 and Rab proteins by inhibiting GDP/GTP exchange. Therefore these molecules prevent GEF activation of the GTPases (Araki et al., 1991; Ueda et al., 1990).

1.5 Rho GTPases Regulators of the Cytoskeleton

Rho GTPases comprise a large subfamily of the Ras-superfamily of GTPases. Among all Rho GTPases, Rac1 (Ras-related C3 botulism toxin substrate 1), Cdc42 (cell division cycle 42) and Rho A (Ras homologous member A) have been most extensively studied (Boettner and Aelst, 2002). At least 10 members of the Rho subfamily are known in mammals:

RhoA-E, RhoG, Rac1 and Cdc42, and TC10, and they share more than 50% sequence identity (Bar-Sagi and Hall, 2000).

Like other GTP-binding proteins, the Rho family GTPases exhibit both GDP/GTP-binding and GTPase activities. The role of the Rho GTPase signaling is pivotal for a plethora of biological processes, but their role in the regulation of the actin cytoskeleton and cell adhesion has been best characterized (Hall, 1998; Mueller, 1999). Insight into the role of the Rho GTPases on the regulation of cytoskeletal processes such as cytokinesis, cell motility, and neurite retraction has attracted particular attention. Current work will undoubtedly identify new molecules and regulatory roles of the Rho GTPases. (Kaibuchi et al., 1999).

Functionally, the GTPases Rho/Rac/Cdc42 are responsible for generating distinct actin-containing structures that regulate the dynamic morphological changes of the growth cone (Symons and Settleman, 2000). Rho proteins regulate formation of stress fibers, which are elongated actin bundles that traverse the cells and promote cell attachment to the extracellular matrix through focal

adhesions (Bateman and Van Vactor, 2001; Brand and Perrimon, 1993; Kozma et al., 1995). Rac proteins regulate the formation of lamellipodia and membrane ruffles, curtain like extensions that form at the leading edge of the growth cone between the filopodia (Ridley and Hall, 1992; Ridley et al., 1992). Activated Cdc42 regulates formation of filopodia, the thin spike like projections that define the leading edge of the growth cone and are at the forefront of the axon projection (Kozma et al., 1995).

Molecules that Interact with Rho Family GTPases.

GEFs for the Rho family GTPases share a common sequence motif Dbl-homology (DH) in the central region of the protein and a conserved amino acid sequence that is the main site of GDP/GTP exchange activity (Cerione and Zheng, 1996; Kaibuchi et al., 1999). Many Dbl GEFs also contain other protein-protein interaction domains, which allow GTPases to be activated in specific signal transduction pathways (Bateman and Van Vactor, 2001). Recently, completed genome sequencing projects have revealed that there are at least three Dbl family GEFs in *Saccharomyces*

cerevisiae, 18 in *Caenorhabditis elegans*, 23 in *Drosophila melanogaster* and 46 in *Homo sapiens* (Zheng, 2001).

The molecular pathway between Dbl family GEFs and Rho GTPases was further strengthened with the identification of the Trio family, which relays extracellular cues to the actin cytoskeleton (Bateman and Van Vactor, 2001).

The Trio Family

Human trio was first identified in a yeast interaction screen using the intracellular domain of the receptor-like tyrosine phosphatase (RPTP) LAR (leukocyte-antigen-related protein) as bait (Debant et al., 1996). LAR family of RPTP are receptors that convey extracellular cues to the actin cytoskeleton during development. An independent yeast interaction screen using the Huntingtin-Associated Protein (HAP1) as bait hooked kalirin, a molecule with a full length structure nearly identical to Trio (Colomer et al., 1997). Whereas Trio is expressed at moderate levels in all tissues, kalirin expression is specific to the central nervous system in adult rats (Bateman and Van Vactor, 2001).

Data from other model genetic systems have begun to shed light on potential roles of Trio signaling during development. The *C. elegans* Trio homolog Unc-73 has been found to regulate actin structure and movement by activating the Rho GTPase Rac. Furthermore, disruption of the Dbl domain of Unc-73 results in multiple axon guidance defects, indicating the importance of the Dbl domain on axon guidance (Steven et al., 1998). *In vitro* analysis of Trio function upstream of Rho GTPases confirms that Trio is required for mediating cytoskeletal rearrangements required for appropriate axon pathfinding (Bellanger et al., 1998; Bellanger et al., 1998). Recently, *Drosophila* Trio and its regulatory role upstream of Rho GTPases have been shown to be required for the guidance of neurites to their appropriate targets in the developing CNS (Awasaki et al., 2000; Bateman et al., 2000; Liebl et al., 2000). As in worms, *Drosophila* Trio is expressed throughout the developing embryo, and high levels are observed in nervous system. Mutations in *Drosophila* Trio produce pleiotropic axonal phenotypes in both the embryonic nervous system and retinal axon

projections (Bateman et al., 2000; Newsome et al., 2000). These defects are similar to those observed in Unc-73 mutants, suggesting some conservation of cellular functions (Bateman and Van Vactor, 2001).

Data from the *Drosophila* visual system have indicated that Trio acts upstream of the GTPase Rac/Cdc42 to activate the serine/threonine kinase Pak (p21-activated kinases) (Newsome et al., 2000). Furthermore, Pak kinase activity is restricted to specific spatial domains within the growth cone by Dock, thereby promoting directed axon extensions. Pak in turn regulates LIM kinase and myosin light chain kinase that control actin dynamics via their substrates cofilin and myosin light chain (Desai et al., 1999; Garrity et al., 1996; Hing et al., 1999). Together, the current genetic and biochemical data support the current model of a signal transduction pathway from Trio to Rac/Cdc42 to Pak that plays an essential role in photoreceptor axon guidance (Hing et al., 1999; Newsome et al., 2000).

Although it has been clear for some time that Rho family GTPases play a central role in the orchestration of

cytoskeletal assembly, our understanding of the components that regulate these important molecules is far more primitive. Functional analysis of the Trio family of proteins in a number of model systems has elucidated its role in neuronal cell migration. Current studies of the Trio molecule suggest that Trio proteins function as integrators of upstream pathways and as activators of multiple downstream pathways.

Although we have a good framework of molecules and their roles in regulating axon guidance, it remains unclear how these mechanisms regulate precise neuronal connectivity in the brain. My dissertation project was intended to broaden our understanding of axonal pathfinding using the developing visual system of *Drosophila* as a model.

1.6 Drosophila as an Experimental Model

Drosophila melanogaster is a well established genetic model for studying *in vivo* functions of genes (Rubin, 1988; Rubin and Lewis, 2000). The amenability of genetic, molecular and cellular techniques in this system makes it especially useful. Furthermore, the high level of conservation across species has extended the understanding obtained from

Drosophila to other systems including humans. For example, out of the 256 human disease causing genes identified, 177 have fly homologs (Kornberg and Krasnow, 2000).

These tools coupled with the recent genome sequence of the fruit fly heralds a new era of gene hunting, exploration, and analysis (Adams et al., 2000).

1.6a *Drosophila* Visual System Development

The visual system of *Drosophila* is an excellent model for identifying and investigating genes that are required for topographic map formation (Clandinin and Zipursky, 2002; Kunes and Steller, 1993; Martin et al., 1995; Newsome et al., 2000). It consists of the compound eyes and the optic lobes that are the visual-processing centers of the brain. The compound eye has approximately 800 identical ommatidia that are organized in a crystal-like array (Figure 1F). Each ommatidium contains exactly twenty cells: eight of which are photoreceptor neurons (R-cells) whose axons project as a bundled fascicle through the optic stalk to distinct ganglion layers of the brain (Cohen, 1993). The patterns of neuronal

connections in the fly visual system are precise, complex, and well characterized.

The stereotyped arrangement of cell types in the ommatidia are generated during the third and final stage of larval development and the early pupal stage. Cell fate determination and patterning begin at the posterior margin of the eye imaginal disc. The onset of pattern formation occurs at a morphological indentation in the eye imaginal disc called the morphogenetic furrow that sweeps across the eye disc in a posterior to anterior direction (Cohen, 1993). Posterior to the morphogenetic furrow, the regular spacing of ommatidial units has been established and the photoreceptor cell fate determined, while anterior to the morphogenetic furrow lies a pool of undifferentiated unpatterned cells. Hence, the morphogenetic furrow demarcates the boundary between the posterior patterned ommatidia and the anterior unpatterned cells.

The establishment of a topographic map in which R-cells in adjacent ommatidia project to adjacent targets largely reflects the intimate relationship between R-cell and target

development. R-cells posterior to the morphogenetic furrow express Hedgehog (HH), a signal that is required for anterior cells of the morphogenetic furrow to enter the pathway of photoreceptor cell determination. R-cells also express the epidermal growth factor receptor (EGFR) and the ligand Spitz (SPI), a signal for ommatidial assembly in the compound eye (Huang and Kunes, 1996; Huang et al., 1998).

The expression of HH and SPI by R-cells posterior to the morphogenetic furrow is required for R-cell recruitment and patterning at the anterior edge of the furrow. The wave of morphogenesis in the eye disc is translated into a wave of R-cell axon innervation of the optic lobe (Huang and Kunes, 1996; Huang et al., 1998). R-cell axons innervating the optic lobe deliver HH, a signal that induces the postsynaptic precursor cells to express the EGFR. Subsequent to the delivery of HH, retinal axons deliver the EGFR ligand SPI that is an essential cue for neuronal differentiation in the brain. SPI is required for the establishment of a five cell synaptic cartridge unit in the brain that will be innervated by incoming R-cell axons projecting from a single ommatidium

(Huang and Kunes, 1998; Huang et al., 1998). Hence, the sequential action of HH and SPI in R-cell bodies and subsequently in their axonal processes orchestrates the assembly of the interconnected arrays of afferent neurons and their targets in the fly visual system (Garrity et al., 1999; Huang and Kunes, 1998; Martin et al., 1995; Newsome et al., 2000). As a result, the projection of R-cell axons to their targets in the developing brain has a one-to-one topographical correspondence to their original positions in the eye imaginal disc (Figure 1G) (Clandin and Zipursky, 2002).

My project was designed to identify and characterize new molecular components involved in the construction of the visual system in *Drosophila*. Specifically, I wanted to further our understanding of how retinal axons find their way to the targets in the brain. It is our expectation that results from this study will be informative for understanding far more complex systems including those in humans.

Chapter 2

Materials and Methods

Drosophila Husbandry

Drosophila melanogaster stocks were grown on standard medium. Stocks were maintained at 25°C or at 18°C. Fly stocks were flipped into a new vial every 14-17 days if reared at 25°C, and every 30 days if being reared at 18°C. Heat shock strains were maintained at 18°C to prevent the induction of the heat shock protein.

Fly Food Medium

Recipe for approximately 100 vials or 25 bottles of fly medium:

Water	1250 milliliters
Dextrose	162 grams
Cornmeal	77 grams
Yeast Extract	41 grams
Fly Agar	12 grams
25% Tegosept	13 milliliters

The 25% stock of the antifungicide Tegosept was prepared by dissolving 25 g into a final volume of 100 ml of 200 proof ethanol.

To cook the food dissolve the dextrose in water, add the cornmeal, yeast extract and fly agar. Boil with regular stirring for 10 minutes. After cooking allow to cool and mix in the 25% tegosept. Pour vials or bottles and allow hardening. Prior to addition of flies several grains of dry yeast were placed on the surface of the food.

G418-Neomyocin Selective Medium

A 0.6 mg/ml final concentration of G418 media was used for selection of neomyocin resistant animals. To 99 ml of standard medium add 1 ml of 60 mg/ml G418 stock.

Embryo Collection Medium

Grape-juice plates containing Bacto-agar, dextrose, sucrose and Torumel yeast were prepared following standard protocol. Plates were coated with yeast paste prior to use for egg collection.

Fly Strains

yw; 137-20 P w+ (26C)/y^+ *CyO*

yw; EP-388 P/ y^+ *CyO*

yw; Gla/ y^+ *CyO*

w; P [neo; FRT] (40A)/*CyO*

y, hsFLP122; arm-*lacZ* P [neoR; FRT] (40A)/*CyO*

p[Gef26+]A2 (homo/hemizygous, on the X); KM5/*CyO*; TM3

KM5/SM6a, *CyO*, Tb (Tb is translocated from 3)

KM5/SM6a, *CyO*, Tb (Tb is translocated from 3)

KM61/SM6a, *CyO*, Tb Gef Deletion

Selection of Virgin Females

Flies were put to sleep on a collection pad with bone dry CO_2 gas diffusing from the bottom of the pad to the surface. Virgin females were collected twice a day. Newly hatched animals were identified by a large clear abdomen

with the presence of a dark spot. Females were separated from males by using a stereomicroscope to identify appropriate genitalia and lack of sex-combs on the front limbs (Ashburner, 1989).

Third Instar Visual System Dissection

The preparation and staining of the late third instar visual systems were conducted as described in He, 2000 (He, 2000). Typically, third instar brains were dissected in 1X phosphate-buffered saline (PBS) using two forceps one to hold the posterior region of the larvae firmly, the second for pulling on the mouth-hooks which were removed with the eye discs and brain attached. Brains were fixed in 4% paraformaldehyde and stained with appropriate antibody overnight at 4°C.

Immunohistochemistry

Fixed visual systems were washed with 1X PBS/Tween (PBT) and blocked with 10% goat serum to block nonspecific staining. Brains were incubated overnight at 4°C in a 1:4 dilution of primary mouse monoclonal antibody 24B10 in

10% goat serum which stains all photoreceptor neurons and with a 1:75 dilution of anti-horseradish peroxidase (HRP) conjugated to fluorescent FITC to label all neurons green. After first antibody incubation tissue was washed 4 times with PBT at room temperature, and then blocked with 10% goat serum for 1 hour at room temperature.

Brains were then incubated overnight at 4°C in a 1:50 dilution of the secondary antibody goat anti-mouse conjugated to the fluorescent dye CY3 (which fluoresces red) in 10% goat serum, and with a 1:50 dilution of anti-HRP conjugated to FITC (which fluoresces green) in 10% goat serum. Stained brains were washed 5 times with PBT over 2 hours. Stained brains were then put through a glycerol series until final treatment with 70% glycerol containing anti-quenching agent prior to mounting for confocal microscopy.

Confocal Microscopy

A Nikon PCM-2000 confocal microscope equipped with dual HeNe-Argon lasers was used. The scope has a FITC

filter set and power stage control, and is operated by Simple-32 software.

Genetic Screening

A large pool of pupal lethal mutants generated by a single P-element insertion on the second chromosome as described in Torok et al. 1993 was screened for developmental defects (Torok et al., 1993). Third instar larval visual systems were collected from these animals, and fluorescently stained with the mature neuronal marker anti-HRP and the R-cell specific neuronal marker 24B10. Confocal microscopy was used for identifying mutants with aberrant neuronal connectivity between photoreceptor R-cell axons and their appropriate targets in the brain.

Genomic DNA Extraction

Approximately 50 animals of both sexes were homogenized in 500 µl of denaturing buffer (100 mM Tris-HCl, 0.1 M EDTA, 1% SDS, 1% DEPC). Subsequently, 14 µl of 8 M KAc was added to every 100 µl of homogenate. The homogenate was then chilled on ice for 1 hour and centrifuged at 6,000 RPM. The supernatant was collected

and a phenol/chloroform extraction was performed. Genomic DNA was then precipitated with isopropanol followed by resuspension in Tris-EDTA (TE) buffer.

Rescuing the P-element and Flanking Genomic DNA

The P-element is a powerful tool that is well suited for rescuing genomic DNA flanking the site of insertion. Genomic DNAs flanking the left and right side of the P-element insertion were rescued by using the appropriate restriction enzyme (Figure 5A). Genomic DNA was digested with a single enzyme according to standard protocol, and circularized using ligase. Circularized DNA was transformed into competent *E. coli* cells using electroporation. Transformants carrying the P-element and flanking genomic sequence were identified by plating on selective NZCYM (Sigma) plates containing 0.07 mg/ml of ampicillin.

Rescuing Flanking Genomic DNA

P-element rescued transformants capable of growing on ampicillin media were cultured overnight in 6 ml of NZCYM media containing a final concentration of 0.01 μg/ml of ampicillin. Cells were collected by centrifugation at

3,000 RPM for 2 minutes and plasmid was extracted using the Qiagen mini-prep protocol. Purified plasmid was digested using the restriction enzyme *HindIII* which cuts off the P-element from the flanking genomic DNA, and also cuts any internal *HindIII* sites of the genomic DNA sequence. Restriction digests were separated on a 1% agarose gel by electrophoresis. All bands were gel purified (using Qiagen gel purification kit) and genomic DNA flanked by *HindIII* cohesive ends were subcloned into the p-Bluescript vector (Figure 5B).

Restriction Endonuclease Digestion

All restriction digestion reactions contained clean DNA, 5 units of enzyme for every 25 µl reaction, and a final concentration of 1X buffer optimized for the specific restriction enzyme. The reaction was incubated at 37°C for 1 hour.

DNA Agarose Gel Electrophoresis

1-2% agarose gels containing ethidium bromide for visualization were cast following standard protocol. All gels

included a 1 kb standard and were run in 1X Tris-EDTA buffer at 100 volts.

Gel Extraction

The Qiagen QIAEX II DNA extraction kit for agarose gels was used to extract and purify DNA. The agarose gel was dissolved in QX-1 buffer (Tris-acetate/EDTA buffer) as outlined by the standard protocol at 50°C. The DNA was then bound to QIAEX II silica particles in the presence of high salt, and the silica beads with the attached DNA was washed with PE buffer prior to elution of DNA with water. A phenol/chloroform DNA extraction following each DNA plasmid preparation was performed to insure the highest quality of DNA possible.

Generation of Recombinant Plasmid

The pBluescript II SK (+) a 2961-bp phagemid derived from pUC19 was the vector used to subclone rescued genomic DNA and RT-PCR (reverse transcriptase–polymerase chain reaction) products (Figure 5B). All pBluescript plasmid was predigested with a single restriction enzyme that cuts only once at the polycloning

site that lies in a functional l*ac-Z* gene, and was treated with Calf Intestinal Alkaline Phosphatase (CIAP) to reduce the background of nonrecombinants. The DNA to be inserted into pBluescript contained complementary cohesive ends complementary to the cut pBluescript plasmid. A ligation reaction included 175 µl of resuspended DNA insert, 20 µl of 10X ligation buffer, 1 µl of concentrated digested pBluescript plasmid, 2 µl of 0.5 u/µl T-4 ligase, and 2 µl of 0.2 M ATP. The 200 µl reaction was incubated overnight at 18°C. DNA was cleaned with a phenol/chloroform extraction, and resuspended in 200 µl of TE buffer, and precipitated with 20 µl of 3.0 M NaAc and 480 µl of 200 proof ethanol at -75°C.

Bacterial Transformation

Stratagene *E. coli* electroporatable XL1-Blue competent cells deficient in all restriction enzyme systems and sensitive to ampicillin were used. Dry plasmid pellet was resuspended in 3 µl of water and 40 µl of competent cells were added and chilled on ice for 5 minutes. Cells were

transferred to BioRad electroporation cuvette and shocked with 1.8 KV using BioRad *E. coli* Gene Pulser. 960 µl of SOC medium was then added to the cuvette and incubated at 37°C for one hour with shaking prior to plating.

Blue/White Selection of Recombinant pBluescript Plasmid

Selection of transformants was performed by plating on NZCYM plates containing 0.07 mg/ml of ampicillin. For blue/white selection isopropylthio-β-D-galactosidase (IPTG) and 5-bromo-4-chloro-3-indolyl-β-D-galactosidase (X-Gal) were spread on the Amp+ plate prior to spreading of transformants. Transformants bearing a recombinant plasmid have a disrupted *lac-Z* gene and are therefore white instead of blue.

Plasmid Extraction

The Qiagen QIAprep Miniprep kit based on the alkaline lysis of bacterial cells followed by adsorption of DNA onto silica in the presence of high salts was used. The procedure consists of the three standard steps: 1) preparation and clearing of bacterial lysate, 2) adsorption of DNA onto the

QIAprep membrane, 3) washing and elution of the plasmid DNA. Bacteria are lysed under alkaline conditions, and the lysate subsequently neutralized and adjusted to high-salt binding conditions for purification on the QIAprep silica-gel mini-prep column. Plasmid was washed with a high salt buffer and was then eluted using 10 mM Tris-Cl, pH 8.5. A 3 ml overnight culture would yield from 10-20 μg of high quality purified plasmid.

Radioactive Labeling of Probes

DNA template was subcloned into the pBluescript polycloning site which is flanked by the forward T3 and reverse T7 primer sequence. A 50 μl reaction was prepared by mixing in a 500 μl micro-centrifuge tube 2 μg of DNA dissolved in 21.5 μl of distilled deionized H_2O (ddH_2O), 5 μl of 10X reaction buffer, 5 μl of 25 mM $MgCl_2$, 1 μl each of 10 mM dATP/dGTP/dTTP, 1 μl of 1 mM dCTP, 10 μl of 3000 Ci/mmol (alpha-^{32}P) dCTP, 2 μl of 10 μM forward primer, 2 μl of 10 μM reverse primer, and 0.5 μl of 5 u/μl DNA

polymerase. To prevent possible evaporation during PCR cycles, the reaction was topped with 25 µl of mineral oil.

Thirty five cycles of the following PCR program was used: denaturing at 94°C for 1 minute, annealing of primer at 50°C for 2 minutes, and chain extension at 72°C for 2 minutes.

cDNA Library Screeining

A Harvard eye disc (HED) and Berkeley eye disc (BED) phage-lambda cDNA libraries were screened. The HED library was plated using C600-hfl *E. coli* cells and the BED library plated using LE-392 *E. coli* cells. Cells were grown in NZCYM medium containing a final concentration of 0.2% maltose. Cells were collected and resuspended in 0.01 M $MgSO_4$ to a final concentration of $1.6X10^9$ cells/ml. 100 µl of cells were mixed with 100 µl of phage suspended in suspension medium (SM). Infected cells were mixed with 3 ml of top agarose which was then poured onto a 150 mm NZCYM agar plate. The plates were incubated overnight at 37°C which allowed the growth of an even bacterial cell lawn disrupted by clear isolated plaques. Plaques were then lifted

onto a nitrocellulose filter and subsequently the filter was treated with denaturing solution (0.5 N NaOH, 1.5 M NaCl) and then transferred to neutralizing solution (1.5 M NaCl, 0.5 M Tris-Cl pH 7.4). Filters were washed in 2X SSC, dried and baked at 80°C for 2 hours (Sambrook et al., 1989).

A genomic ^{32}P labeled denatured PCR probe was incubated with the filters overnight at 42°C in hybridization solution (6X SSPE, 0.05X Blotto, 50% Formamide). Filters were washed with 2X SSC and dried prior to overnight exposure to X-ray film with intensifying screen at -75°C.

Positive plaques were cut and suspended in SM medium and amplified following a similar plating protocol (Sambrook et al., 1989).

RNA Extraction

Approximately 250 µl of intact animals were homogenized in 1.5 ml of RNAWiz (Ambion Kit). The lysate was mixed with chloroform and centrifuged causing the homogenate to separate into 3 phases. The RNA was then precipitated from the aqueous phase following standard Ambion protocol.

Generation of cDNA

An RT-PCR approach was used to generate double stranded cDNA. Only poly-adenylated mRNA from 2 μg of total RNA was reverse transcribed using the primer oligo$(dT)_{18}$ and the enzyme reverse transcriptase. The cDNA generated serves as a template in the PCR reaction. The PCR reaction included the cDNA, dNTPs, buffer, $MgCl_2$, Taq DNA polymerase, and a set of primers specific for *dizzy*. The cDNA was amplified using the following cycle program. The first PCR cycle begins with denaturation of the template at 94°C for 1 minute, annealing of primers at 67°C for 2 minutes and extension at 72°C for 2 minutes. After every 2 cycles the annealing temperature is decreased by 2°C, until the completion of 35 cycles.

Northern Blot

Ambion's NorthernMax kit was used for Northern analysis. 30 μg of total RNA per lane, and Sigma 0.2 - 10 kb marker was separated by electrophoresis in a 1% agarose denaturing formaldehyde gel in 1X MOPS buffer. The RNA was transferred from the denaturing agarose gel to a

positively charged nylon membrane following the manufacturers downward transfer protocol using transfer buffer for 2 hours. The membrane was baked at 80°C for 15 minutes to crosslink the RNA to the positively charged membrane. Denatured double stranded ^{32}P labeled PCR probe was hybridized over-night at 68°C to the membrane in 10 ml of ULTRAhyb per 100 cm^2 of membrane. The membrane was washed with low stringency buffer at 42°C, dried at room temperature and exposed to autoradiographic film with an intensifying screen at -75°C overnight.

Bioinformatics

A fly BLAST search of The National Center for Biotechnology Information (NCBI) genomic data base with the genomic DNA sequence flanking the *dizzy* P-element mapped the precise insertion of the P-element to the left arm of chromosome 2 position 26C 2-3 (http://www.ncbi.nlm.nih.gov).

A GeneScene search (FlyBase) for annotated cDNA sequences located adjacent to the P-element insertion at

position 26C 2-3 led to the identification of a putative cDNA CG9491 (flybase.bio.indiana.edu).

The annotated sequence was used to identify an Expressed Sequence Tag (EST) clone (AT08279) which was obtained from Berkeley *Drosophila* Genome Project. The EST was sequenced and mapped to the 3'-end of the predicted cDNA using the alignment program GCG. The upstream putative sequence was used to design three sets of overlapping upstream primers for RT-PCR (Figure 5D).

The sequence for the three primer sets are:

Set 1
forward primer
(GefAS): 5'-GCCAAGCTTATGGATCCGTATCACCATA

reverse primer
(Gef 2): 5'-CGGAAGCTTCGACCAGCTGCTGTAGCA

Set 2
forward primer
(Gef B): 5'-GCCAGCTTATCCGCGGTACTCCAG

reverse primer
(Gef D): 5'-CCGCAAAGCTTATTCGC

Set 3
forward primer
(Gef C): 5'-GCCAAGCTTCTCGCTATGCGAAGTG

reverse primer

(Gef E): 5'-GCCAAGCTTGCTCTGCGATGCAGAC

Assembly of the RT-PCR sequence and EST sequence was performed using GCG. Using this program the start and stop codons were identified.

Generation of Mosaics

Mosaic animals were generated using the yeast 2-μm plasmid site specific recombinase (FLP) that catalyses recombination between the FLP recombination targets (FRTs) (Golic and Lindquist, 1989). The FRT was inserted into the desired chromosome between the *dizzy* P-insertion and the centromere of the right arm of chromosome 2. Somatic homozygous clones were generated in the eyes of adults by regulating the expression of the recombinase FLP by heat shock. Embryos were collected and heat shocked at 38°C for 30 minutes. The heat shocked embryos were then returned to 25°C to develop into adults. The visual system of these adult animals were screened for homozygous mutant patches (Figure 4D).

DNA Sequencing

The T7 Sequenase chain-termination DNA sequencing method was used (Amersham version 2.0 DNA sequencing kit). All DNA sequenced was subcloned into the pBluescript II SK vector. The DNA synthesis was carried out in two steps. The first was the labeling step in which the primer is extended using limiting concentrations of the deoxynucleoside triphosphates, including radioactively labeled dCTP. In the second step, the concentration of all the deoxynucleoside triphosphates was increased and a chain-terminating nucleotide analog is added. Four separate PCR chain termination reactions each with a different 2',3'-dideoxynucleoside-5'-triphosphate (ddNTP) were performed using the same primer and template. The reactions were loaded onto a polyacrylamide urea denaturing gel. The gel was run at 200 V for four hours, fixed, and dried on blot paper. The dried gel was then exposed overnight to hypersensitive film at room temperature, developed, and sequence read (Sambrook, 1989).

In Situ Hybridization - Embryo Preparation

Embryos were collected every 4 hours from grape-juice agar plates and were rinsed with ddH_2O. Embryos were dechorianated with 50% sodium hypochlorite (commercial bleach) for 3 minutes. Embryos were then washed with ddH_2O and mixed gently in a test tube containing 1 ml of heptane and 1 ml of 4% paraformaldehyde which separates into two phases.

The top layer is heptane, the bottom layer 4% paraformaldehyde, and the embryos are found in the interface. The aqueous bottom layer was removed and 1 ml of methanol added to the heptane and embryos, which after gentle agitation caused the vitelline membrane to split. Vitelline membrane remains in the interphase while the devitellinized embryos fall to the bottom of the test tube. Devitellinized embryos were then rehydrated with PBT and post fixed in 4% paraformaldehyde and PBT. Embryos were incubated for 5 minutes in 1 ml of PBT with 20 μg of proteinase K. Embryos were then rinsed 4 times with PBT,

and were fixed in 4% formaldehyde for 20 minutes with rocking prior to four PBT washes.

In Situ Hybridization - Visual System Preparation

Brains were dissected in 1X PBS and transferred to 4% formaldehyde/PBS containing 0.6% Triton-X-100 at room temperature for 20 minutes. Tissue was washed with 1X PBS/Triton 3 times and incubated for 5 minutes in 1 ml of PBT with 20 μg of proteinase K. Brains were washed four times with PBT.

DIG Labeling of RNA _In-Situ_ Probe

The CG9491 EST clone that mapped to the 3' end of the *dizzy* sequence was used as a template to generate sense and anti-sense single stranded RNA probes. The 3' cDNA sequence was flanked by the restriction sites *EcoRI* and *XhoI* allowing directional insertion into the pOTB7 vector (Figure 4A). To generate the RNA single stranded digoxigenin (DIG) labeled probes the plasmid was linearized by single enzyme digestion and used as a template with the appropriate RNA polymerase in an *in vitro* reverse transcription reaction. Sp6 RNA polymerase was used with

XhoI cut plasmid to generate a sense DIG labeled single stranded RNA probe that was used as a negative *in situ* hybridization probe. T7 RNA polymerase was used with *EcoRI* cut plasmid to generate an anti-sense DIG labeled single stranded RNA probe that was used as a positive *in situ* hybridization probe.

In Situ Probe Hybridization and Detection

The specimens were hybridized overnight with the DIG-labeled single stranded RNA probe, followed by washing with PBS/Tween for 20 minutes five times. They were then incubated for 1 hour at room temperature with anti-DIG antibody (1:5000 solution in PBS Tween), and washed with PBS/Tween and then 3 times with levamisole. Antibody labeling was detected by adding 4.5 µl of NBT and 3.5 µl of X-Phosphate with 1 ml of levamisole. The reaction was terminated after 10 minutes with PBT and then tissue was mounted in 80% glycerol for light microscopy analysis.

Chapter 3

Identification and Characterization of Mutant *dizzy*

Introduction

One important step in elucidating the mechanisms required for precise topographic neuronal connectivity is to identify the relevant candidate genes. Using a forward genetics approach, we have identified from a large scale screen several lethal mutants with aberrant neuronal connectivity in the *Drosophila* visual system. We chose to screen larval and pupal lethal mutants, a typical approach used to identify genes essential for the visual system development. One of the mutants identified is the gene we called *dizzy*, a gene on the second chromosome essential for R-cell connectivity (Bottalico et al., 2003).

Genetic Screening

Second Chromosome P-element Mutants

All mutants screened were generated by the insertion of a single P-element (*P-lacW*) into the second chromosome of *yw* animals (Torok et al., 1993). P-elements are transposable segments of DNA flanked by inverted repeats

that are targeted by the enzyme transposase which can mobilize the P-element to move throughout the genome and insert it into a new position. The insertion of the P-element in the 5'-untranslated region (where the regulatory elements of a gene are located) or in an exon, is capable of disrupting the encoding sequence of a single gene.

We started our screening by selecting mutants whose lethality is at the late third instar or later, since our goal was to isolate genes involved in the visual system development and the photoreceptor clusters begin to form during the third instar stage. The general procedure was to create homozygous larval animals and to examine the projection of the photoreceptor axons.

Generation of Homozygous *dizzy* Animals

All P-element insertion lines were maintained as balanced heterozygous stocks. A balancer is a chromosome that is not able to partake in homologous recombination during meiosis insuring that the mutated locus is not lost as a result of crossing-over. I used the second chromosome balancer $y^{+}CyO$ to balance gene *dizzy*, which contains the y^{+}

allele for scoring homozygous larvae at the third instar (Figure 3A). Homozygous *dizzy* third instar larvae are *y⁻* and thus can be distinguished by the pigmentation of the mouth-hooks.

Collection of Homozygous Third Instar Larvae

Third instar larvae are easily collected from the wall of the fly-bottle because at this larval stage the larvae leave the food to find a suitable location on the wall of the collection bottle to begin pupation. To insure that healthy larvae were collected the density of all stocks was carefully monitored and sufficient yeast and water were added regularly. Homozygous animals were collected from a *dizzy/y⁺CyO* balanced stock and placed in a petri plate containing 1X PBS for stereoscopic examination of their mouth-hooks. The homozygous *dizzy* animals were selected and the visual system consisting of the optic lobes and the eye discs was dissected with a pair of forceps, followed by fixation.

Staining of the Visual System

The fixed visual system was stained with anti-HRP antibody, a pan-neuronal marker labeling all neurons (Jan

and Jan, 1982). It was also conjugated with a fluorescent tag FITC for easy visualization. To examine the projection of the retinal axons, I stained the visual system with the monoclonal antibody 24B10 that recognizes the photoreceptor cells only. The 24B10 antibody was then visualized by a fluorescently labeled secondary antibody conjugated with Cy3.

For a lateral perspective, the two optic lobes were separated and mounted with the eye disc and the optic stalk facing upwards, completed by the application of a cover slip. Alternatively, the optic lobes remained intact and were mounted with ventral nerve cord sitting at the bottom for a horizontal view.

Confocal Microscopy

A Nikon PCM-2000 confocal microscope equipped with dual HeNe-Argon lasers was used to collect high resolution images of the R-cell axon projections from the eye disc to their targets in the brain. Image collection was managed with the Simple-32 software which allows the setting of

density threshold and frame averaging, and images from different focal planes and magnification were collected.

Retinal Axon Projection Defects in *dizzy* Mutants

Imprecise neuronal connectivity between R-cells and their targets in the brain is apparent in the developing fly visual system of third instar larval homozygous *dizzy* mutants. The intact visual system of the *dizzy* mutants were dissected and stained with the mAb24B10 (red) which labels all R-cells and their axon projections, and the neuronal marker anti-HRP (green). In *dizzy* mutants the eye disc patterning of R-cells and their axon projections through the optic stalk are indistinguishable from wild type. The projection defects of *dizzy* mutants are present in the lamina target region of the brain (Figure 3B). *dizzy* mutants have three common target recognition defects. First, a subset of the R1-6 axons fail to stop at their appropriate targets in the lamina and instead overshoot their targets and project further to the medulla region of the brain (Figure 3B). Second, we see frequent crossovers of the R1-

R6 neurons disrupting the even fan-like innervation typical of the lamina target region. Third, as a result of inappropriate target recognition gaps and abnormal axon bundles are present in the lamina.

dizzy is Disrupted by a Single P-element Insertion

The insertion of a transposable P-element into a genomic site often inactivates a gene located at the site of insertion. *dizzy* is disrupted by a single P-element insertion that has been mapped to the left arm of the second chromosome, location 26C, by high resolution cytogenetic analysis of polytene chromosomes from the salivary glands of third instar larvae (Berkeley Drosophila Genome Project http://fruitfly.berkeley.edu/). To confirm that the P-element insertion at site 26C in *dizzy* mutants was responsible for the disruption of precise neuronal connectivity in the visual system of homozygous *dizzy* animals, an excision assay was performed (Figure 3C). Excision of the P-element rescues the *dizzy* mutant phenotype, and the R1-6 axons innervate their appropriate retinotopic targets precisely.

Chapter 4

Tissue Expression and Functional Analysis of *dizzy*

Introduction

Understanding the spatial and temporal expression is an important step in elucidating the function of gene *dizzy*. So using *in situ* hybridization and RT-PCR, I have carried out the analysis of the *dizzy* tissue expression pattern at different developmental stages during embryogenesis. Furthermore, I have created mosaic animals to examine the function of *dizzy* in the visual system of *Drosophila*.

In Situ Hybridization

The tissue expression of a gene is often an indicator of where it may function. To this end, I set out to investigate the expression pattern of gene *dizzy* in the embryos and the visual system of the third instar larvae. I chose to use a non-radioactive procedure where a single stranded RNA probe was synthesized with the incorporation of the residue digoxigenin-11-UTP that can be detected by an anti-DIG antibody. Both sense and antisense probes of *dizzy* were

synthesized using the EST clone AT08279 encoding the *dizzy* cDNA sequence as a template (Figure 4A). This clone contains an insert approximately 1.7 kb in length flanked by the restriction sites *EcoRI* and *XhoI* (Figure 4A). To generate the single stranded DIG RNA labeled probes, the plasmid was linearized by single enzyme digestion and used as a template with the appropriate RNA polymerase in an *in vitro* reverse transcription reaction. The RNA polymerase SP6 was used with *XhoI* cut plasmid to generate a sense DIG labeled single stranded RNA probe as a negative control, while T7 RNA polymerase was used with *EcoRI* cut plasmid to generate an anti-sense DIG labeled single stranded RNA probe to visualize the *dizzy* mRNA expression pattern. The digoxigenin probe was detected by an alkaline phosphatase tagged antidigoxigenin antibody. The probe is visualized by the color reaction of the alkaline phosphatase substrates nitroblue tetrazolium chloride (NBT) and 5-bromo-4-chloro-3-indolylphosphate (BCIP).

Wild-type embryos of different developmental stages and third-instar larvae visual systems were collected and

fixed. All tissue was treated with proteinase K and washed with PBT prior to hybridization overnight with DIG-labeled single stranded RNA. Probed tissue was then incubated for 1 hour at room temperature with anti-DIG antibody. This antibody labeling was detected by adding NBT and X-Phosphate with 1 ml of levamisole. The color reaction was terminated after 10 minutes with PBT and then the tissue was mounted in 80% glycerol for light microscopy analysis.

Embryos and intact visual systems were mounted so that the lateral perspective could be observed using light microscopy. *In situ* staining indicates that *dizzy* messenger is expressed throughout embryogenesis. The negative control DIG-labeled single stranded sense RNA probe did not label any cells blue as illustrated by a stage 15 embryo (Figure 4B). The positive control DIG labeled single stranded RNA detected *dizzy* mRNA in stage 5 embryos, although cellularization has occurred at this stage the possibility of a maternal contribution of *dizzy* mRNA can not be ruled out (Figure 4B). Stage 15 embryos have expression of *dizzy* messenger in the germ band cells that will give rise

to the future CNS (Figure 4B). The third instar visual system has *dizzy* mRNA expressed in the developing eye disc, but no expression in the brain. This suggests that *dizzy* may be required by the developing photoreceptors and not their targets in the brain (Figure 4B).

dizzy mRNA is Expressed at Different Developmental Stages

dizzy mRNA is expressed throughout several developmental stages. Using RT-PCR coupled with agarose gel analysis, I showed that *dizzy* is expressed in embryonic, 1st instar larvae, 3rd instar larvae, and adult tissue. In this approach, total RNA extracted from each developmental stage was extracted and purified. Of the total RNA only mRNA was reverse transcribed using oligo$(dT)_{18}$ as a primer and the enzyme reverse transcriptase to generate cDNA. cDNA from each developmental stage was used as a template for two sets of PCR reactions using a 5-prime primer set for *dizzy* (GEFAS/GEF2) whose product would be approximately 900 bp in length, and the other reaction a *tubulin* positive control primer set (TUBUP2/TUBDN2)

whose PCR product would be 229 bp. The sequence for both primer sets are:

GEFAS 5'-CGGAAGCTTCAGTCGCGAAGAGCTGC

GEF2 5'-CGGAAGCTTCGACCAGCTGCTGTAGCA

TUBUP2 5'-CGGAAGCTTCTGACCATGTCC

TUBDN2 5'-CGGAAGCTTGGCGTGGGTCGCAG

Agarose gel analysis of the PCR reaction products indicate that *dizzy* mRNA is expressed throughout development (Figure 4C). The *dizzy* primer set only amplifies *dizzy* cDNA which is present in all developmental stages. The positive *tubulin* control primer set does indeed PCR amplify the *tubulin* cDNA confirming that the cDNA template is of high quality.

Mosaic Analysis

The generation of mosaic animals that have patches of homozygous mutant tissue in an otherwise heterozygous background is a powerful approach that can be used to study the role of essential genes such as *dizzy* throughout development and also in adults. Mosaic animals were generated to determine which particular cell populations,

those in the eyes or those in the brain, require the function of *dizzy*. To address this issue, I generated mosaic animals that have homozygous clones in the developing eye discs or in the target region of the brain, or both. The developing third instar visual system was fluorescently labeled and mosaic cells were observed using confocal light microscopy. Furthermore, the compound eyes of adult mosaic animals were screened for disruption of the symmetrical organization of ommatidia using a dissecting scope.

To generate mosaic *Drosophila,* I took advantage of the efficient technique which utilizes the yeast 2-μm plasmid site specific recombinase (FLP) that catalyses recombination between the FLP recombination targets (FRTs) (Golic and Lindquist, 1989). By inserting the FRT into the desired chromosome where the interested locus is located, somatic homozygous clones can then be generated at different developmental stages by controlled expression of the recombinase FLP. The homozygous clones are surrounded by heterozygous tissues that express the marker *lacZ*. Due to the absence of the *lacZ* marker, these homozygous clones

will appear as negative patches when stained with the anti-β-galactosidase antibody (anti-β-gal).

To generate *dizzy* mosaic animals, I needed to recombine the *dizzy* mutant locus with an FRT site that lies on the same chromosomal arm near the centromere. To do this, *dizzy* mutant flies were crossed with an FRT strain (Cross 1, Figure 4D). Since the chromosomal location of *dizzy* is 26C, an FRT strain with the FRT site inserted at 40A was used. The FRT structure contains a neomyocin resistant gene that can be used to select FRT bearing animals in G418-neomyocin medium. The recombinant animals were selected during the next cross where G418 resistant animals with red eyes are collected (Cross 2, Figure 4D). The *dizzy* mutant was originally generated by the insertion of the P-element carrying a *mini-white* (w^+) gene encoding red eye color, the selection of red eye animals ensures the existence of the mutant locus. Since Cross 2 relies on the natural occurring recombination, it is the least efficient and most time consuming step. The recombinant animals collected from Cross 2 were expanded as balanced

stocks through Cross 3 (Figure 4D). During the final cross, the recombinase FLP under the control of a heat shock promoter ($hsFLP^{122}$) located on chromosome 1 was introduced into the recombinant offspring of the next generation (Cross 4, Figure 4D). Embryos were collected and heatshocked at 38°C for 30 minutes (Xu and Rubin, 1993). The heat shocked embryos were then returned to 25°C to develop to the third instar larvae. The visual system of these larvae were dissected and stained with both neuronal markers and the anti-β-gal antibody. The anti-β-gal staining will reveal the homozygous clones as negative patches, whereas neuronal markers will determine the pattern of neuronal connectivity. Embryos that were heat shocked for 1 hour at 38°C were transferred to a food vile and were allowed to develop into adults. These animals were screened for defects in the compound eye.

Mosaic third instar larval visual systems were dissected and fixed for antibody staining. Several different neuronal markers for monitoring photoreceptor cells and target neurons were used. Specifically, the mAb24B10 was

used to label photoreceptor cells and their axons, and anti-ELAV antibody to stain target neurons in the lamina. Two-color laser confocal microscopy was utilized to visualize the staining patterns of these antibodies following fluorescent-conjugated secondary antibody labeling. A Cy3 (red) conjugated secondary antibody for neuronal markers (mAb 24B10 and anti-ELAV) was used and a FITC (green) tagged secondary antibody for anti-β-gal.

Observation of homozygous mosaic patches in the eye disc or in the optic lobe of the brain had no visible phenotype. There was no disruption of homozygous mutant photoreceptor cell clusters or of the axon projection patterns to appropriate targets in the lamina. Observation of developing ommatidia clusters indicates that all photoreceptor cells are present in mutant homozygous clones suggesting that *dizzy* does not play a role in photoreceptor cell fate determination. In addition heterozygous photoreceptors innervate homozygous *dizzy* mutant clones in the brain. Mosaic analysis of *dizzy* clones in the developing third instar larval visual system suggested

that the homozygous mutant cells were still able to find their appropriate targets. This is possible because it is common that the *dizzy* mutant cells are guided to their appropriate target by neighboring heterozygous photoreceptor axons that lead their neighbors to appropriate targets. In addition appropriate neuronal connectivity uses several guidance signaling pathways that can compensate for the loss of only one or part of a pathway during early developmental stages.

Since *dizzy* mutants are late pupal lethal with an occasional escaper, I generated mosaic patches in adult animals. Embryos were heat shocked to induce FLP recombinase and these animals were then allowed to develop into adults. Straight wing progeny were collected and screened for mosaic clones. Mosaic patches were found in the compound eye of adults (Figure 4E). Homozygous *dizzy* mutant patches of tissue were found in an eye that is otherwise wild-type. Close observation of photoreceptor cells of the ommatidia of adult animals indicates that they

are all present. The phenotype is a result of the inappropriate organization of the accessory cells.

Chapter 5

Molecular Analysis of the *dizzy* Locus

Introduction

One major task in the characterization of gene *dizzy* is to determine the molecular identity of this gene including its sequence, genomic organization, the protein it encodes, and the functions of these conserved protein domains. To this end, I have used a combination of classical cDNA library screening, RT-PCR and bioinformatics to obtain the full length encoding sequence of gene *dizzy* and the amino acid sequence of the corresponding protein (Bottalico et al., 2003). Cross species comparison reveals that *dizzy* is a guanine nucleotide exchange factor likely to influence photoreceptor axon pathfinding through changes of the cytoskeletal network.

Molecular Characterization of Gene *dizzy*

Rescue of Genomic DNA Flanking the P-element

The transposable P-element is a powerful mutagen in *Drosophila* to silence target genes and functions as a tag to

rescue the flanking sequences around the target locus. By analyzing these flanking sequences, it is possible to identify the chromosomal location of the disrupted gene. The structure of the P-element used in my mutant flies contains two inverted repeats, a *lacZ* marker, a mini-gene *white* (w^+) gene for scoring the P-element, the *Escherichia coli* (*E. coli*) origin of replication and an ampicillin resistance gene (Amp^R) for *in vitro* propagation. In addition, the P-element carries a number of restriction enzyme sites for rescuing the flanking sequences. (Figure 5A).

Using the enzyme *EcoRI*, the right side flanking genomic sequence of the P-element was rescued by ligating *EcoRI* digested genomic DNA to generate circularized DNA, followed by transformation of competent *E. coli* cells. Those transformants showing ampicillin resistance will contain part of the P-element along with the desired flanking sequence. Similar procedures using other restriction enzymes were applied to rescue genomic DNA from the left side of the P-element.

The *EcoRI* rescued plasmid was amplified using overnight cultures, isolated by plasmid extraction, and linearized by digesting with *EcoRI*, followed by agarose gel electrophoresis. The rescued portion of the P-element and the flanking sequence was approximately 8.3 kb in length. To separate the right portion of the P-element bearing the ampicillin resistant gene and bacterial origin of replication, the *EcoRI* rescued plasmid was digested with *EcoRI* and *HindIII*. Restriction digestion of the plasmid with *EcoRI* and *HindIII* followed by agarose gel analysis, and physical mapping indicated that there were four internal *HindIII* sites. Five bands were found on the gel and they were approximately 3.1 kb, 1.8 kb, 1.5 kb, 1.2 kb, and 700 bp, respectively. The 1.8 kb fragment includes the P-element sequence bearing the Amp^R gene and *E. coli* bacterial origin of replication. The remaining four fragments are genomic DNA sequence flanking the P-element.

Screening of cDNA Libraries

To generate probes for the cDNA library screening, the *dizzy* flanking genomic fragments were separated by gel

electrophoresis and purified with the Qiagen gel extraction kit. The three fragments with *HindIII* cohesive ends subcloned into a *HindIII*-cut pBluescript vector were propagated in *E. coli* (Figure 5B). ^{32}P radioactively labeled probes were then generated by PCR amplification.

A *Drosophila* eye disk cDNA library was screened with these probes under stringent hybridization conditions. Out of two rounds of screeing, several *dizzy* positive clones were isolated. While in the process of analyzing these clones, the fly genome project was completed and the entire *Drosophila* genomic sequence became available. By searching the fly genome, I identified a putative sequence as the possible sequence of gene *dizzy*.

Mapping the Precise Insertion Site of the *dizzy* P-element

The availability of the fly genomic sequence provided me with the opportunity to identify the relative relationship of the 3.1 kb, 1.5 kb, 1.2 kb, and 700 bp P-element rescued genomic fragments. The genomic inserts in the recombinant pBluescript vector were sequenced in our laboratory using

the dideoxy-mediated chain termination (Sanger) method for sequence analysis. The rescued genomic fragment sequence along with the size of the *HindIII* restriction fragments allowed me to determine the relative relationship of the rescued genomic fragments to the P-element insertion to the genomic scaffold accession AE003613. This permitted me to map the precise insertion site of the *dizzy* P-element to the genomic sequence region 26C 2-3. My results were confirmed later by the Berkeley fly project in which they used an inverse PCR approach to map the precise insertion site of the P-element to the genomic sequence (accession AQ026067). In this approach they rescued the flanking genomic DNA and used a primer complementary to one strand of the P-element to recover 124 base sequence from the 5' end of the P-element.

Identification of a Putative *dizzy* cDNA Sequence

After mapping the precise insertion site of the *dizzy* P-element to genomic scaffold AE003613, a Gene Scene Search of FlyBase (A data base of the *Drosophila* Genome) for Annotated cDNA sequences located at map positions 26C

2-3 led to the identification of a putative open reading frame disrupted by the *dizzy* P-element insertion accession number CG9491. The putative *dizzy* cDNA sequence was then mapped to the genomic sequence to determine the intron-exon splicing sites of the putative gene *dizzy*.

Identification of a *dizzy* cDNA EST Clone

A valuable resource available through the Berkeley *Drosophila* Genome Project is a database of cDNA Expressed Sequence Tag (EST) clones. These cDNA clones were prepared from high quality RNA that was reverse transcribed using oligo$(dT)_{18}$ primer. Each clone is numbered and it is partially sequenced. cDNA EST libraries from high-quality mRNA isolated from a variety of tissues at different developmental stages were searched using bioinformatic tools for possible EST clones that matched to the putative *dizzy* cDNA sequence. A single EST clone AT08279.5prime (dbESTId 8364398 / GenBank Accession number BF505945) was identified. This EST clone was mapped to the 3-prime end of the putative *dizzy* cDNA

sequence using the 655 bp sequence available for this clone (Figure 5C).

Characterization of the 3' *dizzy* EST

The cDNA of the *dizzy* EST was prepared from testis mRNA. The *dizzy* cDNA insert containing *EcoRI* and *XhoI* cohesive ends was directionally inserted into the polycloning site of the 1815 bp pOTB7 vector (Figure 4A). The *E. coli* carrying the *dizzy* EST recombinant plasmid were obtained and grown in Luria-Bertani (LB) medium overnight at 37°C. Plasmid was purified using the Qiagen mini-prep kit and digested with *EcoRI*, *Xho1*, and both *EcoRI* and *XhoI*. The digests were run on a 1% agarose gel with a 1 kb ladder. Gel analysis indicated that the length of the cDNA insert was approximately 1.7 kb.

Obtaining the Full Length EST Sequence

The EST purified plasmid was sequenced in the laboratory using PM001 (5'-CGTTAGAACGCGGCTACAAT) and T7 (5'-AATACGACTCACTATAGG) primers. The PM001 sequence provides the sense sequence on the side of the *EcoRI* restriction subcloning site, while the T7 primer

provides the antisense sequence on the side of the *XhoI* restriction subcloning site. My sequence confirmed that we obtained the correct EST-clone and that the cDNA sequence provided the stop codon and poly-A tail of *dizzy*. To obtain the full length sequence of the *dizzy* EST the purified plasmid was sent to GeneWiz for sequencing with the PM001 and T7 plasmids. The PM001 sequence was 558 bp in length – the first 163 bp were vector sequence the remaining base pairs matched to the EST-tag sequence that was used to identify the *dizzy* EST clone. The T7 reverse complement sequence of 501 bp included the TGA stop codon, and poly-A tail. Since sequencing with the plasmid primers PM001 and T7 did not permit sequencing of the entire cDNA insert, the PM001 sequence and the T7 sequence was used to design two new primers the ABPMEST (5'CCAAAGATTGCTGCTGCTGCT) and the ABT7EST (5'CCAAAGATTGCTGCTGCT). Using these internal cDNA insert primers the remaining cDNA sequence between the first set of sequence was obtained. Upon assembly of the

overlapping sequences, the full length EST sequenced was assembled (Figure 5C).

Obtaining the 5' End of Gene *dizzy*

The *dizzy* cDNA clone provided the 3' end of *dizzy* including the poly-A tail. Since no other cDNA clones were available, an RT-PCR approach was used to obtain the 5' end of gene *dizzy*. Total RNA was extracted from 3rd instar larval eye discs using RNA-Wiz tri-reagent (Ambion). The RNA was treated with RNase free DNase prior to a phenol/chloroform extraction. The high quality RNA was tested for degradation by looking at the quality of ribosomal RNA on a denaturing formaldehyde gel. The mRNA was reverse transcribed using an oligo$(dT)_{18}$ primer for a reverse transcriptase reaction. This cDNA was cleaned by phenol/chloroform extraction and used as a template for individual PCR reactions.

The putative CG9491 sequence and the 3' cDNA clone sequence was used to design 3 sets of PCR primers (see Materials and Methods). All primers were designed to permit future subcloning of the PCR products into *HindIII*

pBluescript cut vector. The quality of the three PCR products obtained from these primer sets was tested by agarose gel analysis. Single bands present on the gel for primer sets 1-3 matched the predicted lengths expected which were approximately 880 bp, 1.6 kb, and 900 bp in length for the 3 primer sets, respectively (Figure 5D).

The PCR reactions from primer set 1, set 2, and set 3 were all run on an agarose gel in separate lanes. All had a single prominent band that was cut from the gel. The DNA from each band was gel purified using the Qiagen extraction protocol, cleaned with phenol/chloroform, and precipitated. The three PCR DNA bands were then subcloned into *HindIII* cut pBluescript plasmid, transformed into competent *E. coli* cells, and transformants carrying the recombinant plasmid were identified by plating on ampicillin media with IPTG and *X-gal* for blue/white selection. Colonies carrying the recombinant plasmid were white while the colonies carrying non-recombinant plasmid are blue because they have a functional *lac-Z* gene that is not disrupted by the *HindIII*

insert. Restriction analysis of the recombinant plasmid confirmed that they contained the appropriate insert.

The 3 recombinant plasmids bearing the 5' cDNA sequence of gene *dizzy* were commercially sequenced using T3 and T7 primers. The entire cDNA insert of recombinant plasmids bearing the PCR product from primer set 1 and 3 was sequenced. The cDNA insert for primer set 2 was too long to be completely sequenced using the T3 and T7 primers. The first round of sequencing allowed me to determine the orientation of the subcloned PCR products in the pBluescript plasmid. To complete the sequencing of the set 2 PCR product, an upstream and downstream set of primers were designed using the first round of DNA sequence. The sequence of this set of sequencing primers is:

ABBDUPL (upstream): 5'-GCGATCAGATTCACGAAG

ABBDDN (downstream): 5'-CTGAGTGGAACTGCTGCACG

A second round of sequencing using these primers provided the remaining sequence for the set 2 PCR product.

Assembly of the RT-PCR cDNA sequence provided the 5' end of gene *dizzy* starting with the ATG start codon.

Assembly of the Full Length *dizzy* cDNA Sequence

The entire full length sequence of *dizzy* was assembled and the entire open reading frame starting with the ATG start codon to the TGA stop codon plus the poly-A tail was 5025 bp in length (Figure 5D; Figure 5E). The open reading frame was translated and encodes a protein that is 1573 amino acids in length (Figure 5F). The open reading frame sequence was submitted to GenBank on October 16, 2001. The accession number for the *dizzy* cDNA and protein sequence is bankit429519.

Northern Blot Analysis of *dizzy* Embryonic Messenger

To confirm that we obtained the full length sequence of the *dizzy* mRNA a Northern blot analysis was performed. Generally, total embryonic mRNA was prepared and checked for degradation by examining the ribosomal RNA on a denaturing formaldehyde gel. RNA purity was checked using spectrophotometry to confirm that the A260/A280 ratio was between 1.8 and 1.9. In addition the A260 was

used to determine the concentration of RNA. A 1% formaldehyde denaturing gel was loaded with 30 μg of total RNA into 2 lanes and the 3rd lane was loaded with 2 μl of a 0.2-10 kb RNA ladder. After running the gel, the RNA gel was transferred to a positively charged nylon membrane and was prepared for hybridization.

Two ^{32}P labeled cDNA probes were prepared following the same protocol used to generate the probes for the cDNA library screening. A 384 bp *dizzy* probe that recognized the 5' end of *dizzy* and a 229 base pair positive *tubulin* control probe were generated using embryonic cDNA as a template. The primer set for both probes are listed below.

dizzy Primer Set:

GEF1 5'-CGGAAGCTTCAGTCGCGAAGAGCTGC

GEF2 5'-CGGAAGCTTCGACCAGCTGCTGTAGCA

tubulin Primer Set:

TUBUP2 5'-CGGAAGCTTCTGACCATGTCC

TUBDN2 5'-CGGAAGCTTGGCGTGGGTCGCAG

These primer sets were tested using both cold and hot ^{32}P labeled PCR reactions and the PCR products were examined using gel electrophoresis.

The Northern positively charged nylon membrane in which the total RNA was transferred was cut so that one embryonic mRNA lane could be hybridized with the ^{32}P 384 bp *dizzy* probe, while the other embryonic mRNA lane was hybridized with the ^{32}P 229 bp positive control *tubulin* probe. Subsequent to hybridization the blots were dried and exposed to X-ray sensitive film at -75°C overnight. Development of the film indicated that both hybridized blots contained a single band. A standard curve plotting relative mobility (RF) vs. molecular weight was prepared using the relative mobility of the standard mRNA bands. Alignment of the film to the blots permitted me to determine the distance traveled by the detected ^{32}P labeled messenger. Using the standard curve, it was determined that the *dizzy* mRNA was approximately 5.2 kb in length, and the positive *tubulin* mRNA approximately 1.3 kb (Figure 5G). The Northern indicates that there is only one *dizzy* mRNA isoform and

that it is approximately 200 bp longer than the open reading frame. This can be accounted for because the Northern band includes the 5' untranslated region. The positive *tubulin* control mRNA should be approximately 1280 bp, which is close to the 1.3 kb molecular weight determined.

Genomic Organization of the *dizzy* Gene

From the 5' untranslated exon to the last 3' untranslated exon gene *dizzy* extends over 9.3 kb of the genomic sequence. The open reading frame of gene *dizzy* is comprised of 7-exons with 6 intervening introns. The longest exon of gene *dizzy* is approximately 3.7 kb. The 137/20 P-element insertion lies upstream of the ATG start codon in the intron sequence (Figure5H).

Dizzy is a Novel *Drosophila* Guanine Nucleotide Exchange Factor

Pfam search results using the 1573 amino acid Dizzy sequence identified several key domain structures. Dizzy contains a cyclic nucleotide monophosphate binding domain (cNMP) (amino acids 143-233), a PSD-95/DlgA/ZO-1 domain (PDZ) (amino acids 407-496), a Ras/Rap1A-associating

Domain (RA) (amino acids 757-843), and a Ras guanine nucleotide exchange factor domain (RasGEF) (amino acids 865-1051) (Figure 5I). The PDZ domain plays a role in regulating protein-protein interactions, while the RA domain is typical of proteins that bind to the Ras and Rap GTPases. The GEF domain is a catalytic domain capable of activating Ras by regulating the exchange of GDP to GTP. Dizzy is therefore an intracellular signaling molecule that is likely to play a role in regulating Ras GTPase activity.

Domain Structure of Fly Dizzy and Cross Species Conservation

A protein blast search identified putative guanine nucleotide exchange factors in *C. elegans* and humans that were homologous to Dizzy. All contained the signature cNMP, PDZ, RA, and RasGEF domains. The evolutionary conservation of these four domains is remarkable; this is confirmed by the percent identity of these domains across species (Figure 5I). For example, the percent identity of the GEF domain of *C. elegans* and humans to the fly Dizzy GEF

is over 55%. Such strong conservation is indicative of conservation of function.

Genetics at the *dizzy* Locus

Gene *dizzy* is disrupted by two different P-element insertions l(2)k137/20 and EP388 located in region 26C 2-3. One way to confirm that the same gene is disrupted by two different mutations is to perform a complementation test. In this approach, genetic crosses with appropriate visible markers are used to generate animals with a genotype in which the two different mutations are found on separate homologous chromosomes. Homozygous 137/20 and EP388 animals are both pupal lethal (Figure 5J). Animals carrying 137/20 over EP388 are also pupal lethal indicating that there is no complementation between the two P-element insertions. To further study the region of the *dizzy* P-element insertions, a *dizzy* deletion mutant was obtained that lacked the P-element insertion site and much of the 5' end of gene *dizzy*. This deletion mutant was provided by a collaborator, Kevin Edwards, from Illinois State University. Placing the 137/20 P-element insertion over the deletion did

not rescue the pupal lethality. This lack of complementation indicated that the deletion did indeed remove gene *dizzy* (Figure 5J).

Genetic Interaction Between Gene *dizzy* and Rap1

A standard approach to linking two different genes to a similar physiological process is to look for possible genetic interactions between the genes of interest. Our collaborator Kevin Edwards showed that gene *dizzy* and Rap1 (a cousin of Ras) are in the same developmental pathway. In collaboration with K. Edwards we provide additional data supporting a model in which gene *dizzy* acts upstream of Rap1. Unlike the wild type compound eye that has a normal distribution of ommatidia and bristles (Figure 5K), the homozygous (EP388) *dizzy* mutant escapers have an eye with morphological abnormalities. Furthermore, these animals have missing bristles and roughened eye morphology. In Rap1 mutant, the morphology of the eye is severely disrupted, with many bristles missing and the size of the ommatidia changed (Figure 5K).

In animals bearing the *dizzy* EP/EP and the Rap1 mutation, we saw an enhanced mutant phenotype with the eye size reduced, many bristles missing and the typical hexagonal array of the ommatidia altered (Figure 5K). Together, these results suggest that gene *dizzy and* Rap are found in the same developmental pathway and that both genes are required for appropriate development of the compound eye.

Dizzy is Part of the Ras-Rap1 Pathway

Dizzy is a novel *Drosophila* guanine nucleotide exchange factor with a Ras-Rap1 binding domain upstream of a catalytic guanine nucleotide exchange factor domain. The domain structure of Dizzy suggests that it is capable of activating GDP bound Rap1 by catalyzing the exchange of GDP to GTP. Genetic interaction between gene *dizzy* and Rap1 further supports the role of GEF as a mediator of Rap1 a cousin of Ras. Indeed, data from the human Dizzy homolog have shown that Dizzy binds to Rap1 and catalyzes the exchange of GDP to GTP (Liao et al., 1999; Liao et al., 2001).

Chapter 6

General Discussion

Gene *dizzy* and Photoreceptor Axon Pathfinding

Identifying the cellular and molecular mechanisms required for the establishment of precise synaptic connections between neurons and their targets during development is a fundamental goal of neuroscience. Though significant progress has been made in the past two decades in identifying the extracellular guidance cues and the growth cone receptors required for regulating axon pathfinding, it remains elusive how the guidance receptors relay the guidance information to the migrating axons and how different attractive and repulsive guidance cues impact the cytoskeleton (Albright et al., 2000; Dickson, 2002; Mueller, 1999; Tessier-Lavigne and Goodman, 1996).

The *Drosophila* visual system offers a powerful model for identifying and characterizing molecular components critical for axon projection, since retinal axons in the *Drosophila* visual system project over long distances to form synaptic connections with their specific brain targets in a

highly stereotypical fashion (Clandinin and Zipursky, 2002; Kunes and Steller, 1993; Martin et al., 1995; Newsome et al., 2000). Moreover, the amenability of a wide range of molecular, cellular and genetic techniques in fruit flies provides a unique system to investigate the axon guidance pathways (Adams et al., 2000). I chose to use this system to explore molecular mechanisms associated with axon navigation *in vivo*.

In searching for new molecular mediators in axon projection, I used the general strategy of forward genetics where a potential gene is first identified by examining the phenotype of its mutant. To this end, my investigation was initiated by screening a large collection of mutant fly stocks, where unknown target genes were silenced by the insertion of the transposable DNA structure, the P-element (Spradling et al., 1999; Torok et al., 1993). These animals all carried lethal mutations and a subgroup that had later-than-third instar lethality was selected. This is based on the fact that the visual system begins its development in the third instar

larval stage and that animals with early lethality will not be suitable for examining genes critical for the visual system.

To evaluate the possible defects in these animals, the visual system was dissected and stained with antibodies to monitor the photoreceptor pathfinding. One mutant stock showed clear abnormality in retinal axon navigation and I named this gene *dizzy*.

In *dizzy* mutants, photoreceptors sent their axon projections through the optic stalk, but failed to innervate their appropriate targets in the brain (Figure 3B). More specifically, the incoming retinal axons had difficulty in recognizing their proper targets, indicated by the loss of the typical evenly fanned out innervations at the lamina target region (Figure 3B). Instead, these retinal axons in *dizzy* formed thicker-than-usual bundles, sandwiched between large gaps not seen in wild type animals (Figure 3B).

The phenotypic analysis clearly showed that gene *dizzy* is a key regulator for the photoreceptor axon pathfinding and that it would be essential to obtain its molecular identity. I started the molecular analysis of gene *dizzy* by

rescuing the flanking sequences of the P-element in *dizzy* mutant flies, hoping that it would contain part of the *dizzy* encoding sequence that can be used as a probe to isolate cDNA clones from a fly library.

My search for the *dizzy* cDNA was facilitated when the *Drosophila* genome project was completed while I was in the process of screening fly cDNA libraries. It made my own isolation of *dizzy* cDNA clones unnecessary since the genome project made one cDNA clone available. Thus I obtained this clone and sequenced part of it. By comparing this flanking sequence and the genomic sequences from the genome database, I was able to confirm that this cDNA clone indeed encodes gene *dizzy*.

I found that this clone contained an incomplete *dizzy* sequence missing part of the 5' end, and that further sequencing attempts were needed to obtain a full-length *dizzy* sequence. I used an RT-PCR based approach where overlapping oligos would be synthesized and used to amplify the missing segment. This strategy yielded the expected

results and along with my previous sequences, I was able to assemble the full length *dizzy* sequence.

The Dizzy protein elucidated has 1573 amino acids and is a guanine exchange factor (GEF). Furthermore, Dizzy contains a Ras/Rap1 binding domain, indicating Dizzy is likely to function as an activator of Rap1, a Ras related small GTPase.

Evolutionary Conservation of Dizzy

The mounting evidence has established convincingly that the core biological mechanisms are conserved among species ranging from worms, insects to vertebrates (Albright et al., 2000; Dickson, 2002). Comparative genomics analyses have provided further support that many key regulators are operating in similar fashion in different animals. Not surprisingly, some 69% of human disease causing genes have fly homologs (Kornberg and Krasnow, 2000).

Given that positional information exists in both vertebrates and insects during axon projection during the CNS development, it is our expectation that functions of

Dizzy elucidated from the fly visual system will be conserved in other more complex systems. Indeed the protein sequence of Dizzy has shown clear cross species structural conservation.

Using the bioinformatic search engine Pfam, I have found several signature motifs in Dizzy. Specifically, Dizzy contains a cyclic nucleotide monophosphate binding domain (cNMP), a PSD-95/DlgA/ZO-1 domain (PDZ), a Ras/Rap1A-associating Domain (RA), and a Ras guanine nucleotide exchange factor domain (RasGEF) (Figure 5I). The PDZ domain plays a role in regulating protein-protein interactions, while the RA domain is a hallmark of proteins binding to the Ras and Rap GTPases (Gao et al., 2001; Harris and Lim, 2001; Kaprielian et al., 2000; Liao et al., 1999; Liao et al., 2001). The GEF domain is a catalytic domain capable of activating Ras by regulating the exchange of GDP to GTP. Dizzy is therefore a typical intracellular signaling molecule likely to regulate Ras GTPase activities.

Drosophila Dizzy is evolutionarily conserved among invertebrate and vertebrate species. A protein database

search has pulled out Dizzy homologs in *C. elegans* and humans, respectively, and all contain the signature cNMP, PDZ domain, RA and Ras GEF domains. Furthermore, protein sequence comparison of these homologs reveals a truly remarkable degree of conservation over the course of evolution (Figure 5I). For example, the percentage identity of the GEF domain across species is over 55%, a strong indication of functional conservation as well.

Model for Intracellular Signaling of Gene *dizzy* in Axonal Growth Cones

My initial goal was to further our understanding of molecular mechanisms underlining axon pathfinding by seeking new genes critical for photoreceptor axon navigation. The identification and characterization of gene *dizzy* as a novel axon guidance regulator have provided another possible mode used in wiring the CNS. The fact that *dizzy* messenger RNA is predominantly expressed in the developing CNS and eyes highlights its unique role in the construction of the nervous system.

I have constructed a possible Dizzy signaling pathway based on both molecular and genetic data. First, the domain structure of Dizzy clearly indicates that Dizzy is a GEF regulating the activity of Ras/Rap1 small GTPase. Indeed biochemical analysis in vertebrates has shown that mammalian Dizzy binds directly to Rap1 GTPase (Liao et al., 1999; Liao et al., 2001). Second, in collaboration with K. Edwards, it has been shown genetically that the fly gene *dizzy* and *Rap1* function in the same pathway (Figure 5K). Finally, in *dizzy* mutant animals, photoreceptor axons showed frequent failures in defasciculating upon reaching their brain targets, resulting in gaps that are due to misrouted growth cones (Figure 3B). Our morphological examination did not detect any defects in the neural cell fate determination in these animals. In addition, the fact that *dizzy* messengers were detectable only in the eye disc suggested it was unlikely gene *dizzy* is required by the target cells in the brain.

Taken together, these data support a hypothesis that *dizzy* plays a pivotal role in guiding the photoreceptor axons

to their brain targets and that it is likely to influence the navigation through the Rap1 GTPase that in turn regulates the cytoskeleton network. By also incorporating other relevant components, I have constructed a possible cellular signal transduction pathway for gene *dizzy* (Figure 6).

Upon ligand binding, growth cone surface receptors (yet to be identified for Dizzy) are activated, initiating a chain of signaling events leading to the ultimate navigation response. This results in the localization of the Dizzy protein to the cytoplasmic domain of surface receptors and being activated through yet unidentified docking proteins.

The activated Dizzy then binds to the Ras/Rap1 GTPase to activate it. Activated Rap1, in turn, activates CDC42 another GTPase that has been implicated as a key regulator in mediating actin polymerization through the protein Neuronal Wiskott Aldrich Syndrome Protein (N-WASP) (Aspenstrom et al., 1996; Erickson and Cerione, 2001; May, 2001; Mullins, 2000; Snapper and Rosen, 1999). My hypothesis is that Dizzy regulates axon projection through influencing actin reorganization in the growth cone.

Given the complexity of the physical environment growth cones encounter in different species, it is foreseeable that diverse guidance mechanisms have been evolved during the course of evolution. Consequently, different molecular pathways have been uncovered that play a role in guiding axons to their targets. We believe that the Dizzy pathway represents one such mechanism in receiving and interpreting neural guidance cues.

Future Investigations

To extend the understanding of Dizzy, one important unresolved issue is the identity of the immediate adaptor protein linking Dizzy to the surface receptor. One possible approach is to conduct a large scale genetic screening to identify genes in the same pathway as *dizzy*. Given the eye disc specific expression of *dizzy*, it would be especially fruitful to adopt the modified eye disc only screening strategy (Newsome et al., 2000).

Specifically, a screen could be designed so that mutants that have similar photoreceptor axon projection defects in the eye will be selected. These mutants will be

further grouped into upstream and downstream groups of gene *dizzy*. After establishing the molecular identities of the upstream group, it is within expectation that some signature motifs should become clear by comparing the genome data from different species. Once a candidate gene is available, its function as an adaptor can be directly examined through a conventional method such as the yeast two-hybrid system.

The identification of the Dizzy adaptor should shed further light on the function of the Dizzy pathway and enrich our understanding of growth cone navigation in general.

Figures

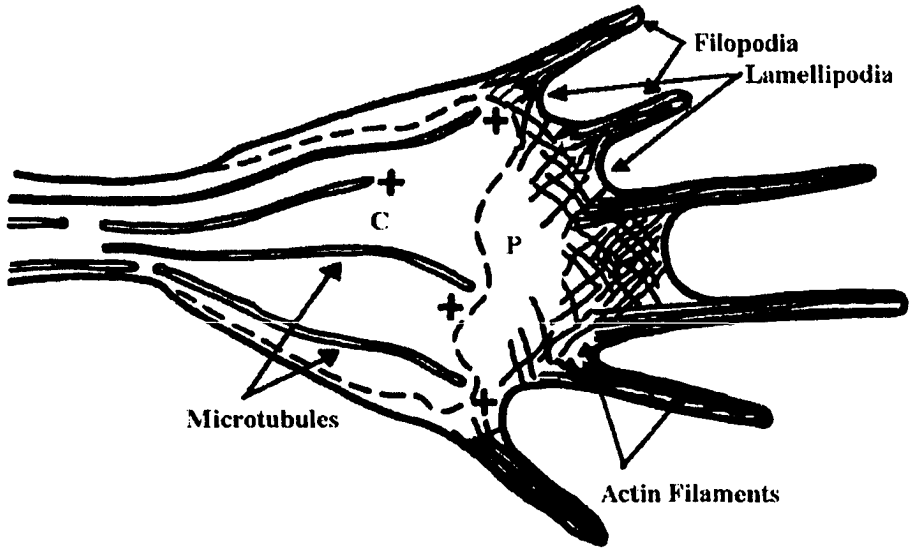

Figure 1A. Schematic of a Neuronal Growth Cone
The finger like projections, filopodia, and web like veils called lamellipodia are labeled. Two cytoskeletal components predominate in the growth cone. Actin filaments are organized in the organelle poor region (P) of the growth cone close to the leading edge. Filopodia contain tightly bundled actin filaments, while at the leading edge of the lamellipodia the actin filaments are organized as a dense interconnected nework. Microtubules are located in the body of the growth cone in the organelle rich region (C). The faster growing plus ends of microtubules are indicated. The dynamics of the cytoskeletal elements regulates the extension and retraction of the growth cone. (adapted from Mueller, 1999)

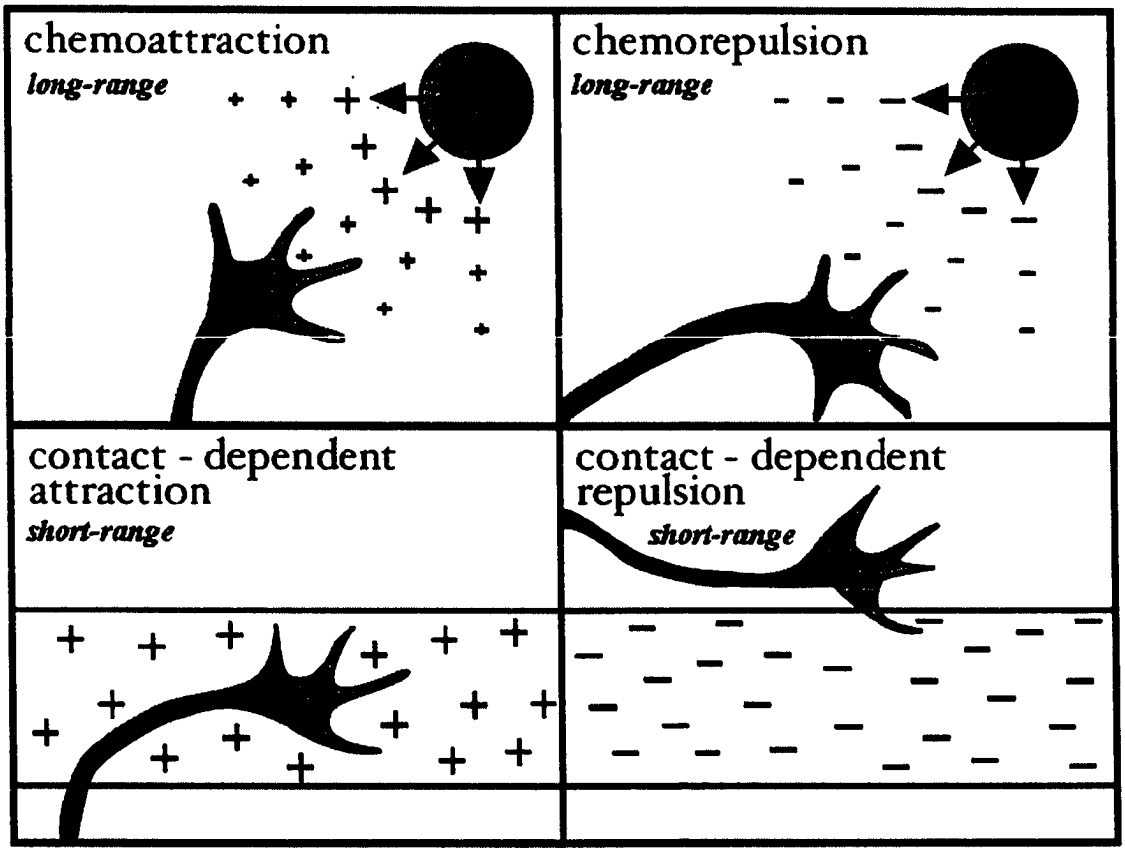

Figure 1B. Four Mechanisms Contribute to the Guidance of Axon Projections at the Growth Cone

Guidance cues can be attractive or repulsive. Growth cones are guided to their targets by long-range diffusible cues and short-range contact dependent cues. There are four axon guidance cues which include: long-range chemoattraction and chemorepulsion, and short-range contact attraction and contact repulsion. (adapted from Mueller, 1999)

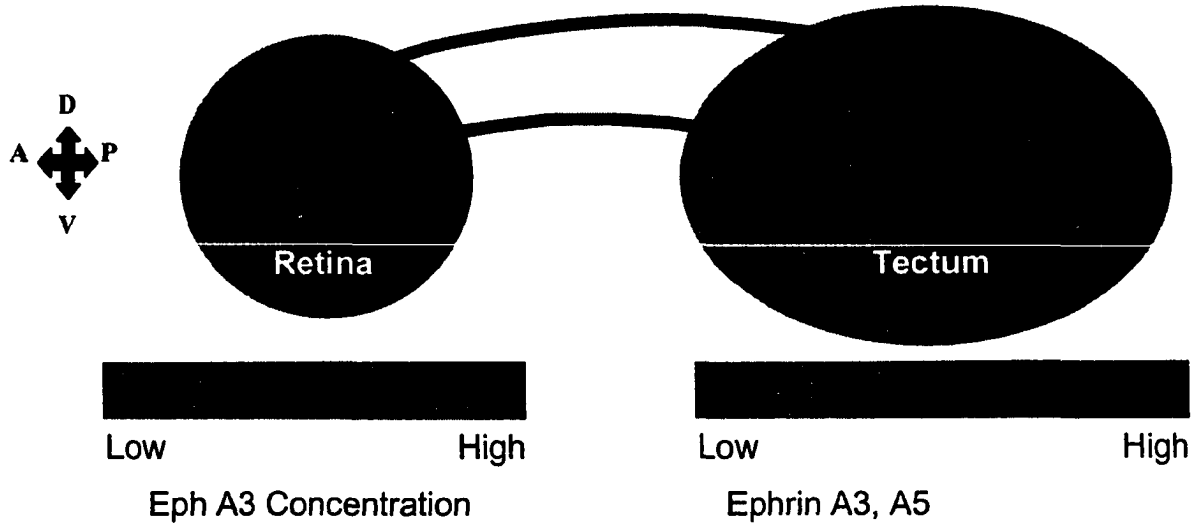

Figure 1C. The Role of Eph Receptors and the Repulsive Ephrin Ligands in Topographic Map Formation Along the Anterior-Posterior Axis

A schematic representation of the vertebrate visual system anterior is to the left and dorsal up. Photoreceptor neurons of the retina express the Eph kinase receptor A3 in a gradient along the anterior posterior axis. In the tectum of the brain, target neurons express the repulsive Eph ligands Ephrin A3 and A5 in a gradient along the anterior posterior axis. Anterior photoreceptor growth cones expressing low levels of Eph kinase send their axon projections to the most posterior tectal targets. The most posterior photoreceptor axons expressing the highest levels of Eph kinase innervate the most anterior targets of the tectum and do not project further to the dorsal region due to the higher levels of Ephrin repulsive ligands.

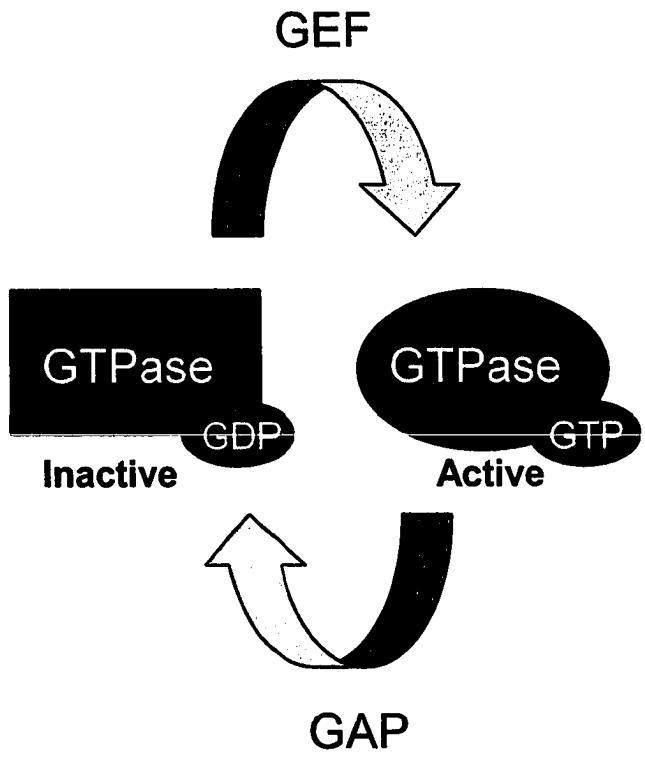

Figure 1D. Schematic Illustration of the Regulation of GTPase Activity

The GTPases have two interconvertible forms: GDP-bound inactive and GTP-bound active forms. GTPase activity is regulated by positive and negative regulators GEFs and GAPs, respectively. GEF stimulates the exchange of GDP for GTP, while GAP proteins stimulate the hydrolysis of GTP to GDP.

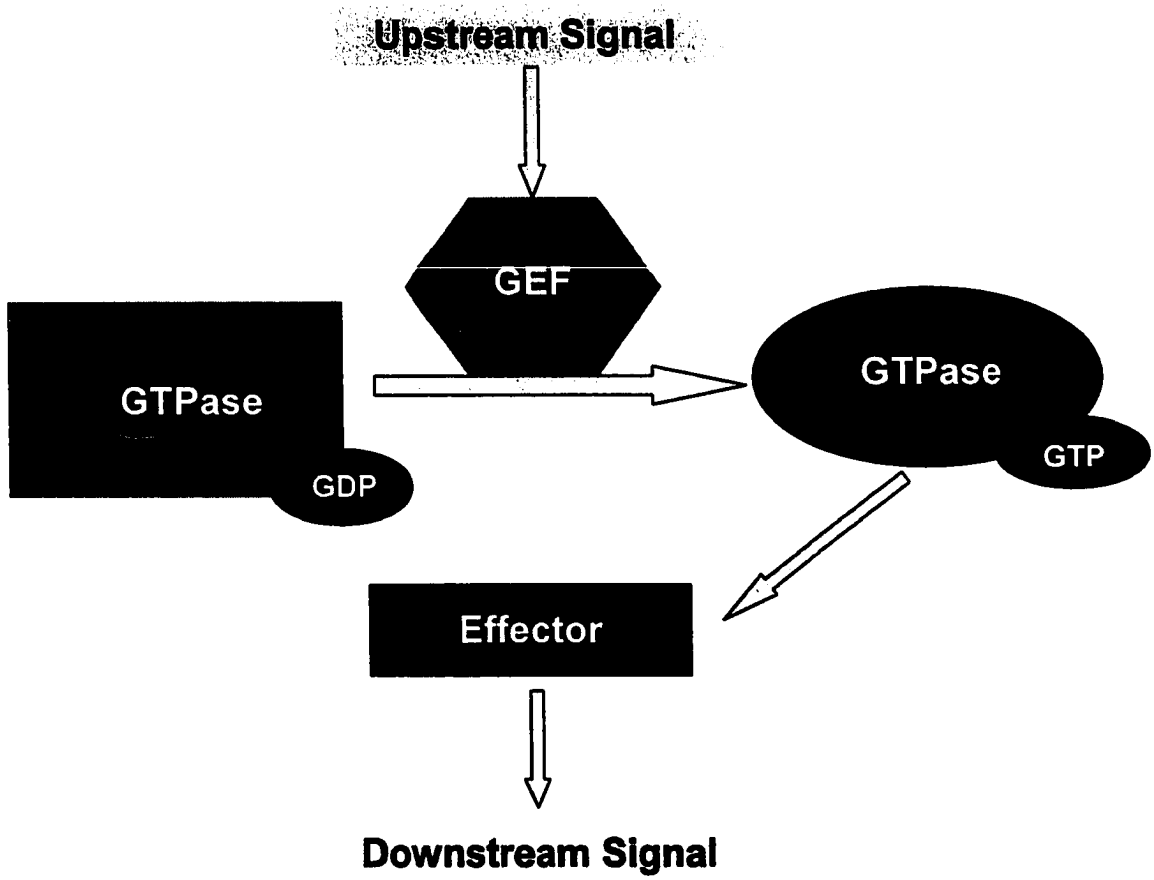

Figure 1E. Schematic Illustration of the Role of GEF in Cell Signaling Upstream signals activate GEF which in turn catalyzes the exchange of GDP to GTP on the GTPase converting it to the active form. Activated GTP bound GTPase can then signal to downstream effectors.

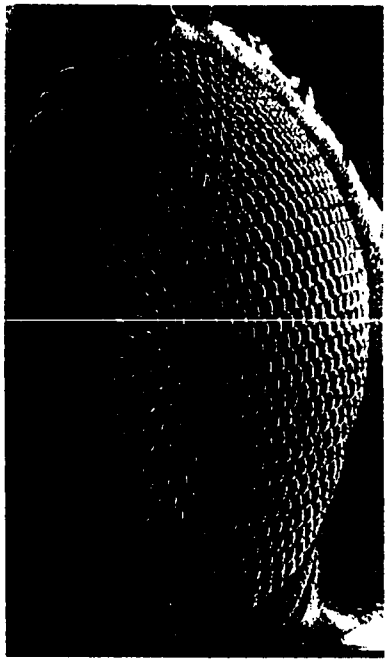

Figure 1F. Scanning Electron Micrograph of the *Drosophila* Compound Eye

The adult eye contains approximately 800 discrete units called ommatidia that are organized in a hexagonal array. Each ommatidium is precisely placed like the bristles. Each ommatidium contains exactly 20 cells 8 are photoreceptor neurons, the remaining are accessory cells.

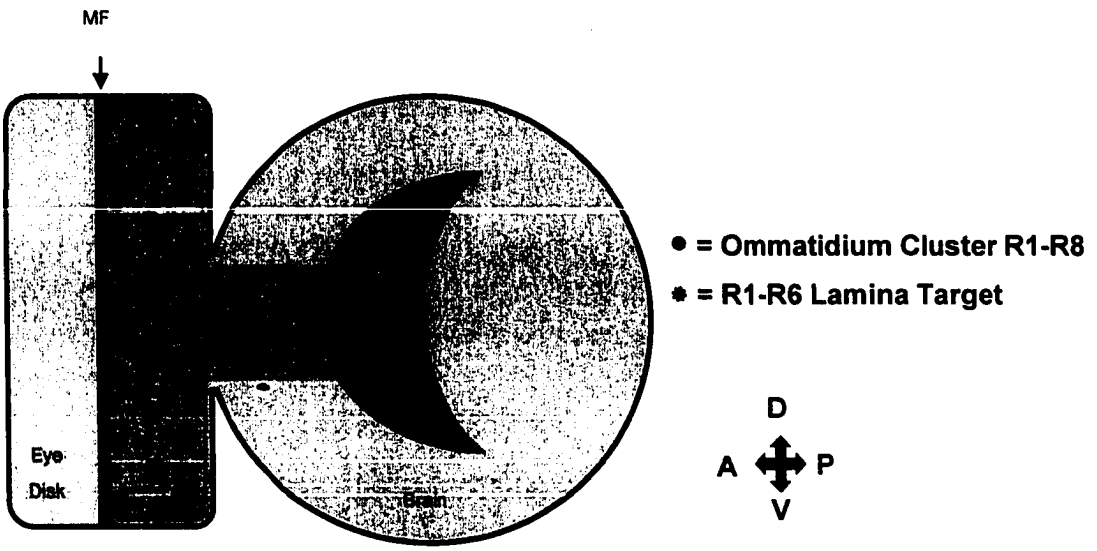

Figure 1G. Schematc Representation of the Lateral Perspective of a Third Instar Larval Visual System.
The onset of neuronal differentiation occurs in the eye disc at the morphogenetic furrow (MF), which sweeps in a posterior to anterior direction across the eye disc. The dots depict a subset of the ommatidia clusters present during this stage. Each cluster contains 8 R-cells which send axon projections as a bundled fascicle through the optic stalk (OS) to corresponding topographic targets in the brain. Photoreceptor axons R1-R6 innervate lamina targets while the R7 and R8 axons project to deeper targets in the medulla (horizontal perspective required). Note that the schematic illustrates only three of the many axon projections present at this stage from posterior clusters and that these axon projections innervate the most posterior region of the lamina in a stereotypic and predictable manner.

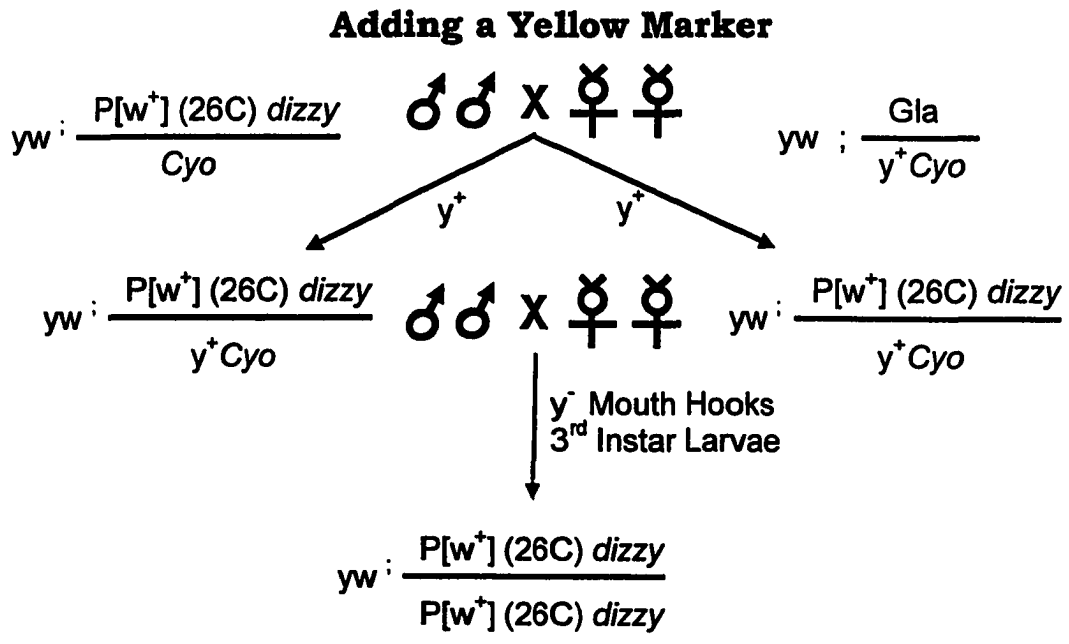

Figure 3A. Genetic Crosses Required to Add a Yellow Marker
Outline of the genetic crosses and stocks required to add the y+ marker required for identifying homozygous third instar *dizzy* mutants.

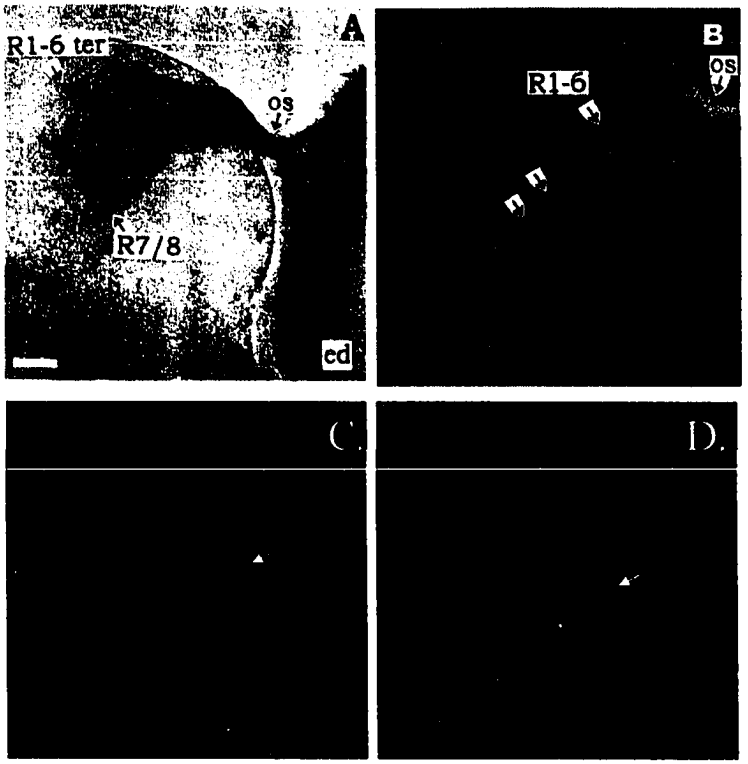

Figure 3B. Phenotype of *dizzy* Mutant

(A) The horizontal perspective of the wild type third instar visual system of *Drosophila.* Retinal axons are stained with antibody mAb24B10, which labels photoreceptor cells and their axons. R1-R6 axons project to their targets in the lamina and terminate there (R1-6 ter), while R7/8 axon projections penetrate further to deeper targets in the medulla. Anterior is to the right, and lateral up. ed, eye disc; os, optic stalk. Scale bar; 12μm

(B) The horizontal perspective of a *dizzy* mutant optic lobe. The visual system was stained with mAb24B10 (colored in red) and anti-HRP (colored in green). Since anti-HRP stains all neurons including R-cells, mAb24B10 positive cells (R-cells) are orange in color. R1-6 axons frequently failed to stop at their appropriate retinotopic targets, and proceed to deeper layers of the brain (arrows without text). Scale bar; 20μm.

(C) Lateral perspective of the wild type third instar visual system. The arrow indicates the even distribution of R1-R6 photoreceptor axon projections at their appropriate targets in the lamina. Anterior is to the left dorsal is up.

(D) Lateral perspective of a homozygous mutant brain. The arrow indicates one of several gaps where R1-R6 photoreceptors typically innervate. There is an uneven distribution of R1-R6 photoreceptor axons in the lamina. Anterior is to the left dorsal is up.

Excision Scheme

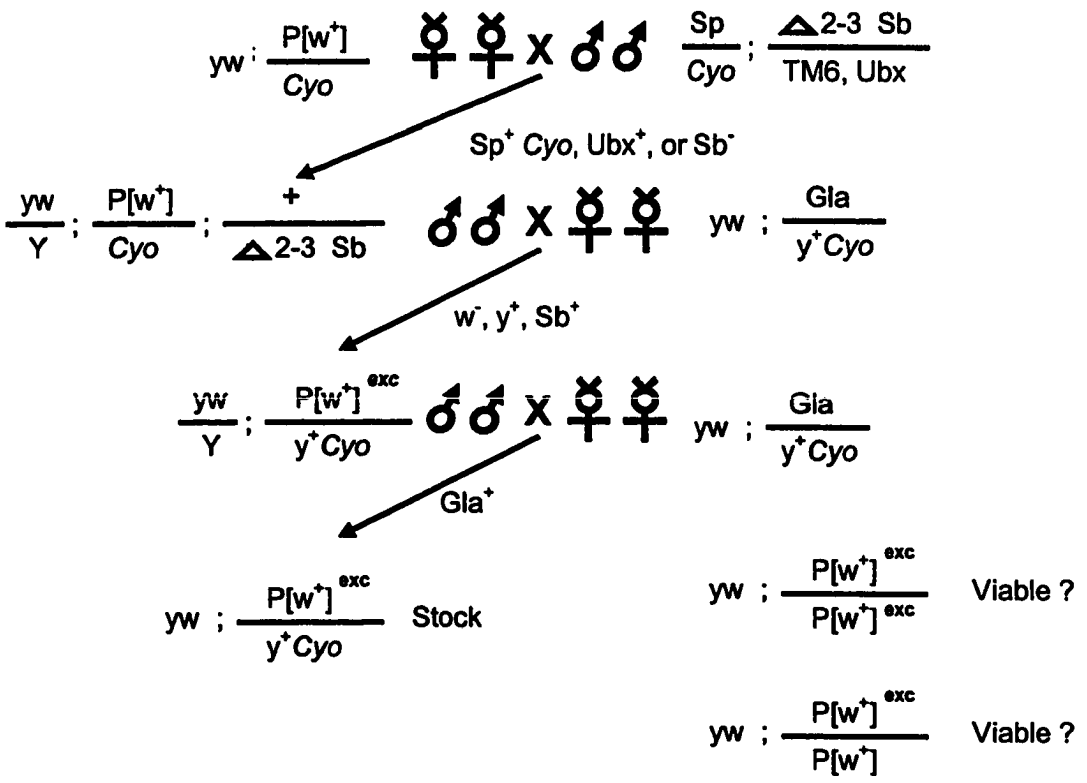

Figure 3C. Genetic Crosses Required to Excise the P-element Insertion

Outline of the genetic crosses and stocks required for removing the P-element insertion to rescue the homozygous *dizzy* mutant phenotype.

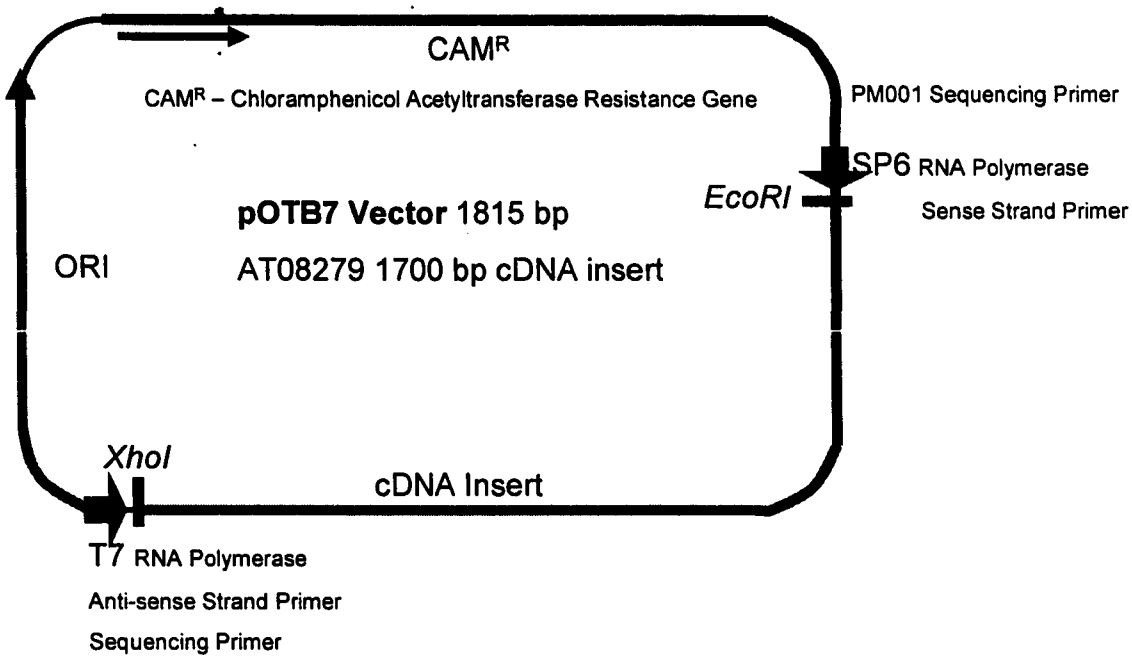

Figure 4A. Schematic of the pOTB7 Vector with *dizzy* cDNA Insert

Schematic of the pOTB7 vector containing the *dizzy* cDNA EST clone AT08279. The RNA polymerase SP6 was used with *XhoI* cut plasmid to generate a sense single stranded DIG-labeled RNA negative control probe, while T7 RNA polymerase was used with *EcoRI* cut plasmid to generate an anti-sense single stranded DIG-labeled RNA probe for *in situ* hybridization.

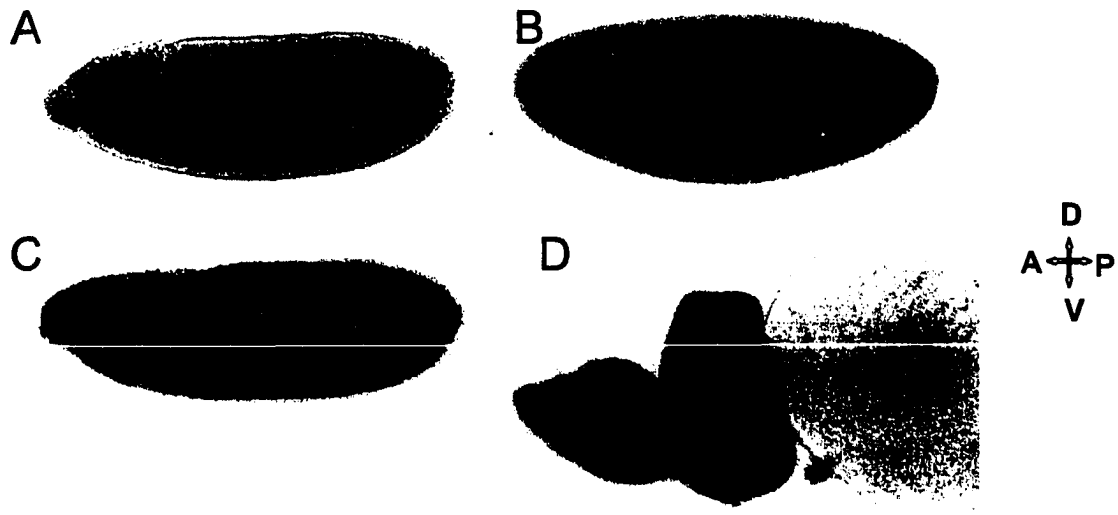

Figure 4B. *In-situ* Hybridization
(A-D) Lateral perspective of whole mount embryos and the third instar visual system. The anterior is to the left and the dorsal up. (A) A control embryo stained with a sense RNA probe.
(B-C) *dizzy* expression in stage 5 and 15 embryos. At stage 5, *dizzy* is detected in the entire embryo, while at stage 15, *dizzy* expression is predominantly in the developing CNS. (D) In the third instar visual system, *dizzy* is highly expressed in the eye-antennal disc.

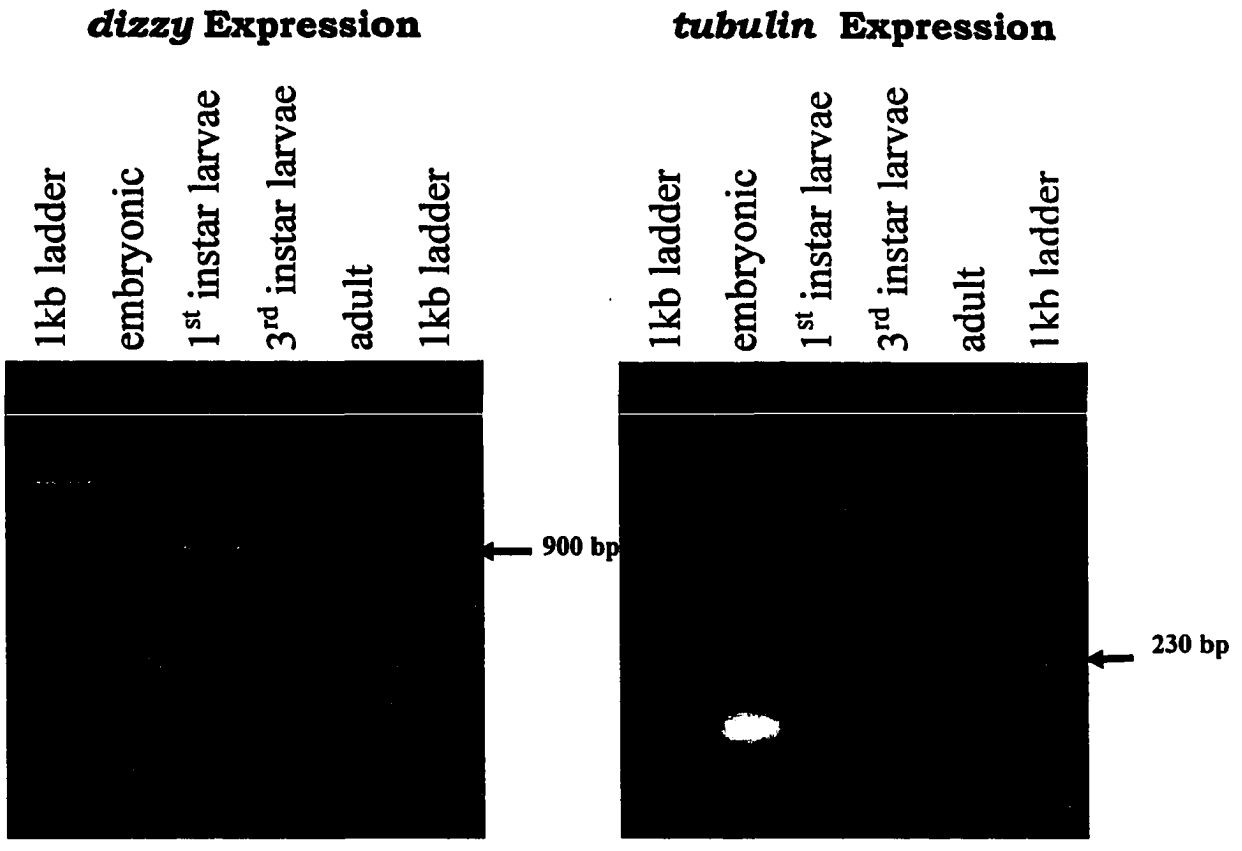

Figure 4C. *dizzy* mRNA is Expressed Throughout Development
Gel analysis of RT-PCR products using cDNA from different developmental stages. RT-PCR products generated using primer set (GEFAS/GEF2) for *dizzy*, and control primer set (TUBUP2/TUBDN2) for *tubulin*. The expected length of the *dizzy* primers is approximately 900 bp and the *tubulin* control 230 bp.

Figure 4D. Genetic Crosses Used to Generate Mosaic Animals
The relevant chromosomes are illustrated with their centromere shown as a filled circle. Crosses 1-3 are required to recombine the P-element insertion *dizzy* mutant onto an FRT-carrying chromosome arm. In **Cross 1** a strain carrying the *dizzy* mutation P[w+] (26C)/*CyO* over a balancer chromosome (*CyO*) is mated to a strain that is heterozygous for a centromere-proximal FRT [arm-*lacZ*] (24A) P[neo^R; FRT] (40A)/*CyO*. Flies carrying the *dizzy* mutation and the [arm-*lacZ*] P[neo^R; FRT] are selected, and in **Cross 2** mated with Gla/y+*CyO* animals. Natural recombinant animals from cross 2 that carry the P[w+] *dizzy* mutation and the P[neo^R; FRT] on the same chromosome are selected from the progeny based on their neomyocin (G418) resistance and red eye phenotype. **Cross 3** is carried out to generate a balanced stock of the natural recombinants selected from cross 2. Somatic clones homozygous for the P[w+] *dizzy* mutation can be produced by crossing the P[w+] *dizzy* mutation and the P[neo^R; FRT] to a strain that carries the same P[neo^R; FRT] and the cell marker FRT [arm-*lacZ*] as well as a hsFLP element on a separate chromosome **(Cross 4)**. Recombination of the FRT sequences by heat-shock induction of the FLP enzyme at the desired developmental stage is then performed to generate homozygous mutant clones which lack the marker *lacZ*.

Mosaic Crosses

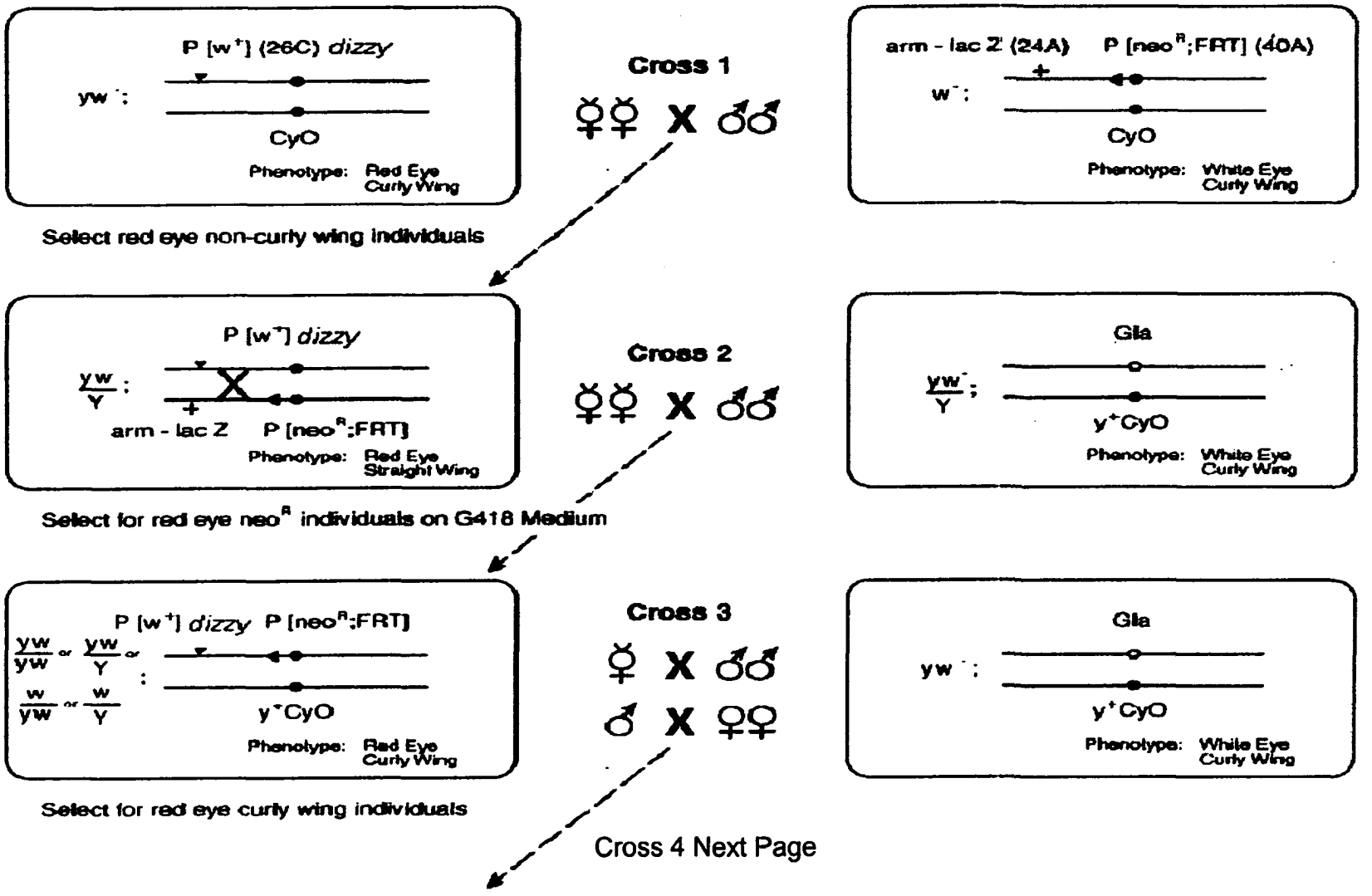

Mosaic Crosses

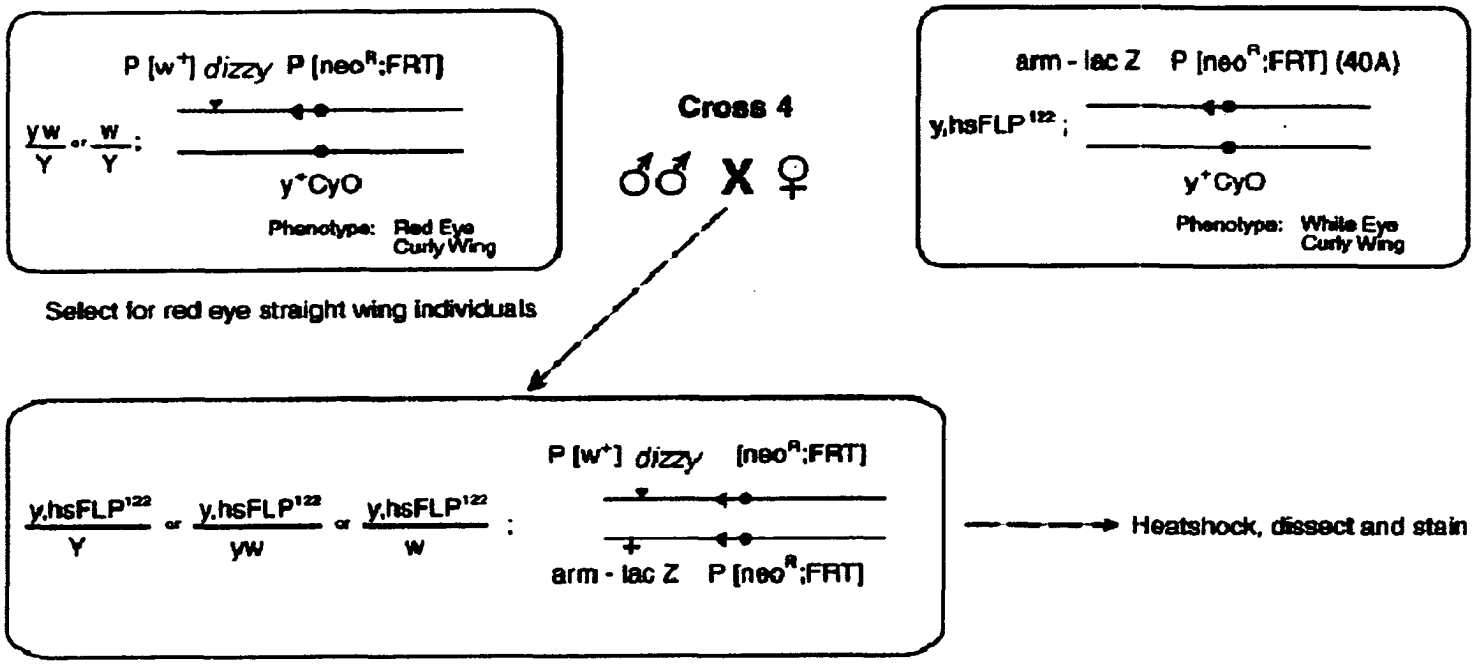

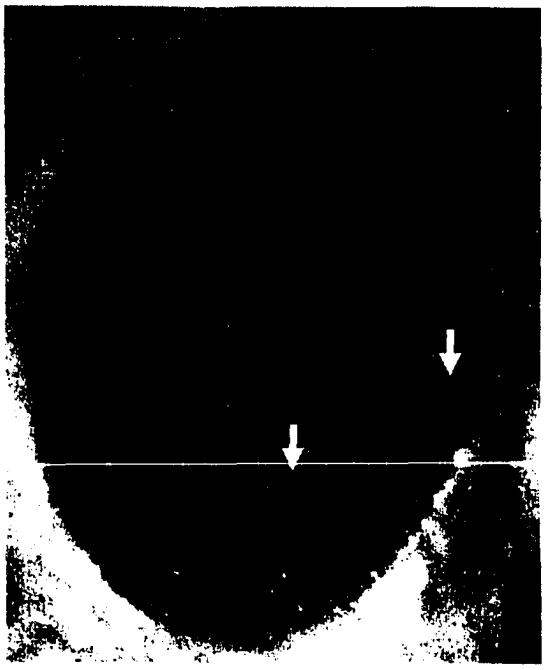

Figure 4E. Adult Mosaic Animal
Induction of FLP recombinase by heat shock of embryos was done at 37°C for 30 minutes. Straight wing progenies were collected and screened for mosaic clones. The arrows indicate the location of homozygous *dizzy* mutant patches of tissue in the eye that is otherwise wild-type. The appropriate organization of the ommatidium facets of the compound eye is disrupted in homozygous tissue.

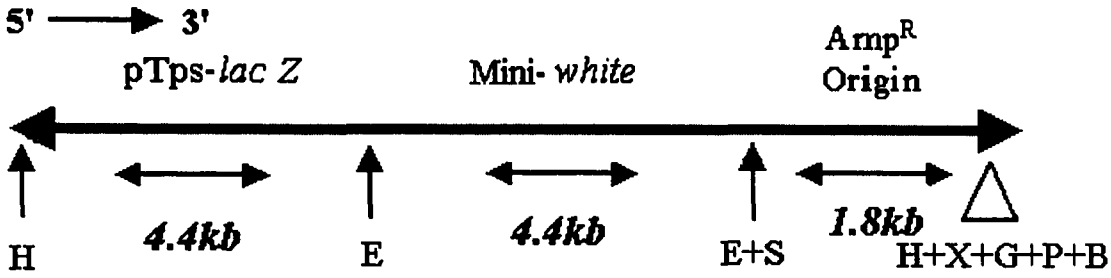

Figure 5A. Schematic Representation of a P-element
A schematic representation of a P-element. The relative location of pTps-*lacZ* marker, mini-*white* gene encoding red eye color, Amp^R (ampicillin resistant gene), and *Escherichia coli* bacterial origin of replication are indicated. The following restriction sites are present in the P-element E (*EcoRI*), H (*HindIII*), S (*SacII*), X (*XbaI*), G (*BglII*), P (*PstI*), and B (*BamHI*). The relative position of restriction enzyme sites are indicated by the vertical arrows and the isosceles triangle. The P-element has a length of 10.6 kb.

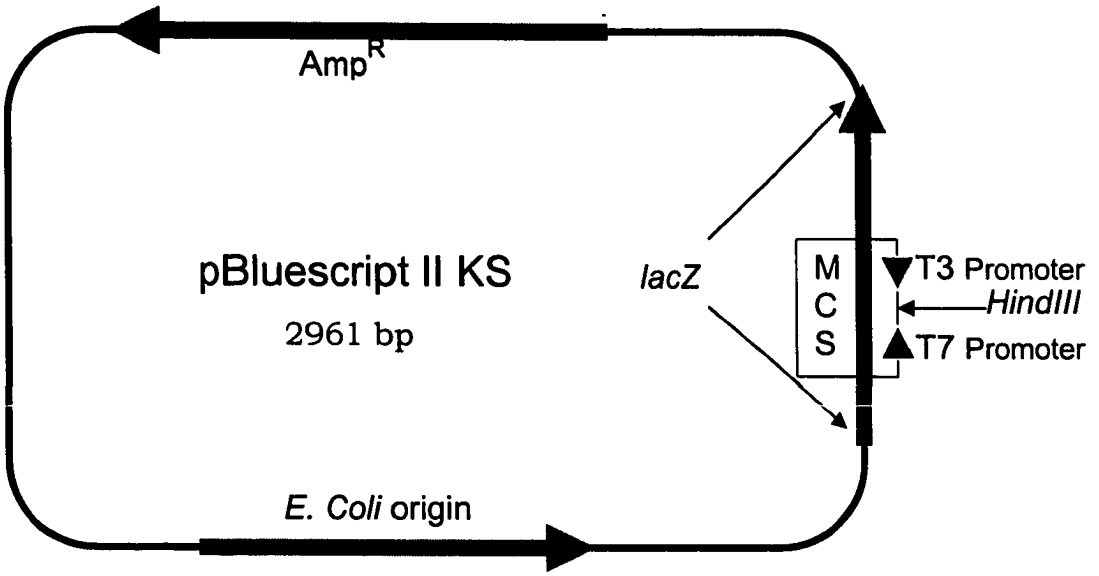

Figure 5B. Schematic of pBluescript II KS (+/-) Phagemid Vector The plasmid carries an Ampicillin (Amp^R) resistance gene for antibiotic selection of the phagemid vector, the *E. coli* bacterial origin of replication, and the *lacZ* gene that allows for blue/white color selection of recombinant phagemids. The *lacZ* multiple cloning site (MCS) includes the *HindIII* restriction site and is flanked by T3 and T7 promoters. (Stratagene Patent)

Obtaining the Full Length cDNA Sequence of *dizzy*

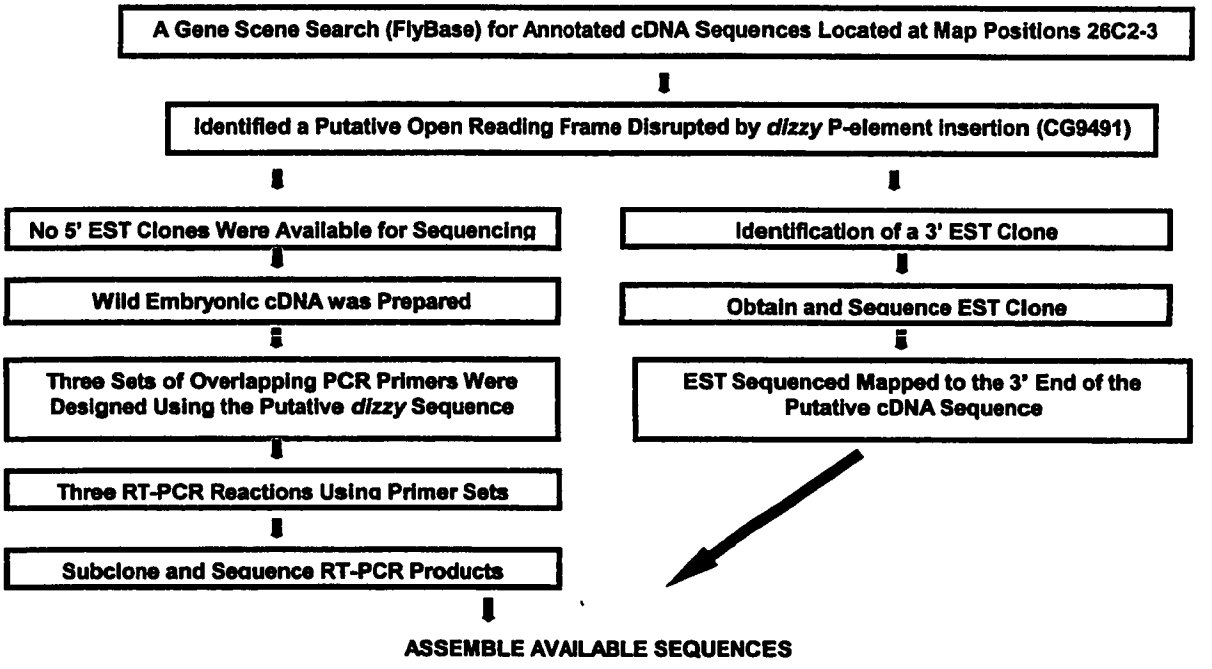

Figure 5C. Flow Chart of the Steps used to Obtain the Full Length cDNA Sequence of Gene *dizzy*

The left side outlines the steps used to obtain the sequence of the 5' end of *dizzy*, while the right side outlines the steps used to obtain the 3' end of gene *dizzy*.

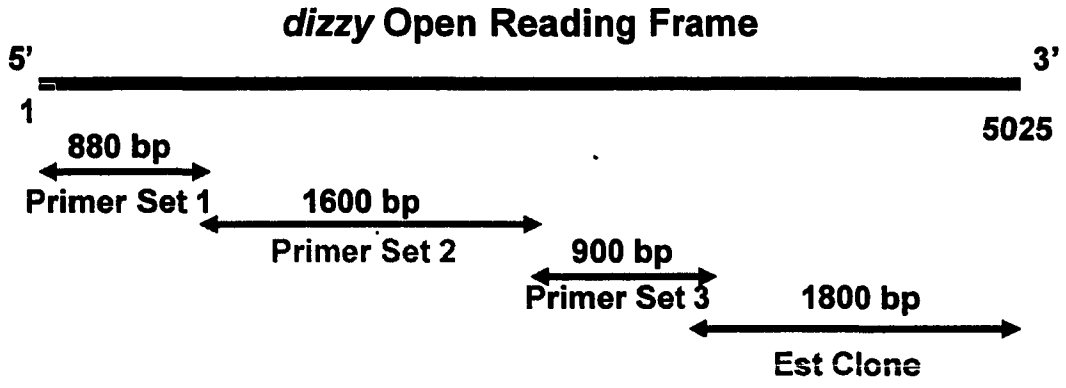

Figure 5D. Assembly of the 5025 bp *dizzy* Open Reading Frame Sequence alignment between three overlapping RT-PCR products and EST-clone. The approximate length of each sequenced clone is indicated in bp.

Gene *dizzy* cDNA Sequence

atggatccgt atcaccatat cagacatcat tatccaccca caagcatagc aggcacagga
gtggtggtgg gcagctcgac tacaatcaac cggccggaac tgcaccaaaa atgcaaccgg
ggctcgcact ccagtgacac cagttcggcg tacagcggca gcgatacaat ggcctcgaac
tatgcctcgt cgctggaggc cgaggagatt gacctctccg gcctggtgga gtccgttgtg
gactctgacg aggaggacct ggcggagagc atggatagtc ttaccgtgcg ggatgccgtg
cgtgactgtc tggaaaagga tccggcggag cgcagcgagg aagatgtgga agtactgctt
agggccttaa ggcattcaca aacattacgc tggcagtgcg aagagcacta tgttccgtga
tggtattcgc cgttgtggac aaggcgggga ccgtggtcat gtcagatggt gaggaactgg
actcatggtc ggtgctcata aacggagcgg tggagatcga gcatgcaaat ggcagtcgcg
aagagctgca gatgggagac tccttcggca ttctacccac catggacaag ctgtaccacc
ggggtgtgat gcgtacgaag tgcgatgact gtcagtttgt gtgcattacg cagacggact
actaccgtat tcagcatcaa ggcgaggaga atacccggcg acatgaggac gagaatggtt
tcgttgttat ggtcactgaa ctccggtcca ttggcggcgt cggcactgat tctgctggca
gtggcggatc ggcgacagga gcttcggctt cgctaaatat gaagcgtggt cacgtagtta
tccgcggtac tccagagcgt ctactacagc agctggtcga ggaaaactcg atgaccgatc
ccacatacgt ggaggacttt ttgctcacac accgcatctt tattcagaac ccacaagagg
tgaccagcaa gttgctgcat tggtttgatt tggagcaggt ggatgcgcac aagacgcagg
aactgcgaga tcgcgtaaca cgcgtcgtgc tcctctgggt gaacaaccat ttcaccgatt
tcgaggcgga ctatgagatg atggagtttc tggaagtctt tgaggcactg ttagagcgaa
aaaagttgct aagtcagctg cgcctgttgc acatagcctg tgccgccaaa gcacggatgc
gcagctgtac cctcactcga tcgtcacgtg acgagccgct caacttccgc atcgtgggcg
gctacgagct tcgaggcgtc gccatagcca ctggaaacgc agcagtgggc atctacattt
cgcacgtcga gccgggatca aaagcccagg atgtgggcct taagcgaggc gatcagattc
acgaagtaaa tggacagtcg ctggaccatg tgactagcaa gcgagccctc gagatactca
caggcaccac ccatttgagc atcagcgtta agagcaactt gcttggcttc aaggagatta
tgcaggctct tgagcatggc ggtggaaccg ctggatccgg aagcatttcc gcaggcagcg
gcagtttcaa gtccgtgcga agtccacgcc gtatttgcgc caatgatatt gctaagttgc
acggtcgctc tgatagcacc accgacgaat tgtccagcgt cagcgcctcg aatcgagcac
acatggtgcg ccttagttcc gtcgatatgc tacttgacca gccggactgc gctccaccgc
aaacgccgcc agtgagtggg agcggtaaca tggcctccaa ttttatgcag caactcttgc
aaagcgttaa caatagttcg gccaagaagt ccggtgggaa ttcaaactcg gatcagcagg
atacgaaggg cggttttatg actctggcgc caaagcgtcg gctgcagaaa gcgctggcaa
agatgaattt actcaataag cagaatcacg gcagcagcct aaacgactcc tcggatacgc
tgctcaacga tcccaagtca aaactttctg cagttagctc gtgcagcagt tccactcagt
cgtctatcaa tggatgcacg gtcagtgggg gtggccggct ctaccagtcg caatcgaatc
cggatttaac cagtctcaac tatgacggag gcagcgatgc gggtggaaac ggtggtggaa
gattgcaagt gaactacctg aacgcccaca ttcaccggcc atcagcggcc agtactttga
caacaaactc gacgcaatcg cacctcttgc ccgattaccc ggaccacgtg ctcaaggtgt
acaaggcaga ccagacgtgc aagtatgtac tcatctacaa ggagacgaca gcccacgagg
tcgcaatgct gacgctgcag gagtttggaa tacacgaccc cagctcgaat ttctcgctat
gcgaagtgag tgttggcgac gggggtatgg taaagcagcg ccggttgccc gatcagctgc
agaacctggc cgagcgaata agctttgcgg cgcgttacta cctcaagtta aacgatagca
ccgaaccgct ggttccagac gaactggccc tggaactggt acgcgagtcg aacgtgcact
tcctgcacct gaatgcatac gagctggcca ttcagctcac tctacaggac tttggaactt
ttcgccagat tgagtccacc gagtacgtgg acgaattgtt cgagttgcgc tcacgctacg
gagtgccaat gctgagcaag tttgccgaac tggtcaatcg tgaaatgttt tgggttgtga
gtgagatttg cgcagagcac aacattgtgc gccgcatgaa gatcgtcaag cagttcatca
aaattgcgcg ccactgcaag gagtgccgta actttaactc catgtttgca atcgtctcgg
ggcttggaca cggagctgtt tcgcgactgc gtcaaacgtg ggagaagctg ccctccaaat
atcagcgact gttcaacgac ctgcaggatc tgatggatcc ctcgcgcaac atgagcaagt
atcggcaact agtgtccgcc gaactactgg cccagcaccc catcatcccg ttctatccga

```
tcgtcaagaa ggatctcacc tttattcacc tgggcaatga tacgagagtt gatggcctaa
tcaactttga gaagctgcga atgctggcca aggaggtacg cctgctcacg cacatgtgca
gttcgccata cgatctgctg tcgatccttg agctcaaggg gcagtcgcca tccaacgctc
tcttctcgct caatcagatg tctgcatcgc agagcaacgc tgccgctggc acagttatcg
ccgccaatgc cggccaggcg actatcaagc ggcgcaagaa gtcgacggcg gcgcccaatc
ccaagaagat gtttgaggag gcgcagatgg tgcggcgggt gaaagcatat ctcaacagcc
tcaaaatact cagtgacgag gacctttgc acaaattctc gctggaatgc gagcccgcgc
acgggtccac gtactcgggc agcatctcgc acgtaaatac ctcacaccga agcggtggtg
gaggcagcat cagtggcggt gctggtggca gctccggtgg tggtggcggg ggcagttcca
gcctcaatgc cggcgaccaa ctgagcatct attcgcatac cagctccagc tcggcgccga
actcctcact atcgcttcgc aagaggcacc caagttcacc cacccttcg actaccagct
caacgagttc taccagcgat catcaaagaa gacagatgca taacaacggc ccaaagtttg
gcacagcctc gccacaagca gttaaaaaga tgctatcgct gtcagagtcc tccaagattc
ggccgcacca gccattcgtg ccgcgtcacg gatccacaat ggccggagtg attccaccac
tgcatcacat gcatgcggcg catggtttca gcacaccgtc gcctggagga gtggtcacct
caccggcaac cagtgcagtg gccaatgtcc agtgtacgcc aagtccaagt ccctgctccc
accgacgact ggcttctgga ggcaacatta ttccctctcg cgcaatacac gagcggtcgc
actcggacac accagctccg ccgccgcctc taccctcggt cgatctctcc cttgagagca
gtagtgtaac tacatttcgc gatttaccat tgcgcaaatc cgtgacttcc ggttccatat
cgtcctgcga cagcggctac gtgcatcagc agcagcatta ccacttgcag taccagcagc
agcaacaaca gaacagctcg caacacgagc catccccgcc ggtctatacc gcagccgact
gccggctgct tcagcagata tcgaacaacg cggtgacccg caacttgaac agtccctgtc
aaagcacaaa cacaccaccc agcacnccta cacctccacc gaaccagccc acagcaacca
ttcagctttc tgcaccgccg acggcagcag catacatgca cgcacgcagc cagcatcagc
agctccagca gcagcagcaa tctttggcca tgccaccacc gccgccaccg cggtacaatg
tgccccccct gggcagtatc tacagccacc accagggcac tgctggcagc aggcacctga
accacatgca tggtaagacg accggaccgc aagagagatg gtttccagat tgccgtccaa
cgacaaaaca acaaatgcaa agcgggagtt gagtcgggtc tttttgaaat aggcgttaca
ccgggttgtt cgacttgttt ttctagtggc ccgccaaatt ttatggatag caccaagtgt
accatatgtc ccatgccacc catgaatcaa aataatttta aagcccagca caacaacgag
acgatcaatt gatatagaaa cgcaaacgga atcaactcga agccaccatt aattccatta
atgtatactt ctttaatact tatgtacaag ctaattttat tacaagcata ctcccttaaa
cgctaaaaaa aaaaaaaaaa aaaaaaaaaa aaaaa
```

Figure 5E. *dizzy* cDNA Sequence

The full length cDNA sequence of gene *dizzy* starting with the 5' ATG and ending with the poly-A tail. Sequence was submitted to NCBI database accession NM_135168.

Dizzy Amino Acid Sequence

translation="MDPYHHIRHHYPPTSIAGTGVVVGSSTTINRPELHQKCNRGSHS
SDTSSAYSGSDTMASNYASSLEAEEIDLSGLVESVVDSDEEDLAESMDSLTVRDAVRD
CLEKDPAERSEEDVEVLLEFTQGLKAFTNITLAVRRALCSVMVFAVVDKAGTVVMSDG
EELDSWSVLINGAVEIEHANGSREELQMGDSFGILPTMDKLYHRGVMRTKCDDCQFVC
ITQTDYYRIQHQGEENTRRHEDENGFVVMVTELRSIGGVGTDSAGSGGSATGASASLN
MKRGHVVIRGTPERLLQQLVEENSMTDPTYVEDFLLTHRIFIQNPQEVTSKLLHWFDL
EQVDAHKTQELRDRVTRVVLLWVNNHFTDFEADYEMMEFLEVFEALLERKKLLSQLRL
LHIACAAKARMRSCTLTRSSRDEPLNFRIVGGYELRGVAIATGNAAVGIYISHVEPGS
KAQDVGLKRGDQIHEVNGQSLDHVTSKRALEILTGTTHLSISVKSNLLGFKEIMQALE
HGGGTAGSGSISAGSGSFKSVRSPRRICANDIAKLHGRSDSTTDELSSVSASNRAHMV
RLSSVDMLLDQPDCAPPQTPPVSGSGNMASNFMQQLLQSVNNSSAKKSGGNSNSDQQD
TKGGFMTLAPKRRLQKALAKMNLLNKQNHGSSLNDSSDTLLNDPKSKLSAVSSCSSST
QSSINGCTVSGGGRLYQSQSNPDLTSLNYDGGSDAGGNGGGRLQVNYLNAHIHRPSAA
STLTTNSTQSHLLPDYPDHVLKVYKADQTCKYVLIYKETTAHEVAMLTLQEFGIHDPS
SNFSLCEVSVGDGGMVKQRRLPDQLQNLAERISFAARYYLKLNDSTEPLVPDELALEL
VRESNVHFLHLNAYELAIQLTLQDFGTFRQIESTEYVDELFELRSRYGVPMLSKFAEL
VNREMFWVVSEICAEHNIVRRMKIVKQFIKIARHCKECRNFNSMFAIVSGLGHGAVSR
LRQTWEKLPSKYQRLFNDLQDLMDPSRNMSKYRQLVSAELLAQHPIIPFYPIVKKDLT
FIHLGNDTRVDGLINFEKLRMLAKEVRLLTHMCSSPYDLLSILELKGQSPSNALFSLN
QMSASQSNAAAGTVIAANAGQATIKRRKKSTAAPNPKKMFEEAQMVRRVKAYLNSLKI
LSDEDLLHKFSLECEPAHGSTYSGSISHVNTSHRSGGGGSISGGAGGSSGGGGGGSSS
LNAGDQLSIYSHTSSSSAPNSSLSLRKRHPSSPTLSTTSSTSSTSDHQRRQMHNNGPK
FGTASPQAVKKMLSLSESSKIRPHQPFVPRHGSTMAGVIPPLHHMHAAHGFSTPSPGG
VVTSPATSAVANVQCTPSPSPCSHRRLASGGNIIPSRAIHERSHSDTPAPPPPLPSVD
LSLESSSVTTFRDLPLRKSVTSGSISSCDSGYVHQQQHYHLQYQQQQQQNSSQHEPSP
PVYTAADCRLLQQISNNAVTRNLNSPCQSTNTPPSTPTPPPNQPTATIQLSAPPTAAA
YMHARSQHQQLQQQQQSLAMPPPPPPRYNVPPLGSIYSHHQGTAGSRHLNHMHGKTTG
PQERWFPDCRPTTKQQMQSGS"

Figure 5F. Dizzy Amino Acid Sequence
The translated open reading frame of *dizzy* encodes a protein that is 1573 amino acids in length.

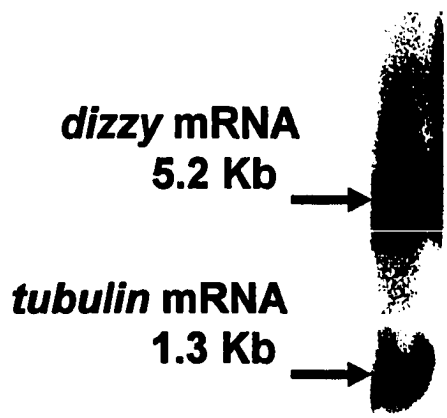

Figure 5G. Northern Blot Analysis of *dizzy* Embryonic Messenger mRNAs were detected with ^{32}P labeled cDNA probes. The *dizzy* cDNA probe detected a single band approximately 5.2 kb in length, consistent with the length of the *dizzy* open reading frame. A *tubulin* cDNA probe was used as a positive control to confirm the quality and quantity of mRNA.

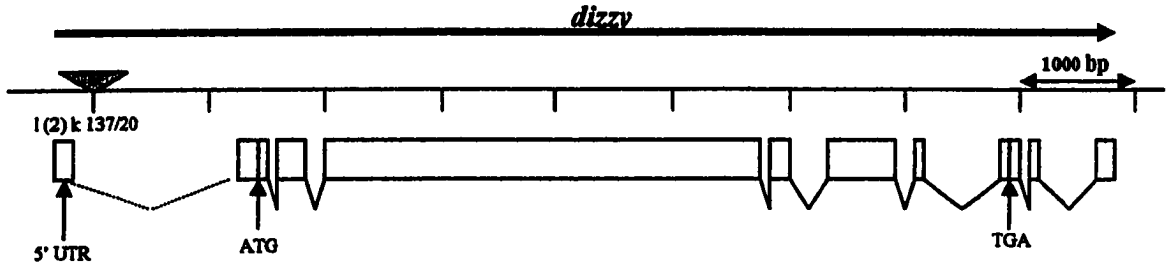

Figure 5H. Genomic Organization of Gene *dizzy*
The intron/exon organization of gene *dizzy*. The open reading frame of gene *dizzy* spans approximately 6.8 kb of the genomic scaffold and is comprised of 7 exons. The l(2) k 137/20 P-element insertion lies upstream of the ATG start codon in the untranslated region.

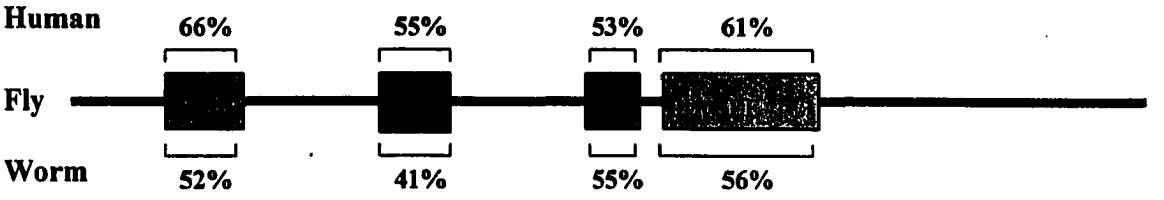

Figure 5I. Dizzy Domain Structure and Evolutionary Conservation
Four domains of Dizzy are conserved among human and worm orthologs. The four domains are:
cNMP = Cyclic Nucleotide Monophosphate-Binding Domain
PDZ = PSD-95/DlgA/ZO-1
RA = Ras/Rap1A-associating Domain
GEF = Guanine Nucleotide Exchange Factor Domain
The percent identity for each domain with its corresponding ortholog is indicated in schematic.

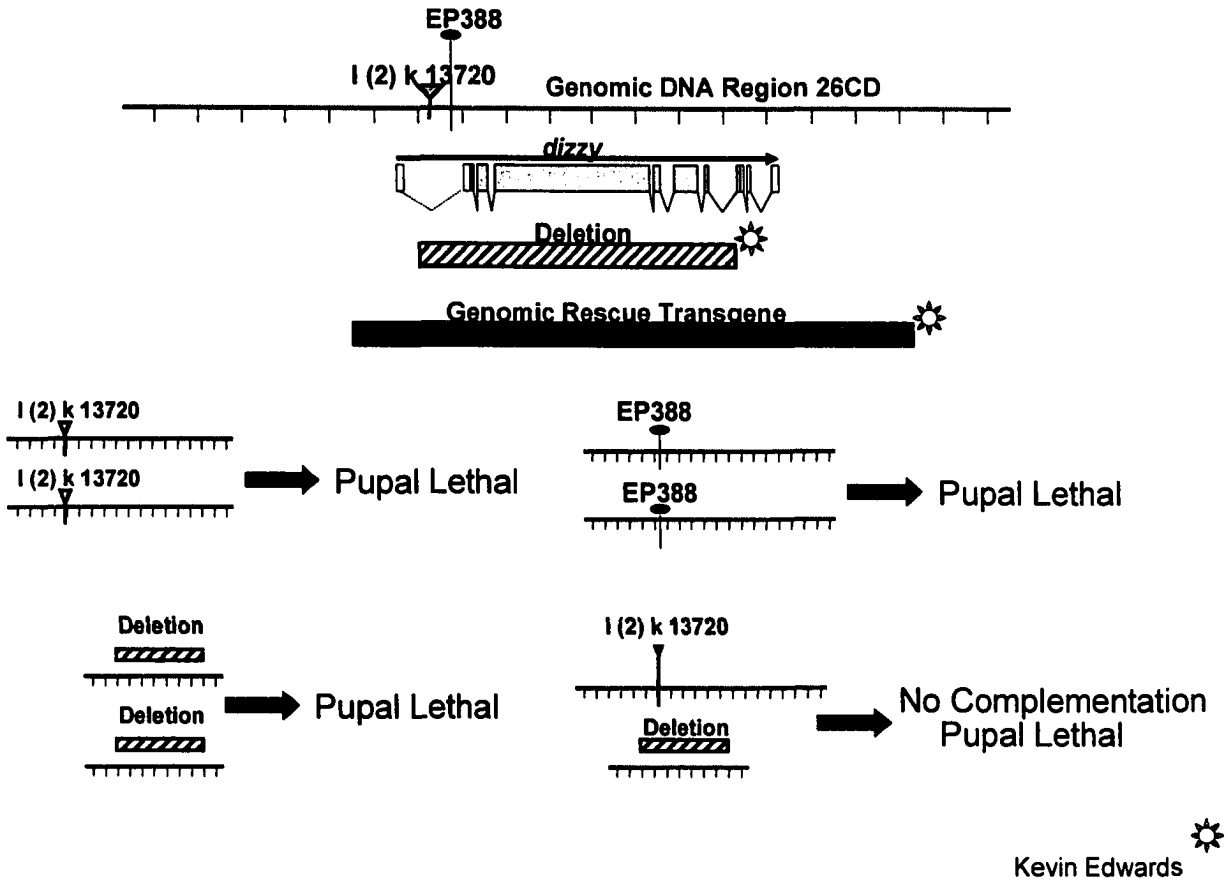

Figure 5J. Genetics at the *dizzy* Locus
Gene *dizzy* is disrupted by two P-element insertions l(2)k137/20 and EP388, the insertion positions are indicated along the top horizontal line which represents the genomic sequence. Below lies the intron/exon structure of gene *dizzy*. We also obtained a deletion mutant that removes six of the encoding exons of gene *dizzy*, the deleted region is represented by the shaded horizontal bar. Several of the complementation tests conducted are illustrated below. All are pupal lethal indicating that there is no complementation and indeed the deletion does remove gene *dizzy*. The dark shaded bar depicts the length and location of the genomic DNA used by a collaborator Kevin Edwards to rescue the *dizzy* mutant.

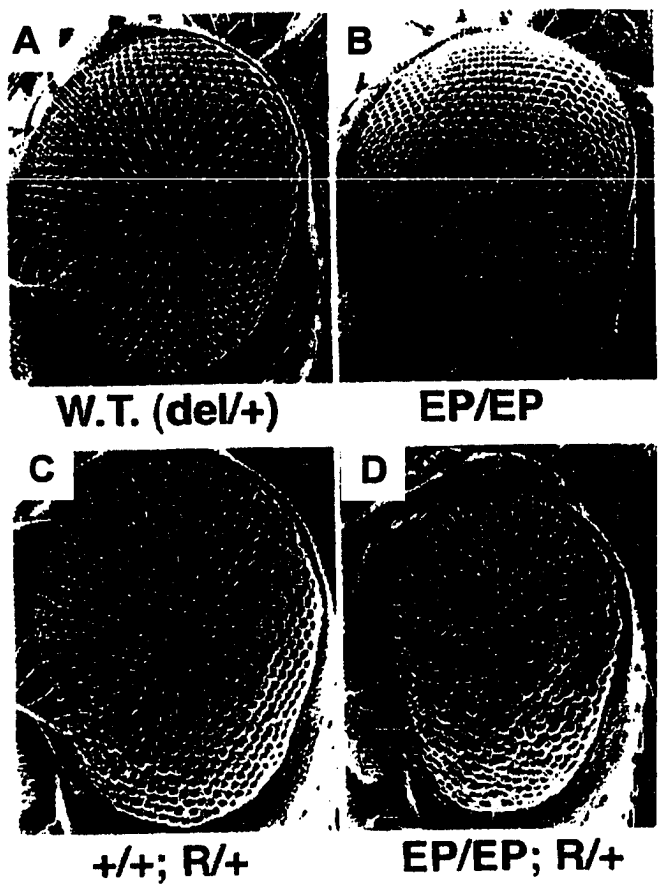

Figure 5K. Genetic Interaction Between Gene *dizzy* and Rap1
The scanning electron micrographs (SEM) of the adult compound eye provide genetic evidence that gene *dizzy* is in the same pathway as Rap1, a Ras family member. SEM of wild-type (W.T.) eye with normal pattern of ommatidia and bristles (Panel A). EP homozygous escapers have a weak phenotype with several bristles disrupted (Panel B). In the Rap1 dominant mutant, we see disruption of ommatidia and bristle patterning (Panel C). EP/EP; Rap/+ double mutants have an enhanced phenotype indicating that Rap1 is in the same pathway as *dizzy*. (Contributed by collaborator Kevin Edwards.)

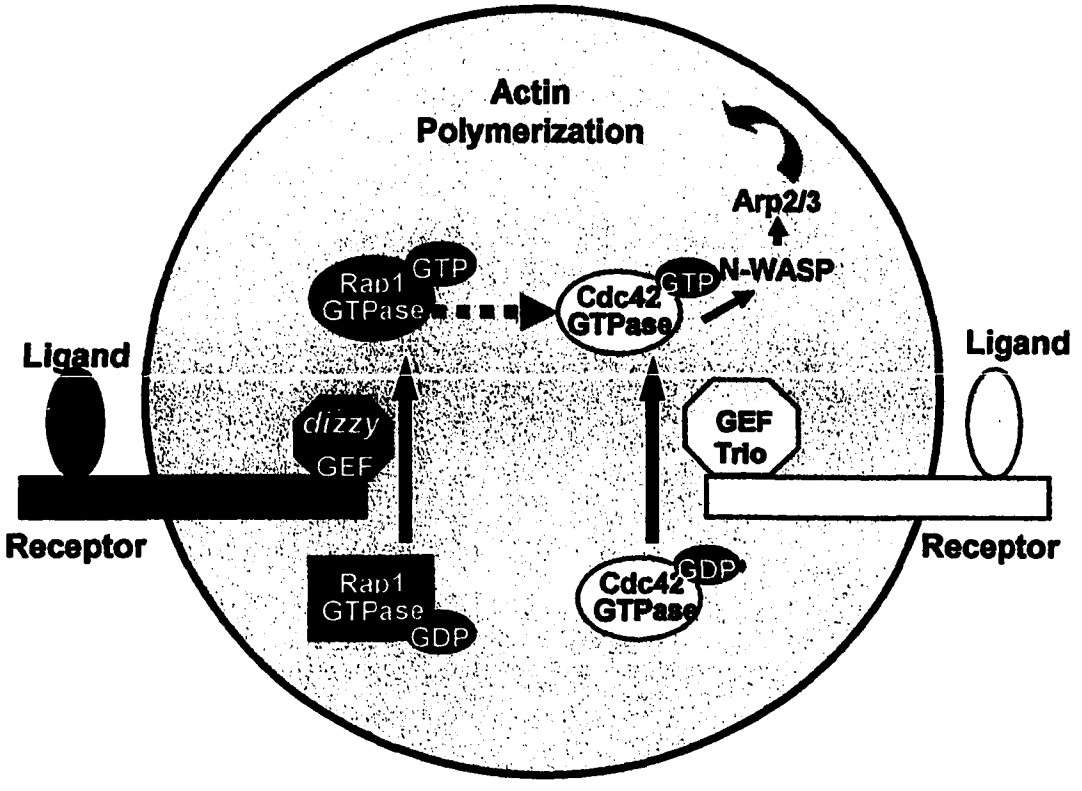

Figure 6. Model for Intracellular Signaling of *dizzy* in the Growth Cone

Transmembrane growth cone receptors are activated by binding of the extracellular ligand. Activated receptors are then capable of transducing the extracellular signal to the intracellular domain. This results in the localization of Dizzy to the intracellular domain of the receptor and activation, in a similar manner to the well characterized GEF Trio. Activated Dizzy is then capable of binding the Ras/Rap1 GTPase, the first step in the process of catalyzing the exchange of GDP for GTP. The exchange of GDP for GTP on Rap1 activates the GTPase which can send signals to the GTP bound activated GTPase CDC42. CDC42 then signals to Neuronal Wiskott Aldrich Syndrome Protein (N-WASP), which activates the seven subunit protein complex Arp2/3 which up regulates actin polymerization.

Chapter 7

References

Adams, M. D., Celniker, S. E., Holt, R. A., Evans, C. A., Gocayne, J. D., Amanatides, P. G., Scherer, S. E., Li, P. W., Hoskins, R. A., Galle, R. F., George, R. A., Lewis, S. E., Richards, S., Ashburner, M., Henderson, S. N., Sutton, G. G., Wortman, J. R., Yandell, M. D., Zhang, Q., Chen, L. X., Brandon, R. C., Rogers, Y. H., Blazej, R. G., Champe, M., Pfeiffer, B. D., Wan, K. H., Doyle, C., Baxter, E. G., Helt, G., Nelson, C. R., Gabor, G. L., Abril, J. F., Agbayani, A., An, H. J., Andrews-Pfannkoch, C., Baldwin, D., Ballew, R. M., Basu, A., Baxendale, J., Bayraktaroglu, L., Beasley, E. M., Beeson, K. Y., Benos, P. V., Berman, B. P., Bhandari, D., Bolshakov, S., Borkova, D., Botchan, M. R., Bouck, J., Brokstein, P., Brottier, P., Burtis, K. C., Busam, D. A., Butler, H., Cadieu, E., Center, A., Chandra, I., Cherry, J. M., Cawley, S., Dahlke, C., Davenport, L. B., Davies, P., de Pablos, B., Delcher, A., Deng, Z., Mays, A. D., Dew, I., Dietz, S. M., Dodson, K., Doup, L. E., Downes, M., Dugan-Rocha, S., Dunkov, B. C., Dunn, P., Durbin, K. J., Evangelista, C. C., Ferraz, C., Ferriera, S., Fleischmann, W., Fosler, C., Gabrielian, A. E., Garg, N. S., Gelbart, W. M., Glasser, K., Glodek, A., Gong, F., Gorrell, J. H., Gu, Z., Guan, P., Harris, M., Harris, N. L., Harvey, D., Heiman, T. J., Hernandez, J. R., Houck, J., Hostin, D., Houston, K. A., Howland, T. J., Wei, M. H., Ibegwam, C., et al. (2000). The genome sequence of Drosophila melanogaster. Science *287*, 2185-95.

Albright, T. D., Jessell, T. M., Kandel, E. R., and Posner, M. I. (2000). Neural science: a century of progress and the mysteries that remain. Cell *100 Suppl*, S1-55.

Andres-Barquin, P. J. (2001). Ramon y Cajal: a century after the publication of his masterpiece. Endeavour *25*, 13-7.

Araki, S., Kaibuchi, K., Sasaki, T., Hata, Y., and Takai, Y. (1991). Role of the C-terminal region of smg p25A in its

interaction with membranes and the GDP/GTP exchange protein. Mol Cell Biol *11*, 1438-47.

Ashburner, M. (1989). Drosophila (New York: Cold Spring Harbor Laboratory Press).

Aspenstrom, P., Lindberg, U., and Hall, A. (1996). Two GTPases, Cdc42 and Rac, bind directly to a protein implicated in the immunodeficiency disorder Wiskott-Aldrich syndrome. Curr Biol *6*, 70-5.

Awasaki, T., Saito, M., Sone, M., Suzuki, E., Sakai, R., Ito, K., and Hama, C. (2000). The Drosophila trio plays an essential role in patterning of axons by regulating their directional extension. Neuron *26*, 119-31.

Baas, P. W., and Luo, L. (2001). Signaling at the growth cone: the scientific progeny of Cajal meet in Madrid. Neuron *32*, 981-4.

Bagnard, D., Lohrum, M., Uziel, D., Puschel, A. W., and Bolz, J. (1998). Semaphorins act as attractive and repulsive guidance signals during the development of cortical projections. Development *125*, 5043-53.

Bar-Sagi, D., and Hall, A. (2000). RAs and Rho GTPases: A Family Reunion. Cell *103*, 227-238.

Barth, M., Hirsch, H. V., Meinertzhagen, I. A., and Heisenberg, M. (1997). Experience-dependent developmental plasticity in the optic lobe of Drosophila melanogaster. J Neurosci *17*, 1493-504.

Bashaw, G. J., and Goodman, C. S. (1999). Chimeric axon guidance receptors: the cytoplasmic domains of slit and netrin receptors specify attraction versus repulsion. Cell *97*, 917-26.

Bateman, J., Shu, H., and Van Vactor, D. (2000). The guanine nucleotide exchange factor trio mediates axonal development in the Drosophila embryo. Neuron *26*, 93-106.
Bateman, J., and Van Vactor, D. (2001). The Trio family of guanine-nucleotide-exchange factors: regulators of axon guidance. J Cell Sci *114*, 1973-80.

Battye, R., Stevens, A., and Jacobs, J. R. (1999). Axon repulsion from the midline of the Drosophila CNS requires slit function. Development *126*, 2475-81.

Bellanger, J. M., Lazaro, J. B., Diriong, S., Fernandez, A., Lamb, N., and Debant, A. (1998). The two guanine nucleotide exchange factor domains of Trio link the Rac1 and the RhoA pathways in vivo. Oncogene *16*, 147-52.

Bellanger, J. M., Zugasti, O., Lazaro, J. B., Diriong, S., Lamb, N., Sardet, C., and Debant, A. (1998). [Role of the multifunctional Trio protein in the control of the Rac1 and RhoA GTPase signaling pathways]. C R Seances Soc Biol Fil *192*, 367-74.

Berlucchi, G. (1999). Some aspects of the history of the law of dynamic polarization of the neuron. From William James to Sherrington, from Cajal and van Gehuchten to Golgi. J Hist Neurosci *8*, 191-201.

Birgbauer, E., Cowan, C. A., Sretavan, D. W., and Henkemeyer, M. (2000). Kinase independent function of EphB receptors in retinal axon pathfinding to the optic disc from dorsal but not ventral retina. Development *127*, 1231-41.

Boettner, B., and Aelst, L. V. (2002). The role of Rho GTPases in disease development. Gene *286*, 155-174.

Bottalico, A. G., Garcia, M. C., Edwards K. and He Q. (2003) A role for gene *dizzy* in the visual system development of Drosophila melanogaster. *Gene (Submitted).*

Bourne, H. R., Sanders, D. A., and McCormick, F. (1990). The GTPase superfamily: a conserved switch for diverse cell functions. Nature *348*, 125-32.

Brand, A. H., and Perrimon, N. (1993). Targeted gene expression as a means of altering cell fates and generating dominant phenotypes. Development *118*, 401-15.

Brennan, C., Monschau, B., Lindberg, R., Guthrie, B., Drescher, U., Bonhoeffer, F., and Holder, N. (1997). Two Eph receptor tyrosine kinase ligands control axon growth and may be involved in the creation of the retinotectal map in the zebrafish. Development *124*, 655-64.

Brose, K., Bland, K. S., Wang, K. H., Arnott, D., Henzel, W., Goodman, C. S., Tessier-Lavigne, M., and Kidd, T. (1999). Slit proteins bind Robo receptors and have an evolutionarily conserved role in repulsive axon guidance. Cell *96*, 795-806.

Buck, K. B., and Zheng, J. Q. (2002). Growth cone turning induced by direct local modification of microtubule dynamics. J Neurosci *22*, 9358-67.

Cerione, R. A., and Zheng, Y. (1996). The Dbl family of oncogenes. Curr Opin Cell Biol *8*, 216-22.

Chan, S. S., Zheng, H., Su, M. W., Wilk, R., Killeen, M. T., Hedgecock, E. M., and Culotti, J. G. (1996). UNC-40, a C. elegans homolog of DCC (Deleted in Colorectal Cancer), is required in motile cells responding to UNC-6 netrin cues. Cell *87*, 187-95.

Changeux, J. P. (2001). Cajal on neurons, molecules, and consciousness. Ann N Y Acad Sci *929*, 147-51.

Chen, H., Bagri, A., Zupicich, J. A., Zou, Y., Stoeckli, E., Pleasure, S. J., Lowenstein, D. H., Skarnes, W. C., Chedotal, A., and Tessier-Lavigne, M. (2000). Neuropilin-2 regulates

the development of selective cranial and sensory nerves and hippocampal mossy fiber projections. Neuron *25*, 43-56.

Cheng, H. J., Bagri, A., Yaron, A., Stein, E., Pleasure, S. J., and Tessier-Lavigne, M. (2001). Plexin-A3 mediates semaphorin signaling and regulates the development of hippocampal axonal projections. Neuron *32*, 249-63.

Clandin, T. R., and Zipursky, S. R. (2002). Making connections in the fly visual system. Neuron *35*, 827-841.

Clandinin, T. R., and Zipursky, S. L. (2002). Making connections in the fly visual system. Neuron *35*, 827-41.

Cohen, S. M. (1993). Imaginal disc Development. In The Development of *Drosophila Melanogaster*, M. Bate and M.-A. A. A., eds. (New York: Cold Spring HArbor), pp. 747-843.

Colomer, V., Engelender, S., Sharp, A. H., Duan, K., Cooper, J. K., Lanahan, A., Lyford, G., Worley, P., and Ross, C. A. (1997). Huntingtin-associated protein 1 (HAP1) binds to a Trio-like polypeptide, with a rac1 guanine nucleotide exchange factor domain. Hum Mol Genet *6*, 1519-25.

Culotti, J. G., and Kolodkin, A. L. (1996). Functions of netrins and semaphorins in axon guidance. Curr Opin Neurobiol *6*, 81-8.

Culotti, J. G., and Merz, D. C. (1998). DCC and netrins. Curr Opin Cell Biol *10*, 609-13.

de la Torre, J. R., Hopker, V. H., Ming, G. L., Poo, M. M., Tessier-Lavigne, M., Hemmati-Brivanlou, A., and Holt, C. E. (1997). Turning of retinal growth cones in a netrin-1 gradient mediated by the netrin receptor DCC. Neuron *19*, 1211-24.

Dearborn, R., Jr., He, Q., Kunes, S., and Dai, Y. (2002). Eph receptor tyrosine kinase-mediated formation of a

topographic map in the Drosophila visual system. J Neurosci *22*, 1338-49.

Debant, A., Serra-Pages, C., Seipel, K., O'Brien, S., Tang, M., Park, S. H., and Streuli, M. (1996). The multidomain protein Trio binds the LAR transmembrane tyrosine phosphatase, contains a protein kinase domain, and has separate rac- specific and rho-specific guanine nucleotide exchange factor domains. Proc Natl Acad Sci U S A *93*, 5466-71.

DeFelipe, J. (2002). Sesquicentenary of the birthday of Santiago Ramon y Cajal, the father of modern neuroscience. Trends Neurosci *25*, 481-4.

Dent, E. W., and Kalil, K. (2001). Axon branching requires interactions between dynamic microtubules and actin filaments. J Neurosci *21*, 9757-69.

Desai, C. J., Garrity, P. A., Keshishian, H., Zipursky, S. L., and Zinn, K. (1999). The Drosophila SH2-SH3 adapter protein Dock is expressed in embryonic axons and facilitates synapse formation by the RP3 motoneuron. Development *126*, 1527-35.

Dickson, B. J. (2002). Molecular mechanisms of axon guidance. Science *298*, 1959-64.

Drescher, U. (2002). Eph family functions from an evolutionary perspective. Curr Opin Genet Dev *12*, 397-402.

Drescher, U., Bonhoeffer, F., and Muller, B. K. (1997). The Eph family in retinal axon guidance. Curr Opin Neurobiol *7*, 75-80.

Erickson, J. W., and Cerione, R. A. (2001). Multiple roles for Cdc42 in cell regulation. Curr Opin Cell Biol *13*, 153-7.

Flanagan, J. G., and Van Vactor, D. (1998). Through the looking glass: axon guidance at the midline choice point. Cell *92*, 429-32.

Flanagan, J. G., and Vanderhaeghen, P. (1998). The ephrins and Eph receptors in neural development. Annu Rev Neurosci *21*, 309-45.

Gao, X., Satoh, T., Liao, Y., Song, C., Hu, C. D., Kariya Ki, K., and Kataoka, T. (2001). Identification and characterization of RA-GEF-2, a Rap guanine nucleotide exchange factor that serves as a downstream target of M-Ras. J Biol Chem *276*, 42219-25.

Garcia, M. C. and He; Q. (2003) Identification and characterization of a novel Drosophila gene *dunc-115*. Mechanisms of Development *(Submitted)*.

Garrity, P. A., Lee, C. H., Salecker, I., Robertson, H. C., Desai, C. J., Zinn, K., and Zipursky, S. L. (1999). Retinal axon target selection in Drosophila is regulated by a receptor protein tyrosine phosphatase. Neuron *22*, 707-17.

Garrity, P. A., Rao, Y., Salecker, I., McGlade, J., Pawson, T., and Zipursky, S. L. (1996). Drosophila photoreceptor axon guidance and targeting requires the dreadlocks SH2/SH3 adapter protein. Cell *85*, 639-50.

Gavazzi, I. (2001). Semaphorin-neuropilin-1 interactions in plasticity and regeneration of adult neurons. Cell Tissue Res *305*, 275-84.

Georgiou, M., and Tear, G. (2002). Commissureless is required both in commissural neurones and midline cells for axon guidance across the midline. Development *129*, 2947-56.

Goodhill, G. J., and Richards, L. J. (1999). Retinotectal maps: molecules, models and misplaced data. Trends Neurosci *22*, 529-34.

Goodman, C. S., and Shatz, C. J. (1993). Developmental mechanisms that generate precise patterns of neuronal connectivity. Cell *72 Suppl*, 77-98.

Gordon-Weeks, P. R. (1988). The ultrastructure of the neuronal growth cone: new insights from subcellular fractionation and rapid freezing studies. Electron Microsc Rev *1*, 201-19.

Habib, M., Demonet, J. F., and Frackowiak, R. (1996). [Cognitive neuroanatomy of language: contribution of functional cerebral imaging]. Rev Neurol (Paris) *152*, 249-60.

Hall, A. (1998). Rho GTPases and the actin cytoskeleton. Science *279*, 509-14.

Hall, A. (1994). Small GTP-binding proteins and the regulation of the actin cytoskeleton. Annu Rev Cell Biol *10*, 31-54.

Harris, B. Z., and Lim, W. A. (2001). Mechanism and role of PDZ domains in signaling complex assembly. J Cell Sci *114*, 3219-31.

Harris, R., Sabatelli, L. M., and Seeger, M. A. (1996). Guidance cues at the Drosophila CNS midline: identification and characterization of two Drosophila Netrin/UNC-6 homologs. Neuron *17*, 217-28.

He, Q. (2000) A functional analysis of the involvement of cytoskeleton proteins in *Drosophila* visual system. Methods in Molecular Biology, 161, 279-283.

Hedgecock, E. M., Culotti, J. G., and Hall, D. H. (1990). The unc-5, unc-6, and unc-40 genes guide circumferential

migrations of pioneer axons and mesodermal cells on the epidermis in C. elegans. Neuron *4*, 61-85.

Heisenberg, M., Heusipp, M., and Wanke, C. (1995). Structural plasticity in the Drosophila brain. J Neurosci *15*, 1951-60.

Hing, H., Xiao, J., Harden, N., Lim, L., and Zipursky, S. L. (1999). Pak functions downstream of Dock to regulate photoreceptor axon guidance in Drosophila. Cell *97*, 853-63.

Holder, N., and Klein, R. (1999). Eph receptors and ephrins: effectors of morphogenesis. Development *126*, 2033-44.

Hong, K., Hinck, L., Nishiyama, M., Poo, M. M., Tessier-Lavigne, M., and Stein, E. (1999). A ligand-gated association between cytoplasmic domains of UNC5 and DCC family receptors converts netrin-induced growth cone attraction to repulsion. Cell *97*, 927-41.

Hong, K., Nishiyama, M., Henley, J., Tessier-Lavigne, M., and Poo, M. (2000). Calcium signalling in the guidance of nerve growth by netrin-1. Nature *403*, 93-8.

Hopker, V. H., Shewan, D., Tessier-Lavigne, M., Poo, M., and Holt, C. (1999). Growth-cone attraction to netrin-1 is converted to repulsion by laminin- 1. Nature *401*, 69-73.

Hornberger, M. R., Dutting, D., Ciossek, T., Yamada, T., Handwerker, C., Lang, S., Weth, F., Huf, J., Wessel, R., Logan, C., Tanaka, H., and Drescher, U. (1999). Modulation of EphA receptor function by coexpressed ephrinA ligands on retinal ganglion cell axons. Neuron *22*, 731-42.

Huang, Z., and Kunes, S. (1996). Hedgehog, transmitted along retinal axons, triggers neurogenesis in the developing visual centers of the Drosophila brain. Cell *86*, 411-22.

Huang, Z., and Kunes, S. (1998). Signals transmitted along retinal axons in Drosophila: Hedgehog signal reception and the cell circuitry of lamina cartridge assembly. Development *125*, 3753-64.

Huang, Z., Shilo, B. Z., and Kunes, S. (1998). A retinal axon fascicle uses spitz, an EGF receptor ligand, to construct a synaptic cartridge in the brain of Drosophila. Cell *95*, 693-703.

Huber, P., Gutbrod, K., Ozdoba, C., Nirkko, A., Lovblad, K. O., and Schroth, G. (2000). [Aphasia research and speech localization in the brain]. Schweiz Med Wochenschr *130*, 49-59.

Itoh, R. E., Kurokawa, K., Ohba, Y., Yoshizaki, H., Mochizuki, N., and Matsuda, M. (2002). Activation of rac and cdc42 video imaged by fluorescent resonance energy transfer-based single-molecule probes in the membrane of living cells. Mol Cell Biol *22*, 6582-91.

Jan, L. Y., and Jan, Y. N. (1982). Antibodies to horseradish peroxidase as specific neuronal markers in Drosophila and in grasshopper embryos. Proc Natl Acad Sci U S A *79*, 2700-4.

Jay, V. (2002). Pierre Paul Broca. Arch Pathol Lab Med *126*, 250-1.

Jones, E. G. (1999). Golgi, Cajal and the Neuron Doctrine. J Hist Neurosci *8*, 170-8.

Kaibuchi, Kuroda, and Amano (1999). Regulation of the Cytoskeleton and Cell Adhesion by the Rho Family GTPases in Mammalian Cells. Annual Review of Biochemistry *68*, 459-486.

Kaprielian, Z., Imondi, R., and Runko, E. (2000). Axon guidance at the midline of the developing CNS. Anat Rec *261*, 176-97.

Keleman, K., and Dickson, B. J. (2001). Short- and long-range repulsion by the Drosophila Unc5 netrin receptor. Neuron *32*, 605-17.

Keleman, K., Rajagopalan, S., Cleppien, D., Teis, D., Paiha, K., Huber, L. A., Technau, G. M., and Dickson, B. J. (2002). Comm sorts robo to control axon guidance at the Drosophila midline. Cell *110*, 415-27.

Kennedy, T. E., Serafini, T., de la Torre, J. R., and Tessier-Lavigne, M. (1994). Netrins are diffusible chemotropic factors for commissural axons in the embryonic spinal cord. Cell *78*, 425-35.

Kidd, T., Bland, K. S., and Goodman, C. S. (1999). Slit is the midline repellent for the robo receptor in Drosophila. Cell *96*, 785-94.

Kidd, T., Brose, K., Mitchell, K. J., Fetter, R. D., Tessier-Lavigne, M., Goodman, C. S., and Tear, G. (1998). Roundabout controls axon crossing of the CNS midline and defines a novel subfamily of evolutionarily conserved guidance receptors. Cell *92*, 205-15.

Kolodkin, A. L., Levengood, D. V., Rowe, E. G., Tai, Y. T., Giger, R. J., and Ginty, D. D. (1997). Neuropilin is a semaphorin III receptor. Cell *90*, 753-62.

Kolodziej, P. A., Timpe, L. C., Mitchell, K. J., Fried, S. R., Goodman, C. S., Jan, L. Y., and Jan, Y. N. (1996). frazzled encodes a Drosophila member of the DCC immunoglobulin subfamily and is required for CNS and motor axon guidance. Cell *87*, 197-204.

Korey, C. A., and Van Vactor, D. (2000). From the growth cone surface to the cytoskeleton: one journey, many paths. J Neurobiol *44*, 184-93.

Kornberg, T. B., and Krasnow, M. A. (2000). The Drosophila genome sequence: implications for biology and medicine. Science *287*, 2218-20.

Kozma, R., Ahmed, S., Best, A., and Lim, L. (1995). The Ras-related protein Cdc42Hs and bradykinin promote formation of peripheral actin microspikes and filopodia in Swiss 3T3 fibroblasts. Mol Cell Biol *15*, 1942-52.

Kunes, S., and Steller, H. (1993). Topography in the Drosophila visual system. Curr Opin Neurobiol *3*, 53-9.

Liao, Y., Kariya, K., Hu, C. D., Shibatohge, M., Goshima, M., Okada, T., Watari, Y., Gao, X., Jin, T. G., Yamawaki-Kataoka, Y., and Kataoka, T. (1999). RA-GEF, a novel Rap1A guanine nucleotide exchange factor containing a Ras/Rap1A-associating domain, is conserved between nematode and humans. J Biol Chem *274*, 37815-20.

Liao, Y., Satoh, T., Gao, X., Jin, T. G., Hu, C. D., and Kataoka, T. (2001). RA-GEF-1, a guanine nucleotide exchange factor for Rap1, is activated by translocation induced by association with Rap1 GTP and enhances Rap1-dependent B-Raf activation. J Biol Chem *276*, 28478-83.

Liebl, E. C., Forsthoefel, D. J., Franco, L. S., Sample, S. H., Hess, J. E., Cowger, J. A., Chandler, M. P., Shupert, A. M., and Seeger, M. A. (2000). Dosage-sensitive, reciprocal genetic interactions between the Abl tyrosine kinase and the putative GEF trio reveal trio's role in axon pathfinding. Neuron *26*, 107-18.

Lukacs, D. (1980). [Pierre Paul Broca, founder of anthropology and discoverer of the cortical speech center]. Orv Hetil *121*, 2081-2.

Marin, O., Blanco, M. J., and Nieto, M. A. (2001). Differential expression of Eph receptors and ephrins correlates with the formation of topographic projections in primary and secondary visual circuits of the embryonic chick forebrain. Dev Biol *234*, 289-303.

Martin, K. A., Poeck, B., Roth, H., Ebens, A. J., Ballard, L. C., and Zipursky, S. L. (1995). Mutations disrupting neuronal connectivity in the Drosophila visual system. Neuron *14*, 229-40.

May, R. C. (2001). The Arp2/3 complex: a central regulator of the actin cytoskeleton. Cell Mol Life Sci *58*, 1607-26.

Meyer, R. L. (1998). Roger Sperry and his chemoaffinity hypothesis. Neuropsychologia *36*, 957-80.

Mitchell, K. J., Doyle, J. L., Serafini, T., Kennedy, T. E., Tessier-Lavigne, M., Goodman, C. S., and Dickson, B. J. (1996). Genetic analysis of Netrin genes in Drosophila: Netrins guide CNS commissural axons and peripheral motor axons. Neuron *17*, 203-15.

Molnar, G., Dagher, M. C., Geiszt, M., Settleman, J., and Ligeti, E. (2001). Role of prenylation in the interaction of Rho-family small GTPases with GTPase activating proteins. Biochemistry *40*, 10542-9.

Mueller, B. K. (1999). Growth cone guidance: first steps towards a deeper understanding. Annu Rev Neurosci *22*, 351-88.

Mullins, R. D. (2000). How WASP-family proteins and the Arp2/3 complex convert intracellular signals into cytoskeletal structures. Curr Opin Cell Biol *12*, 91-6.

Newsome, T. P., Asling, B., and Dickson, B. J. (2000). Analysis of Drosophila photoreceptor axon guidance in eye-specific mosaics. Development *127*, 851-60.

Newsome, T. P., Schmidt, S., Dietzl, G., Keleman, K., Asling, B., Debant, A., and Dickson, B. J. (2000). Trio combines with dock to regulate Pak activity during photoreceptor axon pathfinding in Drosophila. Cell *101*, 283-94.

Nguyen Ba-Charvet, K. T., Brose, K., Marillat, V., Kidd, T., Goodman, C. S., Tessier-Lavigne, M., Sotelo, C., and Chedotal, A. (1999). Slit2-Mediated chemorepulsion and collapse of developing forebrain axons. Neuron *22*, 463-73.

Nguyen-Ba-Charvet, K. T., and Chedotal, A. (2002). Role of Slit proteins in the vertebrate brain. J Physiol Paris *96*, 91-8.

Ohta, K., Mizutani, A., Kawakami, A., Murakami, Y., Kasuya, Y., Takagi, S., Tanaka, H., and Fujisawa, H. (1995). Plexin: a novel neuronal cell surface molecule that mediates cell adhesion via a homophilic binding mechanism in the presence of calcium ions. Neuron *14*, 1189-99.

Opp, G. (1994). Historical roots of the field of learning disabilities: some nineteenth-century German contributions. J Learn Disabil *27*, 10-9.

Orike, N., and Pini, A. (1996). Axon guidance: following the Eph plan. Curr Biol *6*, 108-10.

Rajagopalan, S., Nicolas, E., Vivancos, V., Berger, J., and Dickson, B. J. (2000). Crossing the midline: roles and regulation of Robo receptors. Neuron *28*, 767-77.

Rajagopalan, S., Vivancos, V., Nicolas, E., and Dickson, B. J. (2000). Selecting a longitudinal pathway: Robo receptors specify the lateral position of axons in the Drosophila CNS. Cell *103*, 1033-45.

Rao, Y., and Wu, Y. (2000). [The molecular mechanism of neuronal migration]. Sheng Li Ke Xue Jin Zhan *31*, 198-204.

Raper, J. A. (2000). Semaphorins and their receptors in vertebrates and invertebrates. Curr Opin Neurobiol *10*, 88-94.

Ridley, A. J., and Hall, A. (1992). The small GTP-binding protein rho regulates the assembly of focal adhesions and actin stress fibers in response to growth factors. Cell *70*, 389-99.

Ridley, A. J., Paterson, H. F., Johnston, C. L., Diekmann, D., and Hall, A. (1992). The small GTP-binding protein rac regulates growth factor-induced membrane ruffling. Cell *70*, 401-10.

Ross, E. M., and Wilkie, T. M. (2000). GTPase-activating proteins for heterotrimeric G proteins: regulators of G protein signaling (RGS) and RGS-like proteins. Annu Rev Biochem *69*, 795-827.

Rubin, G. M. (1988). Drosophila melanogaster as an experimental organism. Science *240*, 1453-9.

Rubin, G. M., and Lewis, E. B. (2000). A brief history of Drosophila's contributions to genome research. Science *287*, 2216-8.

Sambrook, J., Fritsh, E. F., and Maniatis, T. (1989). Molecular Cloning, Second Edition: Cold Spring Harbor Laboratory Press).

Schmucker, D., and Zipursky, S. L. (2001). Signaling downstream of Eph receptors and ephrin ligands. Cell *105*, 701-4.

Seeger, M., Tear, G., Ferres-Marco, D., and Goodman, C. S. (1993). Mutations affecting growth cone guidance in Drosophila: genes necessary for guidance toward or away from the midline. Neuron *10*, 409-26.

Snapper, S. B., and Rosen, F. S. (1999). The Wiskott-Aldrich syndrome protein (WASP): roles in signaling and cytoskeletal organization. Annu Rev Immunol *17*, 905-29.

Song, H., Ming, G., He, Z., Lehmann, M., McKerracher, L., Tessier-Lavigne, M., and Poo, M. (1998). Conversion of neuronal growth cone responses from repulsion to attraction by cyclic nucleotides. Science *281*, 1515-8.

Song, H. J., Ming, G. L., and Poo, M. M. (1997). cAMP-induced switching in turning direction of nerve growth cones. Nature *388*, 275-9.

Sotelo, C. (1999). From Cajal's chemotaxis to the molecular biology of axon guidance. Brain Res Bull *50*, 395-6.

Sperry, R. W. (1963). Chemoaffinity in the orderly growth of nerve fiber patterns and connections. Proc. N. A. S. *50*, 703-10.

Spinelli, D. N., Hirsch, H. V., Phelps, R. W., and Metzler, J. (1972). Visual experience as a determinant of the response characteristics of cortical receptive fields in cats. Exp Brain Res *15*, 289-304.

Spradling, A. C., Stern, D., Beaton, A., Rhem, E. J., Laverty, T., Mozden, N., Misra, S., and Rubin, G. M. (1999). The Berkeley Drosophila Genome Project gene disruption project: Single P-element insertions mutating 25% of vital Drosophila genes. Genetics *153*, 135-77.

Steven, R., Kubiseski, T. J., Zheng, H., Kulkarni, S., Mancillas, J., Ruiz Morales, A., Hogue, C. W., Pawson, T., and Culotti, J. (1998). UNC-73 activates the Rac GTPase

and is required for cell and growth cone migrations in C. elegans. Cell *92*, 785-95.

Symons, M., and Settleman, J. (2000). Rho family GTPases: more than simple switches. Trends Cell Biol *10*, 415-9.

Takai, Y., Kaibuchi, K., Kikuchi, A., and Kawata, M. (1992). Small GTP-binding proteins. Int Rev Cytol *133*, 187-230.

Takai, Y., Sasaki, T., and Matozaki, T. (2001). Small GTP-binding proteins. Physiol Rev *81*, 153-208.

Tamagnone, L., Artigiani, S., Chen, H., He, Z., Ming, G. I., Song, H., Chedotal, A., Winberg, M. L., Goodman, C. S., Poo, M., Tessier-Lavigne, M., and Comoglio, P. M. (1999). Plexins are a large family of receptors for transmembrane, secreted, and GPI-anchored semaphorins in vertebrates. Cell *99*, 71-80.

Tamagnone, L., and Comoglio, P. M. (2000). Signalling by semaphorin receptors: cell guidance and beyond. Trends Cell Biol *10*, 377-83.

Tanaka, E., and Sabry, J. (1995). Making the connection: cytoskeletal rearrangements during growth cone guidance. Cell *83*, 171-6.

Tessier-Lavigne, M. (1995). Eph receptor tyrosine kinases, axon repulsion, and the development of topographic maps. Cell *82*, 345-8.

Tessier-Lavigne, M., and Goodman, C. S. (1996). The molecular biology of axon guidance. Science *274*, 1123-33.

Torok, T., Tick, G., Alvarado, M., and Kiss, I. (1993). P-lacW insertional mutagenesis on the second chromosome of Drosophila melanogaster: isolation of lethals with different overgrowth phenotypes. Genetics *135*, 71-80.

Ueda, T., Kikuchi, A., Ohga, N., Yamamoto, J., and Takai, Y. (1990). Purification and characterization from bovine brain cytosol of a novel regulatory protein inhibiting the dissociation of GDP from and the subsequent binding of GTP to rhoB p20, a ras p21-like GTP-binding protein. J Biol Chem *265*, 9373-80.

Van Vactor, D., and Flanagan, J. G. (1999). The middle and the end: slit brings guidance and branching together in axon pathway selection. Neuron *22*, 649-52.

Wilkinson, D. G. (2001). Multiple roles of EPH receptors and ephrins in neural development. Nat Rev Neurosci *2*, 155-64.

Winberg, M. L., Noordermeer, J. N., Tamagnone, L., Comoglio, P. M., Spriggs, M. K., Tessier-Lavigne, M., and Goodman, C. S. (1998). Plexin A is a neuronal semaphorin receptor that controls axon guidance. Cell *95*, 903-16.

Yu, H. H., and Kolodkin, A. L. (1999). Semaphorin signaling: a little less per-plexin. Neuron *22*, 11-4.

Zheng, Y. (2001). Dbl family guanine nucleotide exchange factors. Trends Biochem Sci *26*, 724-32.

Zhou, F. Q., and Cohan, C. S. (2001). Growth cone collapse through coincident loss of actin bundles and leading edge actin without actin depolymerization. J Cell Biol *153*, 1071-84.

Zinn, K., and Sun, Q. (1999). Slit branches out: a secreted protein mediates both attractive and repulsive axon guidance. Cell *97*, 1-4.